

3 MAY 1989



**FOREIGN  
BROADCAST  
INFORMATION  
SERVICE**

---

# ***JPRS Report***

# **Science & Technology**

---

***Japan***

ISTEC SUPERCONDUCTIVITY  
WORKSHOP

JPRS-JST-89-010

3 MAY 1989

## SCIENCE & TECHNOLOGY

### JAPAN

#### ISTEC SUPERCONDUCTIVITY WORKSHOP

43070708 Tokyo ISTEC WORKSHOP ON SUPERCONDUCTIVITY in English  
1-3 Feb 89 pp 5-8, 12-15, 24-27, 31-34, 39-50, 59-66, 71-74, 79-122

[Selected papers presented at the ISTEC Workshop on Superconductivity held 1-3 February 1989 in Oiso; sponsored by the International Superconductivity Technology Center]

#### CONTENTS

Scientific Program.....	1
Critical Current in High-Field Superconductors [K. Tachikawa].....	5
Temperature and Magnetic Field Dependence of the Critical Current in Polycrystalline $\text{Ba}_2\text{YCu}_3\text{O}_y$ [H. Obara, H. Yamasaki, et al.].....	9
Flux Pinning Mechanism in High $T_c$ Oxide Superconductors [T. Matsushita].....	13
Weak Links in High $T_c$ Superconductors [M. Wakata, S. Miyashita, et al.].....	17
Study of the Magnetic Loss in the Copper-Oxide Based Superconductors by Complex Susceptibility Measurement [A. Maeda, K. Uchinokura].....	21
Magnetization and Critical Current of YBCO and BSCCO Materials [D. Ito, E. Shimizu, et al.].....	25

Critical Current and Flux Creep in YBaCuO Prepared by the Quench and Melt Growth Technique [Masato Murakami, Mitsuru Morita, et al.].....	29
High Jc BiSrCaCuO and TlBaCaCuO Superconducting Thin Film [H. Itozaki, S. Tanaka, et al.].....	33
Effects of Boundary Defects on Critical Current Densities of ErBa <sub>2</sub> Cu <sub>3</sub> O <sub>7-δ</sub> [K. Takagi, T. Aida, et al.].....	37
In-situ Growth of YBa <sub>2</sub> Cu <sub>3</sub> O <sub>7-x</sub> Thin Films by Activated Reactive Evaporation [T. Terashima, K. Iijima, et al.].....	41
Ba <sub>1-x</sub> K <sub>x</sub> BiO <sub>3</sub> Thin Films Preparation With ECR Ion Beam Oxidation and Their Properties [Y. Enomoto, T. Murakami, et al.].....	45
Low Temperature Formation of Bi(Pb)-Sr-Ca-Cu-O Thin Films by a Successive Deposition Method With Excimer Laser [Tomoji Kawai, Masaki Kanai, et al.].....	49
AS-Grown Preparation of Superconducting Epitaxial Ba <sub>2</sub> YCu <sub>3</sub> O <sub>x</sub> Thin Films Sputtered on Epitaxially Grown ZrO <sub>2</sub> /Si(100) [H. Myoren, Y. Nishiyama, et al.].....	53
Synthesis and Characterization of Artificially Layered Bi-Sr-Ca-Cu Oxide Films [Junichi Sato, Masatsugu Kaise, et al.].....	57
Epitaxial Film Growth of Artificial (BiO)/(SrCaCuO) Layered Structure [J. Fujita, T. Tatsumi, et al.].....	61
Growth of C-Axis Oriented Tl-Ca-Ba-Cu-O Thin Films [Yo Ichikawa, Hideaki Adachi, et al.].....	65
Microstructure Dependence of Critical Current Density in Ag Sheathed Ba <sub>2</sub> YCu <sub>3</sub> O <sub>6+x</sub> Tapes [K. Osamura].....	69
Ag-Sheathed High Tc Superconducting Tape with Jc=10 <sup>4</sup> A/cm <sup>2</sup> [T. Matsumoto, M. Okada, et al.].....	73
Critical Current Density of Bi(Pb)-Sr-Ca-Cu-O Tape [K. Togano].....	77
BiPbSrCaCuO Superconducting Wires With High Critical Current Density [Ken-Ichi Sato, Takeshi Hikata, et al.].....	81

# SCIENTIFIC PROGRAM

**WEDNESDAY, FEBRUARY 1**

13:00 - 13:20

## Opening Remarks

T. Akutsu (Senior Managing Director, ISTEC)

S. Tanaka (Workshop Chairman, /Vice President, ISTEC)

K. Kajimura (Chairman of Program Committee, /Electrotechnical Lab.)

## OPENING SESSION

13:20 - 14:40

Chairperson: W. Klose (Karlsruhe Nuclear Research Center)

13:20 - 14:00

CONSIDERATIONS LIMITING CRITICAL CURRENTS IN HIGH TEMPERATURE SUPERCONDUCTORS

M. Tinkham (Harvard University)

14:00 - 14:40

CRITICAL CURRENT IN HIGH-FIELD SUPERCONDUCTORS

K. Tachikawa (Tokai University)

14:40 - 15:10

COFFEE BREAK

## SESSION I: MICROSTRUCTURE

15:10 - 18:30

Chairperson: K. Osamura (Kyoto University)

15:10 - 15:40

MICROSTRUCTURES AND INTRAGRAIN CRITICAL CURRENT DENSITIES IN  $\text{YBa}_2(\text{Cu}_{1-x}\text{M}_x)_3\text{O}_7$

M. Suenaga (Brookhaven National Lab.)

15:40 - 16:10

THE EFFECT OF IMPURITY ELEMENTS ON THE MICROSTRUCTURE AND CURRENT CARRYING CAPACITY OF BULK AND THIN FILM YBCO MATERIAL

C. R. M. Grovenor (University of Oxford)

16:40 - 17:10

TEMPERATURE DEPENDENCE OF THE TRANSPORT CRITICAL CURRENT IN POLYCRYSTALLINE  $\text{Ba}_2\text{YCu}_3\text{O}_y$

H. Obara (Electrotechnical Lab.)

17:10 - 17:30

BREAK

Chairperson: N. Koshizuka (ISTEC)



- 17:30 - 18:00 COMPLEX STRUCTURAL BEHAVIOUR OF THE SUPERCONDUCTING  
COPPER OXIDES  
M. Hervieu (CRISMAT-ISMRA)
- 18:00 - 18:30 FLUX PINNING MECHANISM IN HIGH  $T_c$  OXIDE SUPERCONDUCTORS.  
T. Matsushita (Kyushu University)

WELCOME RECEPTION

19:00 - 21:00

## THURSDAY, FEBRUARY 2

### SESSION II: WEAK LINK AND GRAIN BOUNDARY

09:00 - 12:00

Chairperson: T.K. Worthington (IBM Thomas J. Watson Research Center)

- 09:00 - 09:30 SUPERCONDUCTIVITY IN THE  $\text{LaBa}_2\text{Cu}_3\text{O}_{7-y}$  COMPOUNDS WITH Ag  
RELATED ADDITIVES  
F. Mizuno (ISTEC, Nagoya Division)
- 09:30 - 10:00 ELECTRON MICROSCOPY STUDIES OF  $\text{YBa}_2\text{Cu}_3\text{O}_{7-x}$  GRAIN  
BOUNDARIES  
S.E. Babcock (University of Wisconsin-Madison)
- 10:00 - 10:30 WEAK LINKS IN HIGH  $T_c$  SUPERCONDUCTORS  
M. Wakata (Mitsubishi Electric Corporation)

10:30 - 11:00 COFFEE BREAK

Chairperson: M. Hervieu (CRISMAT-ISMRA)

- 11:00 - 11:30 STUDY OF THE MAGNETIC LOSS IN THE COPPER-OXIDE BASED  
SUPERCONDUCTORS BY COMPLEX SUSCEPTIBILITY  
MEASUREMENT  
A. Maeda (The University of Tokyo)
- 11:30 - 12:00 MAGNETIZATION AND CRITICAL CURRENT OF YBCO AND BSCCO  
MATERIALS  
D. Ito (Toshiba Corporation)

LUNCH

### SESSION III: FLUX CREEP

14:00 - 15:30

Chairperson: T. Matsushita (Kyushu University)

- 14:00 - 14:30 THE MENACE OF GIANT FLUX CREEP  
T.K. Worthington (IBM Thomas J. Watson Research Center)
- 14:30 - 15:00 DISSIPATION BELOW  $T_c$  IN THE HIGH TEMPERATURE  
SUPERCONDUCTORS  
T.T.M. Palstra (AT&T Bell Laboratories)
- 15:00 - 15:30 CRITICAL CURRENT AND FLUX CREEP IN  $\text{YBaCuO}$  PREPARED BY  
THE QUENCH AND MELT GROWTH TECHNIQUE  
M. Murakami (Nippon Steel Corporation)

**SESSION IV: THIN FILM**

16:00 - 18:00

*Chairperson:* I.F. Corbett (Rutherford Appleton Lab.)

- 16:00 - 16:30 HIGH Jc BiSrCaCuO AND TiBaCaCuO SUPERCONDUCTING THIN FILM  
H. Itozaki (Sumitomo Electric Industries, Ltd.)
- 16:30 - 17:00 RELATION BETWEEN GROWTH QUALITY AND CRITICAL CURRENT DENSITY IN SPUTTERED YBaCuO THIN FILMS  
J. Geerk (Karlsruhe Nuclear Research Center)
- 17:00 - 17:30 EFFECTS OF BOUNDARY DEFECTS ON CRITICAL CURRENT DENSITIES OF ErBa<sub>2</sub>Cu<sub>3</sub>O<sub>7-x</sub> THIN FILMS  
K. Takagi (Hitachi Ltd.)
- 17:30 - 18:00 CRITICAL CURRENTS IN MAGNETIC FIELDS, mm-WAVE SURFACE RESISTANCE AND INFRARED PROPERTIES OF EPITAXIAL YBaCuO FILMS  
H.E. Hoenig (SIEMENS Corporate Research)

**LUMP SESSION I: THIN FILM PREPARATION**

Room Hakucho

*Chairperson:* Y. Bando (Kyoto University)

19:30 - 22:30

- 19:30 - 19:50 IN-SITU GROWTH OF YBa<sub>2</sub>Cu<sub>3</sub>O<sub>7-x</sub> THIN FILMS BY ACTIVATED REACTIVE EVAPORATION  
Y. Bando (Kyoto University)
- 19:50 - 20:10 Ba<sub>1-x</sub>K<sub>x</sub>BiO<sub>3</sub> THIN FILMS PREPARATION WITH ECR ION BEAM OXIDATION AND THEIR PROPERTIES  
Y. Enomoto (NTT, Opto-Electronics Labs.)
- 20:10 - 20:30 LOW TEMPERATURE FORMATION OF Bi(Pb)-Sr-Ca-Cu-O THIN FILMS BY A SUCCESSIVE DEPOSITION METHOD WITH EXCIMER LASER  
T. Kawai (Osaka University)
- 20:30 - 20:50 AS-GROWN PREPARATION OF SUPERCONDUCTING EPITAXIAL Ba<sub>2</sub>YC<sub>3</sub>O<sub>x</sub> THIN FILMS SPUTTERED ON EPITAXIALLY GROWN ZrO<sub>2</sub>/Si(100)  
Y. Osaka (Hiroshima University)
- 20:50 - 21:10 SYNTHESIS AND CHARACTERIZATION OF ARTIFICIALLY LAYERED Bi-Sr-Ca-Cu OXIDE FILMS  
K. Ogawa (National Research Inst. for Metals)
- 21:10 - 21:30 EPITAXIAL FILM GROWTH OF ARTIFICIAL (BiO)/(SrCaCuO) LAYERED STRUCTURE  
J. Fujita (NEC Corporation)
- 21:30 - 21:50 GROWTH OF C-AXIS ORIENTED Ti-Ca-Ba-Cu-O THIN FILMS  
Y. Ichikawa (Matsushita Electric Industrial Co.)
- 21:50 - 22:30 DISCUSSION

**LUMP SESSION II: FLUX PINNING***Chairperson:* K. Yamafuji (Kyushu University)Room Tsuru  
19:30 - 22:30**Speakers:**

M. Murakami (Nippon Steel Corporation)  
K. Osamura (Kyoto University)  
K. Togano (National Research Inst. for Metals)  
T. Matsushita (Kyushu University)

**FRIDAY, FEBRUARY 3****SESSION V: TAPE AND WIRE**

09:00 - 11:00

*Chairperson:* K. Ogawa (National Research Inst. for Metals)

- 09:00 - 09:30      MICROSTRUCTURE DEPENDENCE OF CRITICAL CURRENT DENSITY  
IN Ag SHEATHED  $\text{Ba}_2\text{YCu}_3\text{O}_{6+x}$  TAPES  
K. Osamura (Kyoto University)
- 09:30 - 10:00      Ag-SHEATHED HIGH  $T_c$  SUPERCONDUCTING TAPE WITH  
 $J_c=10^4 \text{ A/cm}^2$   
T. Matsumoto (Hitachi Ltd.)
- 10:00 - 10:30      CRITICAL CURRENT DENSITY OF Bi(Pb)-Sr-Ca-Cu-O TAPE  
K. Togano (National Research Inst. for Metals)
- 10:30 - 11:00      BiPbSrCaCuO SUPERCONDUCTING WIRES WITH HIGH CRITICAL  
CURRENT DENSITY  
K. Sato (Sumitomo Electric Industries, Ltd.)

11:00 - 11:20

**Closing Remarks**

M. Suenaga (Brookhaven National Lab.)

*Chairperson:* T. Kobayashi (ISTEC)

# CRITICAL CURRENT IN HIGH-FIELD SUPERCONDUCTORS

K. TACHIKAWA

TOKAI UNIVERSITY, FACULTY OF ENGINEERING

Hiratsuka, Kanagawa 259-12, Japan

## ABSTRACT

Metallurgical factors affecting the critical current density of practically important alloy and compound superconductors are summarized. There are different kinds of effective pinning centers depending on both the material and the intensity of applied magnetic field.

In this paper, problems related to the critical current density  $J_c$  in different high-field superconductors are reviewed. In Nb-Ti alloy wires, pinning centers introduced by a severe cold working and a precipitation of  $\alpha$ -Ti phase are effective in a high field region and in a low field region, respectively [1]. A proper combination of cold working and precipitation yields a high  $J_c$  in Nb-Ti wires. In addition, pinning by the matrix between superconducting filaments is predominant in a low field region in ultra fine filamentary Nb-Ti wires developed for AC applications [2].

Meanwhile, in compound superconductors dislocations and precipitations are not present, and the predominant pinning centers are grain boundaries. Thus, the  $J_c$  of Nb<sub>3</sub>Sn and other compound superconductors is strongly dependent on their grain size [3]. A high upper critical field  $H_{c2}$  in compound superconductors yields high  $J_c$  in high fields. The  $H_{c2}$  enhancement by Ti doping to Nb<sub>3</sub>Sn improves the  $J_c$  in high fields as shown in Fig. 1 [4]. The V<sub>3</sub>Ga also exhibits appreciably better  $J_c$  in high fields than pure Nb<sub>3</sub>Sn. The insitu processed V<sub>3</sub>Ga wire consisted of very fine superconducting filaments shows an extremely high  $J_c$  may be due to a pinning by matrix between the filaments like the ultra fine filamentary Nb-Ti wire [5].

In the compound with large grain size, the  $J_c$  in low field is reduced, and a so-called peak effect appears. In the bronze processed tape with columnar grain structure grown perpendicular to the core, an anisotropy in  $J_c$  with respect to the direction of applied field is observed as shown in Fig. 2 [3]. When the field is applied perpendicular to the columnar axis a peak effect



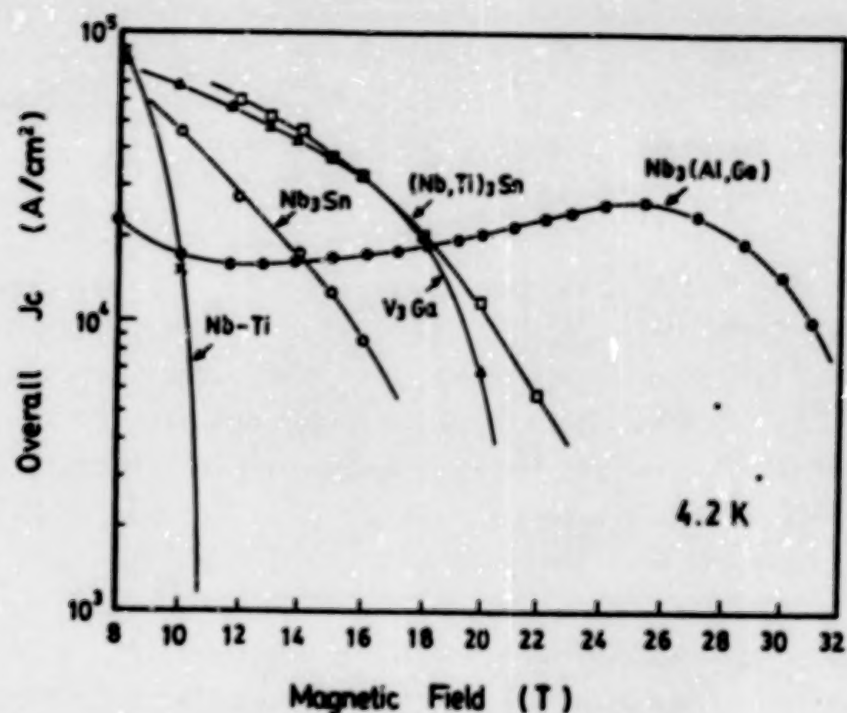


Fig. 1  $J_c$  versus magnetic field curves of different high-field superconductors.

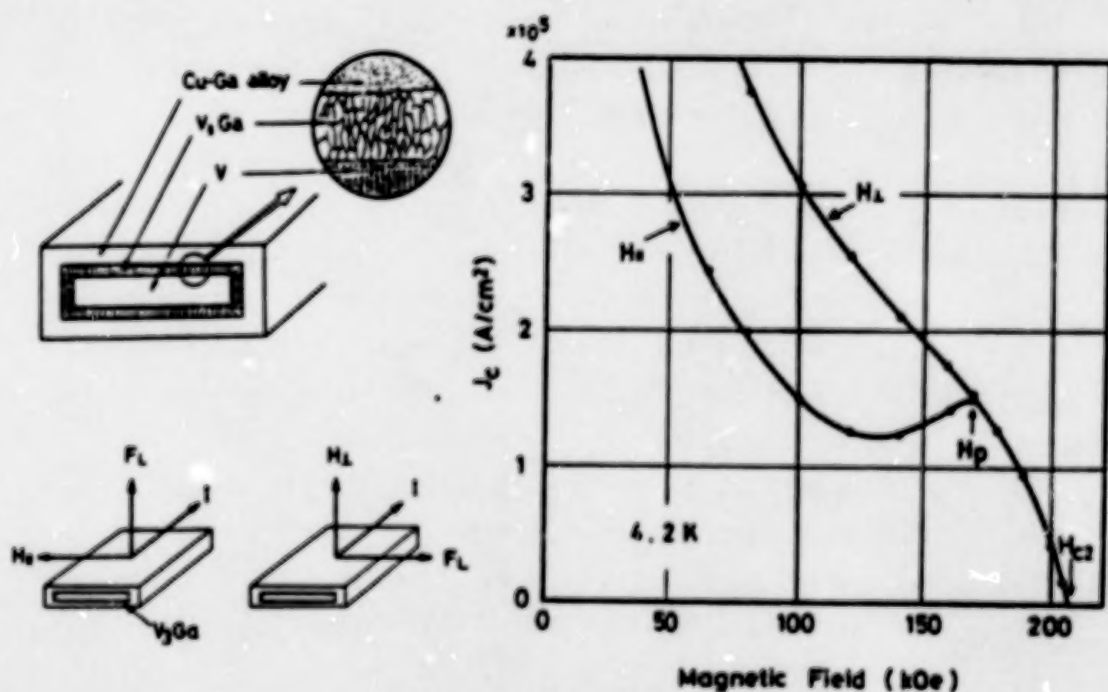


Fig. 2 Anisotropy in  $J_c$  with respect to the direction of magnetic field applied parallel and perpendicular to the surface of bronze processed V<sub>3</sub>Ga tape.

appears. The  $J_c$  in low fields is closely related to the grain structure of compound, whilst the  $J_c$  in fields higher than the peak field does not depend on the grain structure at all. There seems to be another more intrinsic pinning mechanism in high field region.

The fabrication of  $Nb_3Al$  and other superconductors with high-field performance superior than that of  $Nb_3Sn$  has been studied. The Al5  $Nb_3(Al,Ge)$  transformed via the supersaturated bcc phase has a very fine grain size and shows a  $J_c$  of exceeding  $1 \times 10^6 A/cm^2$  at 20T [6]. The rapid quenching from high temperatures facilitates the retention of stoichiometric Al5  $Nb_3Al$  phase and yields a high  $J_c$  in high fields. The  $Nb_3(Al,Ge)$  produced by a continuous electron beam irradiation process keeps an enough high  $J_c$  for practical use at 30T as shown in Fig. 1 [6].

The thin films of B1  $NbN$  prepared by a sputtering shows a  $J_c$  of  $10^6 A/cm^2$  at 20T [7]. However, the  $J_c$  of  $NbN$  films drops rapidly with increasing film thickness as shown in Fig. 3, which is a problem in  $NbN$  for high-field applications. The  $J_c$  of  $PbMo_8S_8$  Chevrel phase wires prepared by a powder method has been improved through a precise composition adjustment and a

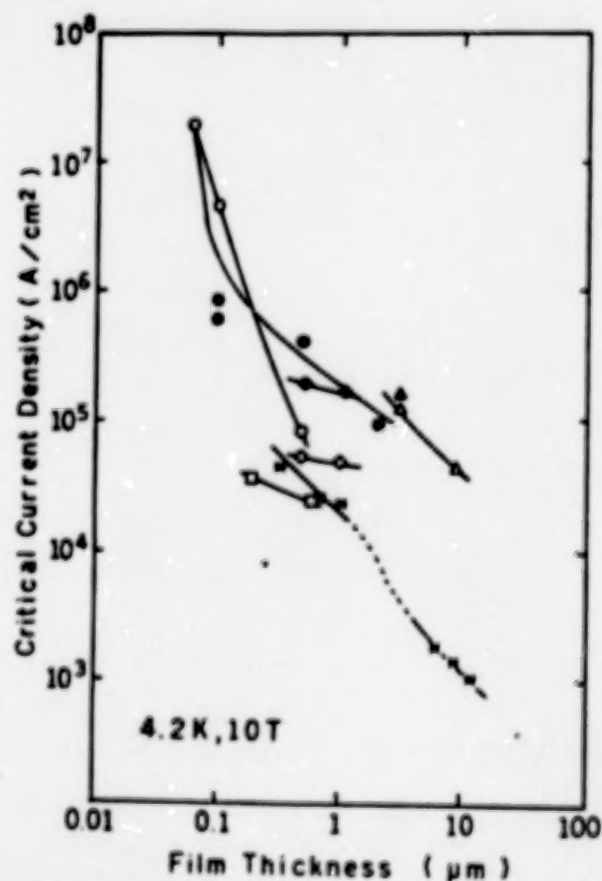


Fig. 3 Dependence of  $J_c$  of  $NbN$  films on their thickness. Data are summarized from different references.

reduction of strain effect. A  $J_c$  of  $\sim 1 \times 10^4 \text{ A/cm}^2$  has been obtained at 20T [8]. The enhancement in  $J_c$  of Chevrel phase wire provides a bright prospect for the improvement in  $J_c$  of high- $T_c$  oxide wires.

A mechanical strain produces an appreciable effect on the  $J_c$  in high fields. The improvement of  $H_{c2}$  by a third element addition such as Ti to  $\text{Nb}_3\text{Sn}$  reduces the strain effect in high fields. The  $J_c$ 's of  $\text{V}_3\text{Ga}$  and  $\text{Nb}_3\text{Al}$  show smaller strain effects than that of  $\text{Nb}_3\text{Sn}$ . The  $J_c$  of C15  $\text{V}_3(\text{Hf}, \text{Zr})$  and Bi NbN are almost independent on strain.

The electromagnetic stability of high-field superconductors has crucial importance for magnet applications. High- $J_c$  superconducting tape like insitu  $\text{V}_3\text{Ga}$  shows a pronounced degradation in  $J_c$  when wound into a coil. Meanwhile, low- $J_c$  tape like diffusion processed  $\text{V}_3\text{Ga}$  is much stable. A peak effect in  $J_c$  against magnetic field may cause the one also against temperature, providing an excellent stability.

There seems to be different kinds of effective pinning centers in metallic high-field superconductors depending on the material and the intensity of applied magnetic field. There are still several problems unsolved for the quantitative understanding of  $J_c$  in high-field superconductors.

## References

1. H.Wada, K.Itoh, K.Tachikawa, Y.Yamada and S.Nurase, J. Japan Inst. Metals, 48, 1126 (1984).
2. H.Tateishi, T.Ohnishi, K.Ohatsu, H.Takei and M.Nagata, Proc. Int. Symp. on Flux Pinning and Electromagnetic Properties in Superconductors, 208 (1985).
3. Y.Tanaka, K.Itoh and K.Tachikawa, J. Japan Inst. Metals, 40, 515 (1976).
4. K.Tachikawa, K.Kamata, H.Moriiai, N.Tada, T.Fujinaga and K.Saito, Advances in Cryogenic Engr. and Materials, 32, 947 (1986).
5. H.Kumakura, K.Togano, T.Takeuchi and K.Tachikawa, IEEE Trans.on Magnetics, MAG21, 760 (1985).
6. K.Togano and K.Tachikawa, Advances in Cryogenic Engr. and Materials, 34, 451 (1987).
7. J.R.Gavaler, A.T.Santhanam, A.I.Braginski, N.Ashikin and M.A.Janocko, IEEE Trans. on Magnetics, MAG-17, 573 (1981).
8. Y.Kubo, K.Yoshizaki, F.Fujiwara, K.Noto and K.Watanabe, to be published in Proc. MRS symp. on Advanced Superconductors, (Tokyo, 1988).

# TEMPERATURE AND MAGNETIC FIELD DEPENDENCE OF THE CRITICAL CURRENT IN POLYCRYSTALLINE $\text{Ba}_2\text{YCu}_3\text{O}_7$

H. OBARA, H. YAMASAKI, Y. KIMURA,  
Y. HIGASHIDA<sup>†</sup> and T. ISHIHARA<sup>†</sup>

ELECTROTECHNICAL LABORATORY  
Umezono 1-1-4, Tsukuba-shi, Ibaraki 305, JAPAN

<sup>†</sup>JAPAN FINE CERAMICS CENTER  
Mutsumi 2-4-1, Atsuta-ku, Nagoya-shi, Aichi 456, JAPAN

## ABSTRACT

Temperature and magnetic field dependence on the critical current density  $J_c$  of polycrystalline high- $T_c$  oxide superconductor,  $\text{Ba}_2\text{YCu}_3\text{O}_7$ , have been measured. At low temperature,  $J_c$  showed different temperature dependence between field cooling and zero-field cooling, that is, the  $J_c$  value measured when the sample was cooled in a fixed magnetic field, was different from that measured when the sample was cooled in zero magnetic field and then a magnetic field was applied. This irreversible behavior of  $J_c$  disappeared at reduced temperature difference  $1 - t$  proportional to  $H^{2/3}$  ( $H$  is magnetic field). Moreover we have observed that the slope  $dV/dI$  just above  $J_c$  began to increase rapidly with increasing temperature above 70 K. These experimental results can be attributed to the effects of grain boundaries or anisotropy of this system.

## INTRODUCTION

The discovery of high temperature oxide superconductors [1-4] has brought a great impact on basic science and technology, and has stimulated a remarkably wide range of research activity. In regard to technological aspects, there is a need to prepare specimens which have higher critical current density,  $J_c$ . Transport critical current density of polycrystalline bulk samples, however, have been much lower than that of thin films [5] and the magnetization measurement has indicated that  $J_c$  is very high inside each grain [6]. It is very important to investigate the  $J_c$  behavior in polycrystalline bulk samples and to find out the factor which determines  $J_c$ .

High- $T_c$  oxide superconductors have some different natures, compared with the conventional superconducting materials, such as  $\text{Nb}_3\text{Sn}$  and  $\text{NbTi}$ , which have been applied for high current conductors. One of the remarkable properties of high- $T_c$  oxide superconductors is its anisotropy. Anisotropic behavior of  $J_c$  is observed in good quality thin films and the anisotropy is considered to play an important role for  $J_c$  [7], also for polycrystalline samples.

Recently, Yeshurun and Malozemoff [8] have proposed a thermally activated flux-creep model in the high- $T_c$  superconductor and Tinkham [9] extended this model to account for the experimentally measured width of the resistive transition in a magnetic field. From this point of view, the flux-creep in high- $T_c$  superconductor reduces  $J_c$  and is a severe problem for application.

In the present work, we have measured temperature and magnetic field dependence of  $J_c$  of polycrystalline  $\text{Ba}_2\text{YCu}_3\text{O}_7$  very carefully, and discussed the observed  $J_c$  behavior in correlation with the anisotropy, grain boundaries and the flux creep of this system.



## EXPERIMENTAL

$Ba_2YCu_3O_7$  samples were prepared by sintering  $BaCO_3$ ,  $Y_2O_3$  and  $CuO$  mixed powders of an appropriate composition. Starting materials were mixed in alcohol and heated at  $930^\circ C$  for 12 h in air. Such calcining processes were repeated twice, and the calcined powder was finally pressed and heated at  $950^\circ C$  for 24 h and at  $500^\circ C$  for 24 h in oxygen. Samples were in the form of a bar, 2 cm long, with a cross-sectional area of about  $2mm^2$ . Critical current was determined by the  $1 \mu/cm$  criterion.

The critical temperature of samples was determined by the ac magnetization measurement, which was done in an atmosphere of helium and by using an operating frequency of 930 Hz and an ac field of 1 Oe.

The measurement of  $J_c$  was performed using a four-terminal technique in magnetic fields ranging from 0.05 T to 1.5 T, which is calibrated by an NMR measurement. Temperature was controlled by a closed-cycle refrigerator system capable of covering the temperature range from 20 K to 300 K and monitored by Pt resistance thermometer in zero magnetic field and by Au/Au-Fe thermocouple in nonzero magnetic field. Samples were mounted on a copper block with Apiezon grease for thermal contact and with epoxy plates for electrical insulation. Moreover, the sample holder was in an atmosphere of helium which made the temperature of the sample holder uniform. Before making the electrical contacts, samples were mechanically polished and gold was deposited on the contact area. After the deposition of gold, samples were heated at  $550^\circ C$  and slowly cooled in an oxygen flow. Finally the wires were attached on gold electrode using silver paint. These processes are very important in obtaining low resistance contacts to measure  $J_c$  [10]. If electric contacts are not good, samples are heated at the current contacts and the voltage vs current (V-I) curves become quite different from those measured with a sample in liquid  $N_2$ . In the present work, we have obtained good electric contacts ( $< 10^{-4} \Omega cm^2$ ) and ensured that V-I curves were almost the same as those measured in liquid  $N_2$ .

## RESULTS AND DISCUSSION

Typical V-I characteristics of the sample at several temperatures are shown in Fig. 1. Considerably low resistance contact ( $< 10^{-4} \Omega cm^2$ ) enables us to measure  $J_c$  of samples without heating at the current contacts. Using only silver paint for electrical contacts or without Apiezon grease for thermal contact, the apparent resistance above  $J_c$  was quite larger than that measured in liquid  $N_2$ . Therefore, the good electrical contacts are indispensable to the measurement of  $J_c$  in a helium gas atmosphere.

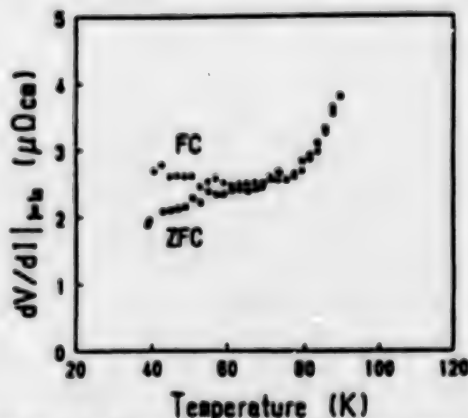
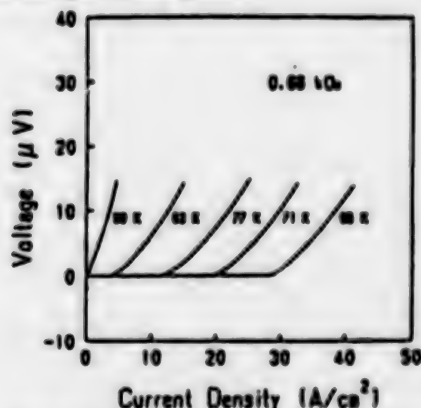


Fig. 1 Typical voltage-current (V-I) characteristics at several temperatures. Fig. 2 The slope,  $dV/dI$ , just above  $J_c$  vs temperature in the  $fc$  case and the  $zfc$  case.

The temperature dependence of the slope,  $dV/dI$ , just above  $J_c$  was shown in Fig. 2. It is seen from this figure that  $dV/dI$  begins to increase rapidly with increasing temperature above 70 K. Below 70 K,  $dV/dI$  shows almost no temperature dependence in the field cooling (fc) case and small temperature dependence in the zero field cooling (zfc) case.

Figure 3 shows the temperature dependences of  $J_c$  when samples were cooled in the magnetic field (fc) and Fig. 4 shows that when samples were cooled in zero magnetic fields and the field was applied at low temperature ( $\leq 30$  K) (zfc). The temperature dependence of  $J_c$  changes at around 70 K. From the magnetization measurement, no anomaly was observed at about 70 K and sample inhomogeneity was not the origin of this phenomenon. This phenomenon can be considered as the dimensional crossover effects which originates in anisotropy of the superconductor or the effects of grain boundaries.

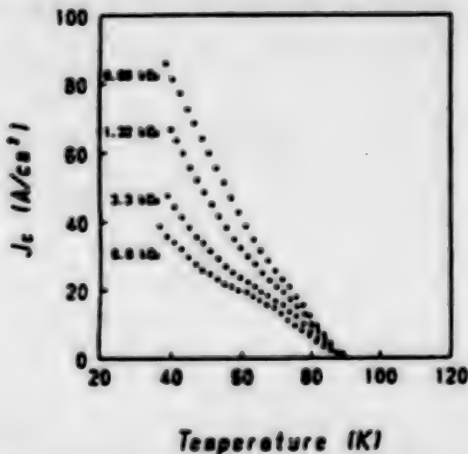


Fig. 3 Temperature dependence of  $J_c$  when the magnetic field applied in normal states (fc).

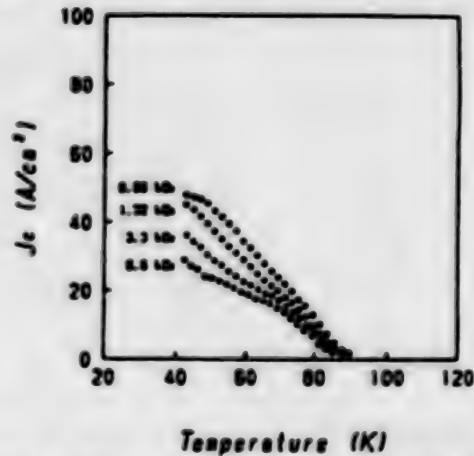


Fig. 4 Temperature dependence of  $J_c$  when the field was applied after sample was cooled in zero magnetic field (zfc).

Most remarkable thing is that the difference of temperature dependence of  $J_c$  appears between field cooling and zero-field cooling less than 70 K (see Fig. 5). Further, magnetic field dependence of the reduced temperature difference,  $1-t$ , when this irreversible behavior of  $J_c$  disappears are plotted in Fig. 6. It is seen from this figure that the reduced temperature difference when the irreversible behavior of  $J_c$  disappears is proportional to  $H^{2/3}$ .

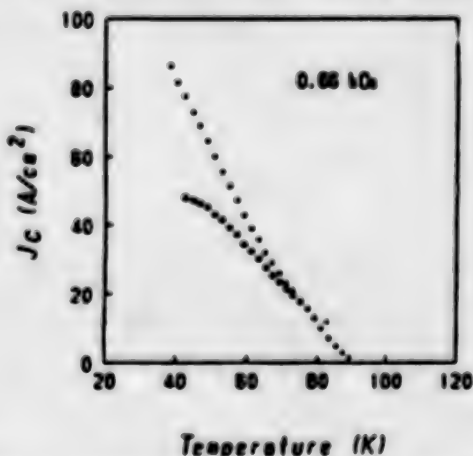


Fig. 5 Temperature dependence of  $J_c$  in 0.66 kOe.

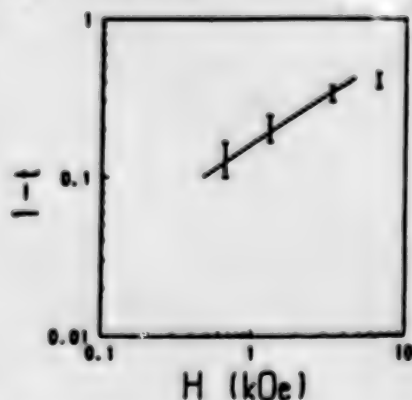


Fig. 6 Magnetic field dependence of the reduced temperature difference,  $1-t$ , when the irreversible behavior of  $J_c$  disappears. (Solid line represents the relation  $1-t \propto H^{2/3}$ .)

This magnetic field dependence of the irreversible behavior of  $J_c$  is similar to the magnetic

irreversibilities [8]. Yeshurun and Malozemoff considered that the supercurrents which can persist over the duration of an experiment give an irreversible contribution to the magnetization. Recently Matsushita et al.[11] explained a self-field of the closed intragrain currents as being a cause of history dependence of  $J_c$  in a weakly-coupled high- $T_c$  superconductor. If we can consider that the irreversible behavior of  $J_c$  comes from a self-field of the intragrain shielding currents, the correlation between the irreversible  $J_c$  behavior and the irreversible magnetization is reasonable and our experimental results confirm the model of Ref. 11.

At the present stage, however, we can not thoroughly explain the temperature dependence of  $J_c$  and further study is necessary to clarify the mechanism of  $J_c$  of high- $T_c$  oxide superconductors.

## CONCLUSION

In the present work, we have measured temperature and magnetic field dependence of  $J_c$  of polycrystalline  $Ba_2YCu_3O_7$ , very carefully and observed that the  $J_c$  behavior changes at about 70K and the irreversible behavior of  $J_c$  at low temperature. Still the mechanism of  $J_c$  is not clear, our experimental results will become a hint to clarify the mechanism of  $J_c$  in high- $T_c$  oxide superconductors.

## ACKNOWLEDGEMENT

The authors would like to express their thanks to S. Maekawa for his encouragement throughout this research and Chichibu Cement Ltd. for sample preparation.

## REFERENCES

- [1] J. G. Bednortz and K. A. Müller: Z. Phys. B64 (1986) 189.
- [2] K. Kishio, K. Kitazawa, S. Kanbe, I. Yasuda, N. Sugii, H. Takagi, S. Uchida, K. Fueki and S. Tanaka: Chem. Lett. 162 (1987) 429.
- [3] M. K. Wu, J. R. Ashburn, C. J. Torng, P. H. Hor, R. L. Hor, R. L. Meng, L. Gao, Z. J. Huang, Y. Q. Wang and C. W. Chu: Phys. Rev. Lett. 58 (1987) 908.
- [4] H. Maeda, Y. Tanaka, M. Fukutomi and T. Asano: Jpn. J. Appl. Phys. 27 (1988) L209.
- [5] Y. Enomoto, T. Murakami, M. Suzuki and K. Moriwaki: Jpn. J. Appl. Phys. 26 (1987) L1248.
- [6] H. Kumakura, M. Uehara, Y. Yoshida and K. Togano: Phys. Lett. A 124 (1987) 367.
- [7] T. Matsushita, M. Iwakuma, Y. Sudo, B. Ni, T. Kisu, K. Funaki, M. Takeo and K. Yamafuji: Jpn. J. Appl. Phys. 26 (1987) L1524.
- [8] Y. Yeshurun and A. P. Malozemoff: Phys. Rev. Lett. 60 (1988) 2202.
- [9] M. Tinkham: Phys. Rev. Lett. 61 (1983) 1658.
- [10] J. W. Ekin, A. J. Panson and B. A. Blankenship: Appl. Phys. Lett. 52 (1988) 33.
- [11] T. Matsushita, B. Ni, K. Yamafuji, K. Watanabe, K. Noto, H. Morita, H. Fujimori and Y. Muto: to be published.

# FLUX PINNING MECHANISM IN HIGH $T_c$ OXIDE SUPERCONDUCTORS

T. MATSUSHITA

KYUSHU UNIVERSITY, DEPT. OF ELECTRONICS  
6-10-1 Hakozaki, Higashi-ku, Fukuoka 812, JAPAN

## ABSTRACT

Although the critical current density in sintered ceramic superconductors is very low, that in single crystalline thin films and the local critical current density in materials prepared by the quench and melt growth technique are quite high. What kind of defective structure is the dominant pinning centers contributing to the high critical current densities? Contributions from various kinds of defects, i.e., twinning planes, grain boundaries, point defects, normal precipitates etc., are theoretically estimated. These results are compared with observed values of the critical current density.

## INTRODUCTION

Critical current density is one of the key factors for power application of superconductors. At this moment, obtained critical current density in bulk oxide superconductors is far below the level of Nb-Ti at low temperatures. However, this is mainly caused by a weak-link nature of grain boundaries in this material [1] and does not show a poor potentiality of this material. In fact, high critical current densities have been observed in single crystalline thin films [2,3]. It has also been found that the current with very high density flows locally in materials prepared by the quench and melt growth technique [4]. The bulk critical current density much smaller than this is considered to be caused by nonsuperconducting second phase layers that prevent the current from flowing uniformly. These experimental results suggest that high critical current density will be obtained even in bulk materials, if the barriers such as weak-link grain boundaries and nonsuperconducting layers are removed.

In this case, the interest will be concentrated on the dominant pinning centers that cause high critical current density. The pinning centers that seem effective are twinning planes and point defects. In this paper, contributions from these pinning centers to the critical current density are theoretically estimated. Critical current characteristics of other pinning centers are also investigated.

## THEORETICAL ESTIMATE OF $J_c$

### (a) twinning plane

Twinning planes are the defects observed commonly in 123 materials. It was clarified by the decoration technique [5] that fluxoids are distributed so as to fit the twinning planes. This experimental result proves that these planar defects are effective for flux pinning. Since the density of these defects are fairly high, their contribution to the critical current density is expected to be large. The fact that the intragrain current density is small in Bi- and Tl-systems that do not contain twinning planes supports this hypothesis.

The electron scattering mechanism [6], i.e., a variation in the coherence length due to the electron scattering by the defects, works for



flux pinning interaction through a variation of the core energy. The notable point for these planar defects is, however, that these are effective for pinning only when fluxoids parallel to them cross them [7]. In this case, the critical current density is estimated as [8]

$$J_c^{TP} = \frac{K}{(BB_{c2\perp})^{\frac{1}{2}}} \left(1 - \frac{B}{B_{c2\perp}}\right), \quad (1)$$

$$K = 1.35 \left(\frac{\sqrt{3}}{\pi}\right)^{\frac{1}{2}} \frac{A\zeta B_c^2}{\mu_0 d} \left[1 - \left(\frac{T}{T_c}\right)^2\right]^{\frac{1}{2}}, \quad (2)$$

where  $B_c$  is the thermodynamic critical field,  $B_{c2\perp}$  is the upper critical field along the c-axis,  $d$  is a mean spacing of the twinning planes and  $A\zeta$  is a constant characterizing the pinning strength of planar defects. We expect  $A\zeta \sim 0.2$  from experimental results on ordinary high-field superconductors. Similar estimation is given also by Kes et al. [9].

As for the intragrain critical current density in polycrystals with random crystalline orientation, the anisotropies in  $B_{c2}$  and flux pinning should be taken into account. The current density is derived after the average with respect to the angles of the field direction from the c-axis and the twinning plane [8].

#### (b) point defect

Many people have pointed out that point defects are effective in oxide superconductors because of their small coherence length. Although it is true that they are effective in flux pinning, they are effective also for low  $\kappa$  materials with large coherence lengths. Küpfer et al. [10] showed that the intragrain critical current density increased by a factor about 10 due to point defects nucleated by neutron irradiation. The pinning interaction energy of a point defect is estimated as  $U_p \approx (B_c^2/2\mu_0)\xi w^2$ , where  $w$  is a size of the defect [11]. Hence, the elementary pinning force is approximately given by  $f_p \approx U_p/\xi \approx (B_c^2/2\mu_0)w^2$ . Since  $w$  is usually very small, their strength  $f_p$  is also small. Hence, these are effective when their volume density is so high that these work collectively.

We treat the case where the mean spacing of the point defects  $d_p$  is much smaller than the fluxoid spacing  $a_f$ . Then, the number of pins in a coherent region of a fluxoid of a length  $4\pi a_f$  is approximately  $n_p = 4\pi a_f^3 N_p$ , with  $N_p$  denoting the concentration of the defects,  $1/d_p^3$ . The pinning strength of the defects in the coherent region is of the order of  $\sqrt{n_p} f_p$ . From a statistical summation [12] we have

$$J_c^{PD} = \beta \frac{\sqrt{n_p} f_p}{4\pi a_f^3 B} = \left(\frac{N_p}{4\pi a_f^3}\right)^{\frac{1}{2}} \frac{\beta B_c^2 w^2}{2\mu_0 B} \quad (3)$$

at low fields, where  $\beta$  is a constant of the order of 0.5.

#### (c) grain boundary

Grain boundaries are known to cause a percolative characteristic of

the current because of their weak-link nature. But this is only for the boundaries normal to the direction of the transport current. The boundaries parallel both to the fluxoids and the transport current, which are perpendicular to the direction of the Lorentz force, work as pinning centers. Hence, the grain boundaries are expected to contribute to the intragrain current density. This contribution through the electron scattering mechanism is given by eqs. (1) and (2), where the grain size is substituted into  $d$ . There exists another contribution through the anisotropy in  $B_{c2}$  and it is discussed in Ref. 13.

(d) normal precipitate

Precipitates of  $Y_2BaCuO_5$  phase are found to distribute in specimens prepared by the quench and melt growth technique [4, 14]. Normal and insulating precipitates are known as strong pinning centers. When their size is much larger than the fluxoid spacing  $a_f$ , the critical current density due to these precipitates can be estimated from [15]

$$J_c^P = \frac{\pi B_c^2 \xi}{4\mu_0 B a_f} S_v, \quad (4)$$

where  $S_v$  is the effective surface area of precipitates in a unit volume of the superconductor, i.e.,  $S_v = N_p D^2$  with  $D$  denoting the size of precipitates.

(e) porosity

Porosities also contribute to the flux pinning through the same mechanism with insulating precipitates. Hence, eq. (4) is applicable for porosities.

(f) thickness modulation in thin film

If the thickness of film varies along the direction of fluxoid motion, the fluxoid suffers a variation in the energy when it moves. This gives rise to flux pinning interaction. The critical current density due to this interaction is given by

$$J_c^{TM} = \frac{B_c^2}{8\mu_0 d} \left( \frac{\sqrt{3}\pi}{B_{c2} B} \right)^{\frac{1}{2}} \frac{\delta t}{t}, \quad (5)$$

where  $\delta t/t$  is a rate of thickness modulation and  $d$  is a mean wave length of this modulation. The idea to use cracks in a thin films as strong pinning centers [16] originates from the same mechanism.

## DISCUSSION

Here we mainly discuss quantitatively the critical current density due to twinning planes and point defects.

First, we discuss the flux pinning by twinning planes. Most thin films have oriented  $c$ -axis normal to the film surface. Hence, twinning planes probably pin the fluxoids, when the magnetic field is applied normal to the film surface. The theoretical result from eqs. (1) and (2)

gives the estimate comparable to experiments (see Ref. 8). Thin films of Bi- and Tl-systems have only small critical current densities in this field geometry [17]. This will be attributed to the absence of twinning planes. In the field parallel to the film surface, the surface pinning is considered to work. The intragrain current density in ceramics can also be explained quantitatively by the pinning due to twinning planes.

Küpfer et al. [10] showed that the intragrain current density is increased up to about  $3 \times 10^9$  A/m<sup>2</sup> at  $T = 77$  K and  $B = 2$  T by nucleating point defects by neutron irradiation. Since this value is more than ten times as large as the original intragrain current density, it can be mainly attributed to the pinning by point defects. These pinning centers are isotropic and we use the mean coherence length  $\xi \sim (\xi_x^2 \xi_z)^{1/3} = 3.7 \times 10^{-9}$  m. If we assume that  $w \sim \xi/2$  and  $d_p = 6.3 \times 10^{-9}$  m, the observed intragrain current density can be explained by eq. (3). Since the pin density assumed here is quite high, it seems to be reasonable that the degradation in  $T_c$  occurs for higher neutron fluence. Hence, the above value seems to be the maximum of  $J_c$  by point defects.

## REFERENCES

- 1) D. Dimos, P. Chaudhari, J. Mannhart and F. K. LeGoues: Phys. Rev. Lett. 61 (1988) 219.
- 2) Y. Enomoto, T. Murakami, M. Suzuki and K. Moriwaki: Jpn. J. Appl. Phys. 26 (1987) L1248.
- 3) S. Tanaka and H. Itozaki: Jpn. J. Appl. Phys. 27 (1988) L622.
- 4) T. Matsushita, B. Ni, M. Murakami, M. Morita, K. Miyamoto, M. Saga and S. Matsuda: submitted to Phys. Rev. B.
- 5) L. Ya. Vinnikov, L. A. Gurevich, G. A. Yemelchenko and Yu. A. Ossipyan: Solid State Commun. 67 (1988) 421.
- 6) See, for example, G. Zerweck: J. Low Temp. Phys. 42 (1981) 1.
- 7) A. DasGupta, C. C. Koch, D. M. Kroeger and Y. T. Chou: Philos. Mag. B 38 (1978) 367.
- 8) T. Matsushita and B. Ni: to be published in IEEE Trans. Magn. MAG-25 (1989).
- 9) P. H. Kes, A. Pruymboom, J. van den Berg and J. A. Mydosh: to be published in Cryogenics 29 (1988).
- 10) H. Küpfer, I. Apfelstedt, R. Flükiger, C. Keller, R. Meier-Hirmer, B. Runtzsch, A. Turowski, U. Wiech and T. Wolf: to be published in Cryogenics 29 (1988).
- 11) E. V. Thuneberg, J. Kurkijärvi and D. Rainer: Phys. Rev. B 29 (1984) 3913.
- 12) T. Matsushita: Jpn. J. Appl. Phys. 20 (1981) 1153.
- 13) T. Matsushita, M. Iwakuma, Y. Sudo, B. Ni, T. Kisu, K. Funaki, M. Takeo and K. Yamafuji: Jpn. J. Appl. Phys. 26 (1987) L1524.
- 14) M. Murakami, M. Morita, K. Miyamoto and S. Matsuda: to be published in Proc. of Osaka Univ. Int. Symp. on New Developments in Applied Superconductivity, Suita, 1988.
- 15) T. Matsushita: Jpn. J. Appl. Phys. 20 (1981) 1955.
- 16) T. Matsushita: Jpn. J. Appl. Phys. 27 (1988) L1712.
- 17) H. Itozaki, K. Higaki, K. Harada, S. Tanaka, N. Fujimori and S. Yazu: to be published in Proc. 1st Int. Symp. on Superconductivity, Nagoya, 1988.

## WEAK LINKS IN HIGH $T_c$ SUPERCONDUCTORS

M. WAKATA, S. MIYASHITA, K. EGAWA, H. HIGUMA, T. OGAWA, K. YOSHIKAZI,  
MITSUBISHI ELECTRIC CORP., MATERIALS & ELECTRONIC DEVICES LAB.  
1-1-57 MIYASHIMO, SAGAMIHARA, KANAGAWA 229, JAPAN  
S. YOKOYAMA, K. SHIMOHATA, M. MORITA AND T. YAMADA  
MITSUBISHI ELECTRIC CORP., CENTRAL RESEARCH LAB.  
8-1-1 TSUKAGUCHI-HONMACHI, AMAGASAKI, HYOGO 661, JAPAN

### ABSTRACT

Our studies on the weak links in high  $T_c$  superconductors are reviewed. For Y-Ba-Cu-O system the V-I characteristics up to a high current region measured by using the pulsed currents and the magnetization properties are shown. It is found the type of the weak links in this system is that of S-N-S or S-S'-S junctions. For Bi-Pb-Sr-Ca-Cu-O system the origin of the weak links is the superconducting phase with  $T_c$  of 90-100K.

### INTRODUCTION

The critical current densities for the sintered samples of oxide superconductors are much lower and have stronger field dependence than those for the single-crystal like films because of the existence of the weak links. The evidences of weak links are reported by many researchers, for example, the discrepancy between the transport and the magnetization  $J_c$ 's [1], the existence of a low resistive state above the  $I_c$  [2], the direct measurements of intra- and inter-grain  $J_c$ 's [3] and so on.

In this paper we review our studies on the weak-links in high temperature superconductors. We have also observed a low resistive state above the  $I_c$  so measured the V-I characteristics up to much higher current region and found two-step transition [4,5]. Furthermore, we have observed the complicated structure in magnetization curves at lower field than 100 Oe [6]. From such measurements it can be estimated that the weak links in  $YBa_2Cu_3O_{7-y}$  are S-N-S or S-S'-S type.

In Bi-Pb-Sr-Ca-Cu-O system the temperature and the field dependence of the susceptibility are measured [7]. It is found that the superconducting phase with  $T_c$  of 90-100K should be responsible for the weak links.

### WEAK LINKS IN $YBa_2Cu_3O_{7-y}$

Figure 1 shows the V-I characteristic at 53K for the  $YBa_2Cu_3O_{7-y}$  thin film with the  $T_c$  of 60K prepared by sputtering. Two-step transition is clearly seen. Above the critical current,  $I_{c1}$ , the linear relation between the voltage and the current holds in a wide range of the current. The resistivity defined by the slope,  $\rho_1$ , is lower than the normal state resistivity,  $\rho_n$ . Above the current,  $I_{c2}$ , which is one order higher than  $I_{c1}$ , the voltage is abruptly increased as increasing current and finally, the normal state appears. This behavior should be considered as follows: Above the  $I_{c1}$  ( $J_{c1}$ ), which is the critical current (density) restricted by the weak-links, the superconducting coupling among the high  $J_c$  regions disappears. Therefore, the weak link regions become normal state, nevertheless, the high  $J_c$  regions hold their superconductivity. Above the  $I_{c2}$  ( $J_{c2}$ ) the transition to the normal state begins in the high  $J_c$  regions.



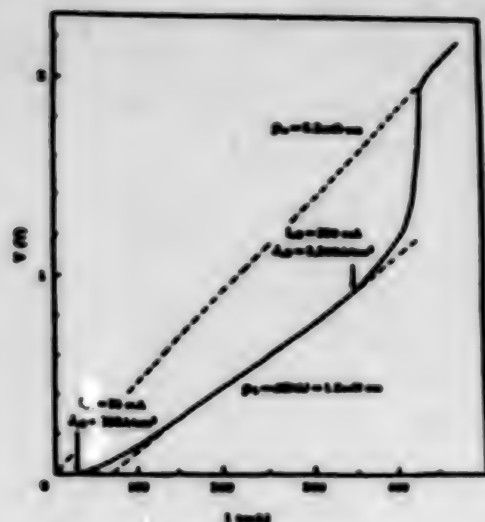


Fig. 1 The V-I characteristic at 53K of the  $\text{YBa}_2\text{Cu}_3\text{O}_{7-y}$  thin film with the  $T_c$  of 60K prepared by sputtering.

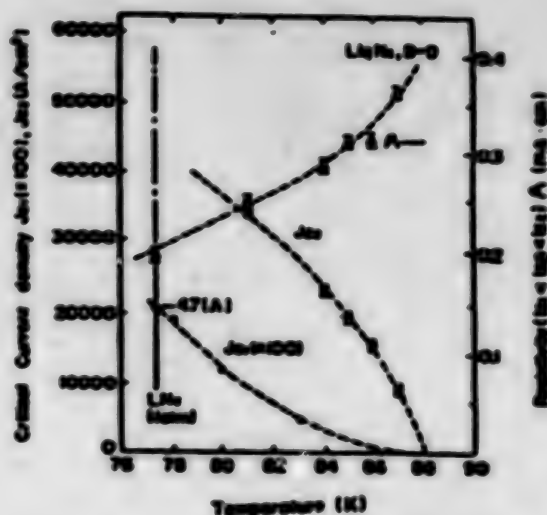


Fig. 2 The temperature dependence of the  $J_{c1}$ , the  $J_{c2}$  and the  $p_1$  for the sintered  $\text{YBa}_2\text{Cu}_3\text{O}_{7-y}$  measured by pulsed currents.

This V-I characteristic is measured in He gas by using DC current so that the quantitative reliability is open to question because of the ohmic heat generated especially, at the current contacts. Then we have tried such measurements in liquid  $\text{N}_2$  by using pulsed current. The temperature can be controlled by changing the pressure.

Figure 2 shows the temperature dependence of the  $J_{c1}$ , the  $J_{c2}$  and the  $p_1$  for the sintered  $\text{YBa}_2\text{Cu}_3\text{O}_{7-y}$  with the  $p_0$  of about  $1.4 \text{ m}\Omega\text{cm}$ . Apparently the temperature dependences of the  $J_{c1}$  is different from that of the  $J_{c2}$ . On the other hand the resistivity,  $p_1$ , is decreased as decreasing temperature, which indicates the type of weak links in this sample is not that of S-I-S junctions but maybe that of S-N-S or S-S'-S junctions.

We have found two kinds of minima or maxima in the magnetization of the sintered  $\text{YBa}_2\text{Cu}_3\text{O}_{7-y}$  samples. At 77K one is at about 0.005 T and the other at about 0.03 T. It was thought that this was related with the existence of the weak links in the samples, so the transport current dependence of the magnetization was measured. The bar shaped sample with the  $I_c$  of 6 A at 77K is used for the measurement. The DC transport current,  $I_T$ , and the field is parallel to the direction of the sample length.

Figure 3 shows the results of the measurements in the field range of  $\pm 0.04 \text{ T}$  (a) and  $\pm 0.15 \text{ T}$  (b). As shown in Fig. 3(a) the hysteresis of the magnetization is decreased as increasing  $I_T$  up to the  $I_c$ . Above the  $I_c$  the minimum at the low field (about 0.005 T) is vanished and magnetization curve becomes independent of  $I_T$  at least up to several times of  $I_c$ . In higher field magnetization as shown in Fig. 3(b) the transport current affects only field range of about  $\pm 0.06 \text{ T}$  but the minimum at about 0.03 T does not change.

These results suggest that there are two kinds of current paths in this sample, one is the current which flows over whole range of the sample and the other is inside each high  $J_c$  regions. In fact, the critical current density calculated from the hysteresis of the magnetization,  $\Delta M p_1(I_T=0A) - \Delta M p_1(I_T > I_c)$  has the similar value to the  $J_{c1}$ . Furthermore, the critical current density calculated from the hysteresis at higher field than 0.06 T has the same order as the  $J_{c2}$  if the mean size of high  $J_c$  regions is assumed to be the same as the mean grain size, which is about  $10 \mu\text{m}$ .

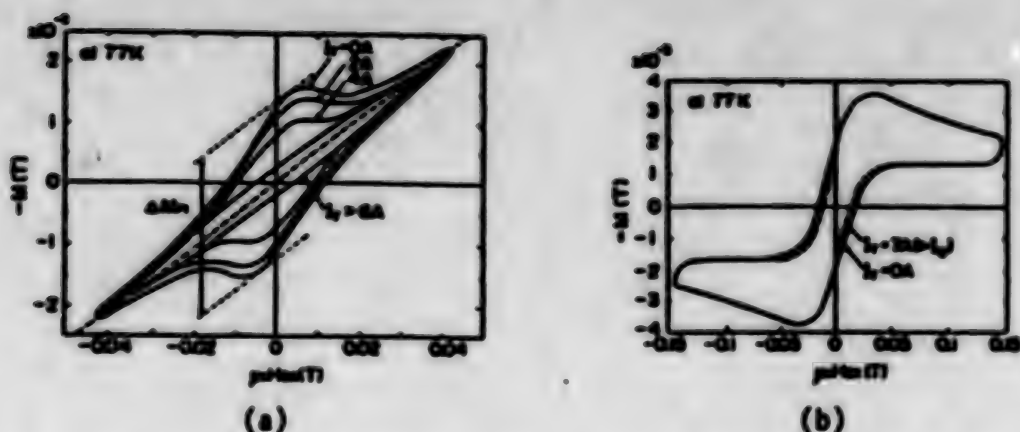


Fig. 3 The magnetization curves at 77K for the sintered  $\text{YBa}_2\text{Cu}_3\text{O}_{7-y}$  in the field range of  $\pm 0.04$  T (a) and  $\pm 0.15$  T (b).

#### WEAK LINKS IN Bi-Pb-Sr-Ca-Cu-O SYSTEM

In this study we used two sintered samples. The sample 1 has the nominal composition of  $\text{Bi}_{1.7}\text{Pb}_{0.3}\text{SrCaCu}_3\text{O}_y$  and is sintered at  $845^\circ\text{C}$  for 240hr in air. The temperature dependence of the resistivity and the susceptibility shows sharp transition about 110K. However, the X-Ray diffraction analysis (XD) reveals that the sample consists of 110K and 80K phases. The  $T_c(\mu=0)$  is 107K. The  $J_c$  at 77K is  $93 \text{ A/cm}^2$  at zero field and exponentially decreased as increasing the field. Therefore, it was thought that the  $J_c$  was also restricted by the weak links in this system like in Y-Ba-Cu-O system. So the V-I characteristic and the transport current dependence of the susceptibility were measured as follows: The sample was inserted into a solenoid coil, the DC current was supplied to the sample at 77K and the sample voltage and the inductance of the coil were measured. The results are shown in Fig. 4.

In the V-I curve the linear relation is appeared in higher current range than 6 A. The resistivity,  $\rho_l$ , defined by the slope is one order lower than the normal state resistivity,  $\rho_n(77\text{K})$ , which is obtained by the linear extrapolation of the temperature dependence of the resistivity. Meanwhile, the inductance of the coil is abruptly increased near  $I_c$  and saturated in the low resistive state. However, the value is still lower than the inductance of the coil without the sample.

Figure 5(a) shows the temperature dependence of the susceptibility measured by the same method as in Fig. 4, where the coil voltage, V, is varied from 0.01 to 5 V. The V of 0.01 V corresponds to the field of about 0.5 Oe at 90K. As shown in this figure the transition is sharp when the V is 0.01 V. However, when the V is 0.1 V two-step transition is clearly seen. Compared with the transition by 110K phase the onset temperature is decreased and the width is abruptly spread as increasing the V in the second transition.

Figure 5(b) shows the results of the same kind of measurements for the pelletized powder obtained by grinding the sample 1. The transition by 80K phase, which is not seen in the sintered sample is clearly seen in this figure, which coincides with the results by XD. Therefore, it can be said that 80K phase exists covered with 110K phase in the sample 1. Furthermore, two-step transition as seen in Fig. 5(a) can not seen in this pelletized powder. So another superconducting phase as seen in Fig. 5(a) when  $V > 0.1\text{V}$  should be responsible to the weak links in this sample.

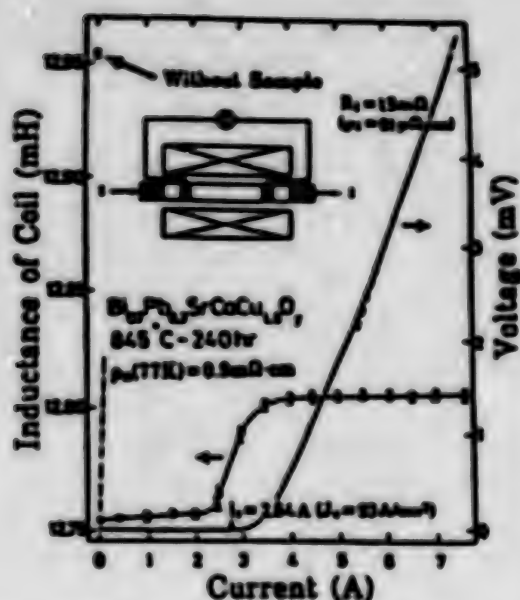


Fig. 4 The V-I and the L-I characteristics for the sample 1 at 77K.

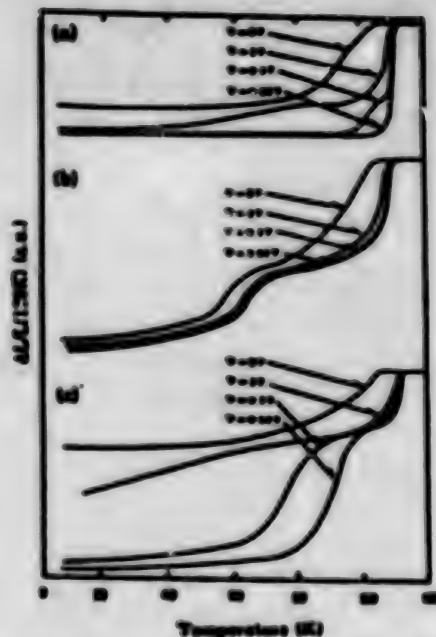


Fig. 5 The temperature and the field dependence of the susceptibility for the sample 1 (a), the pressed powder obtained by grinding the sample 1 (b) and the sample 2 (c).

The existence of the superconducting phase with the  $T_c$  of 90 to 100K is confirmed in many samples. For example, the sample 2 has the nominal composition of  $\text{BiPb}_{0.2}\text{SrCaCu}_2\text{O}_y$  sintered at  $840^\circ\text{C}$  for 50hr in  $\text{N}_2\text{-7.5}\%\text{O}_2$  flowing gas mixture. In the XRD pattern all the main peaks correspond to those for 110K phase and other weak peaks to those for 80K phase. However, as shown in Fig. 5(c) the temperature dependence of the susceptibility reveals the existence of two superconducting phases with  $T_c$  of 110 and about 100K even if the  $V$  is 0.01V. The field dependence as shown in Fig. 5(c) is almost the same as in Fig. 5(a) except  $V=0.01$  V. This superconducting phase has the same structure as 110K phase or amorphous like one.

## CONCLUSIONS

In this study we have found that the weak links in the  $\text{YBa}_2\text{Cu}_3\text{O}_y$  are S-N-S or S-S'-S type and those in Bi-Pb-Sr-Ca-Cu-O system are the superconducting phase with  $T_c$  of 90-100K. Further investigations are needed to achieve higher  $J_c$  by removing such weak links.

## REFERENCES

- [1] K. Funaki et al: Jpn. J. Appl. Phys. Lett. 26 (1987) L1445
- [2] J. W. Ekin et al: J. Appl. Phys. 62 (1987) 4825
- [3] J. Mannhart et al: Phys. Rev. Lett. 61 (1988) 2476
- [4] M. Wakata et al: 5th Seminar on Frontier Technology (1988) Shuzenji
- [5] K. Shimohata et al: Proc. Int. Work Shop at Osaka Univ. (1988)
- [6] S. Yokoyama et al: Proc. ISS'88 (1988) Nagoya
- [7] S. Miyashita et al: Proc. ASC'88 (1988) San Francisco



STUDY OF THE MAGNETIC LOSS  
IN THE COPPER-OXIDE BASED SUPERCONDUCTORS  
BY COMPLEX SUSCEPTIBILITY MEASUREMENT

A. MAEDA and K. UCHINOKURA

DEPARTMENT OF APPLIED PHYSICS, FACULTY OF ENGINEERING,  
THE UNIVERSITY OF TOKYO  
HONGO 7-3-1, BUNKYO-KU, TOKYO 113, JAPAN

ABSTRACT

Magnetic loss in the copper-oxide based ceramic superconductors was studied by ac susceptibility measurement. This method is a useful tool for the characterization of the nature of grain boundaries, and thus can be used for the study of critical current and that of the preparation of high-quality samples. Two examples of the study of the ac magnetic susceptibility are shown for the preparation of high-quality samples; one is the preparation of  $\text{LaBa}_2\text{Cu}_3\text{O}_y$  and the other is that of  $(\text{Bi,Pb})_2\text{Sr}_2\text{Ca}_2\text{Cu}_3\text{O}_y$ .

INTRODUCTION

Critical current density  $J_C$  is the most important parameter for the application of superconductors. Especially, in the case of polycrystalline samples, critical current is restricted by that of weak links between superconducting grains (intergrain  $J_C$  or transport  $J_C$ ), which is a few orders of magnitude smaller than the so-called intragrain  $J_C$ , which is determined by the pinning force of magnetic flux in the mixed state of type-II superconductors. The effort of the improvement of intergrain  $J_C$  is important not only for the application but also for the basic research with ceramic samples, because preparation of the high-quality samples is crucial for obtaining reliable data on physical and chemical properties.

It is well known in ceramic superconductors that the real part of ac magnetic susceptibility around zero magnetic field strongly depends on the amplitude of the alternating magnetic field below some temperature  $T_0$ , which is lower than the superconducting onset transition temperature  $T_C$ . And the imaginary part becomes large just below  $T_0$ . This behavior of ac magnetic susceptibility was well explained by the weak-link formation model[1]. Thus, it is possible to estimate the nature of grain boundaries in ceramic superconductors by ac susceptibility measurements. In this paper, we will show examples of the studies on the preparation of high-quality samples using ac magnetic susceptibilities performed on two materials, and propose that the complex susceptibility measurement is a useful tool for the study of transport  $J_C$  in ceramic superconductors. The materials used in this study are  $\text{LaBa}_2\text{Cu}_3\text{O}_y$ , which is important from the application point of view and  $(\text{Bi,Pb})_2\text{Sr}_2\text{Ca}_2\text{Cu}_3\text{O}_y$ , which has importance also from the basic research of the understanding of the mechanism of high- $T_C$  superconductors.

EXPERIMENTALS



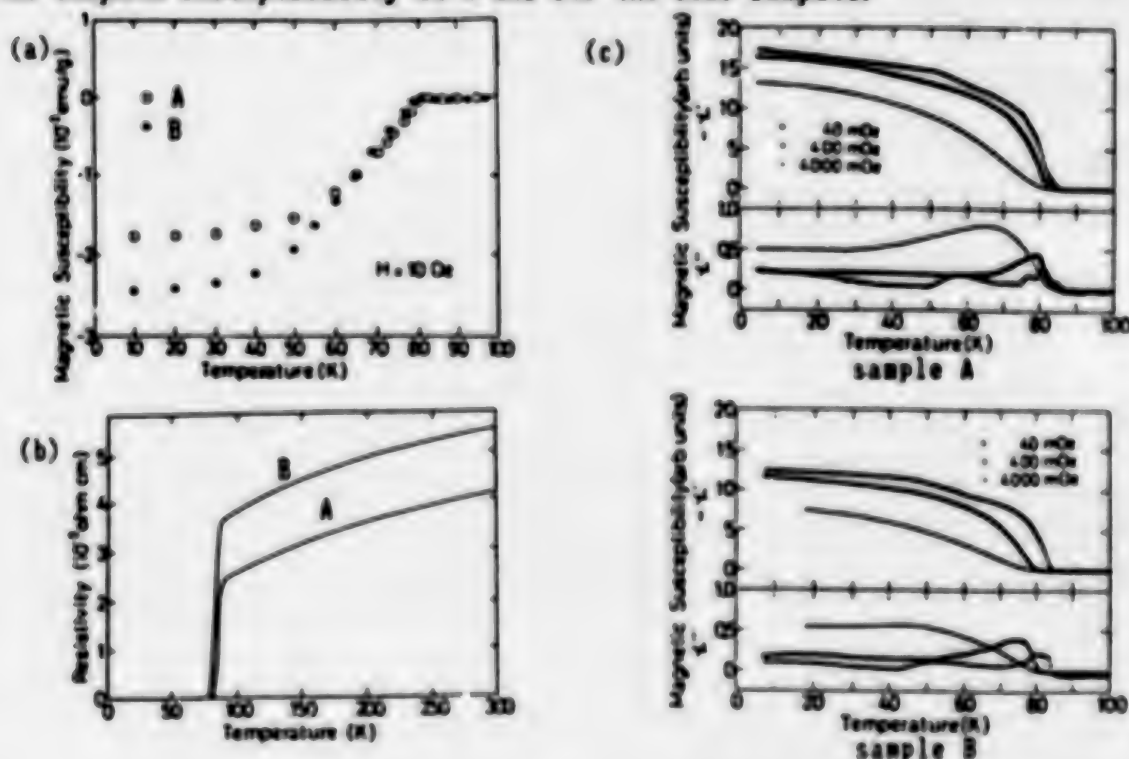
Samples were prepared by an ordinary solid-state reaction method using the starting materials of oxide, carbonate, or nitrate powders. Details are published in separate papers[2,3]. Samples were characterized by powder X-ray diffraction technique, dc resistivity measurement, dc susceptibility measurement with SQUID magnetometer, and complex susceptibility measurement. Complex susceptibility measurement was performed by measuring the temperature dependence of complex impedance of a small solenoid including samples.

## RESULTS AND DISCUSSION

### (1) 1-2-3 compounds ( $\text{LaBa}_2\text{Cu}_3\text{O}_y$ )

The so-called 1-2-3 material  $\text{LaBa}_2\text{Cu}_3\text{O}_y$  ( $\text{La}=\text{Y}$ , rare earth elements)[4] is a 90 K superconductor. Especially,  $\text{LaBa}_2\text{Cu}_3\text{O}_y$  attracts much attention from application point of view because of the low cost of La. However, preparation of good crystals had been difficult, partly because of the special reason for this material and partly because of the common reason for 1-2-3 materials. That is, for the synthesis of high-quality 1-2-3 materials, sufficient annealing by oxygen at low temperature is necessary. In fact, at the initial stage, annealing around at 300 K was successful to form the 90 K superconducting phase in this material[5]. However, there are some reports that low-temperature annealing sometimes degrades the superconducting characteristics[6]. Sometimes we also found a similar situation. Thus, some other factors have to be overcome. Here, it should be noted that superconducting properties in polycrystalline samples are determined both by those of the bulk and the grain boundaries. Especially, the latter is closely related with the intergrain  $J_C$  (transport  $J_C$ ). Figure 1(a) shows the bulk superconducting properties measured

Figure 1 (a) The temperature dependence of the dc magnetic susceptibility of  $\text{LaBa}_2\text{Cu}_3\text{O}_y$  samples sintered at 1050 C in  $\text{N}_2$  for 12 h and post annealed in  $\text{O}_2$  for different time (A; 20 h, B; 74 h). (b) The temperature dependence of dc resistivity for the same samples. (c) The temperature dependence of the complex susceptibility at 2 kHz for the same samples.

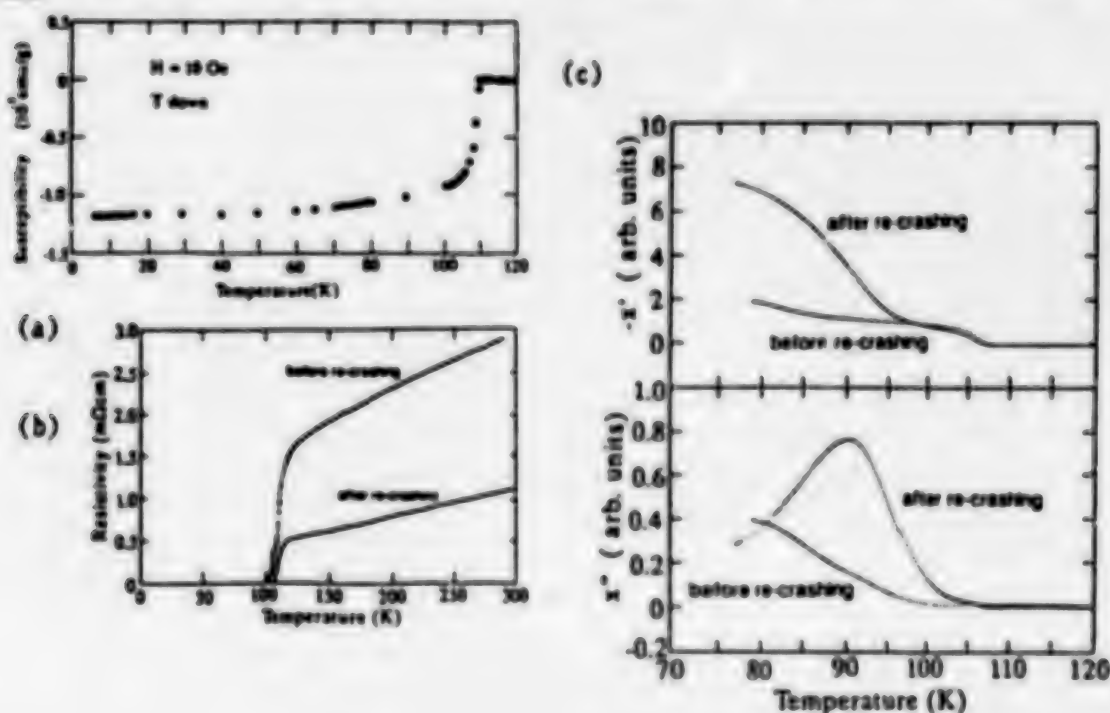


by the dc SQUID magnetometer (Meissner-effect) for  $N_2$ -sintered samples of  $LaBa_2Cu_3O_7$ , which were post-annealed in  $O_2$  for different time. This figure clearly shows that the introduction of oxygen surely improves the bulk superconducting properties. On the other hand, superconducting properties measured in resistivity (Fig. 1(b)) shows that the superconducting characteristics were degraded by the annealing. Thus, we should ascribe the origin of the degradation of superconducting characteristics to that of grain boundaries. This can be observed much more easily in complex susceptibility around zero magnetic field (Fig. 1(c)). The magnitude of  $\chi''$  decreases with increasing annealing time. The structure in  $\chi''$  becomes much broader and the peak moves to the lower temperature. All of these behaviors can be ascribed to the destruction of the weak links at the grain boundaries. This degradation is probably due to the water included in the oxygen gas flowing in the annealing process. In fact, the introduction of the dry oxygen gas during the annealing process led to the synthesis of a sample which has zero-resistance at 92 K[7]. The extreme improvement was also confirmed by the ac susceptibility measurement.

(2)  $(Bi,Pb)_2Sr_2Ca_2Cu_3O_y$  (2-2-2-3 phase)

$Bi_2Sr_2Ca_2Cu_3O_y$  is a member of the group which has the highest  $T_C$ [8], and contains the triple  $CuO_2$  layers in the unit cell[9]. Although one year has passed since the discovery of this material, there are few reliable data of the physical properties of this material, which is due to the difficulty in preparation of high-quality single-phase samples. Recently, Takano et al.[10], and subsequently Endo et al.[11] showed that the introduction of Pb and sintering in low oxygen partial pressure produce good single-phase samples in a well-reproducible way. We also succeeded in obtaining almost single-phase samples with almost complete Meissner effect by using essentially the same method. However, the temperature dependence of the resistivity has a small tail at  $T_C$ , as is shown in Fig. 2(b). The

Figure 2 (a) The temperature dependence of the dc magnetic susceptibility at 10 Oe for  $(Bi,Pb)_2Sr_2Ca_2Cu_3O_y$ . (b) The temperature dependence of the dc resistivity of the same sample. (A; before and B; after the treatment described in the text). (c) The temperature dependence of the ac complex susceptibility at 2 kHz for the same samples. Amplitude was fixed at 4 Oe.



reason for this mysterious behavior seem to be the increase of porosity due to the volume expansion during sintering process, which is easily confirmed by the ac susceptibility measurement as shown in Fig. 2(b). Loss structure in the imaginary part remains finite down to liquid nitrogen temperature, which demonstrates that the coupling of the superconducting grains is extremely weak despite the large volume fraction of superconducting phase. Thus, the pellet was re-crashed, pressed again and sintered at slightly lower temperatures (820-830 C) for a couple of hours. This treatment removes the tail in the temperature dependence of the resistivity and also decreases the magnitude of the resistivity by a factor of 3-4. As a result, high-quality single-phase 2-2-2-3 superconducting polycrystals with the resistivity of 1.1 (0.6) m cm at 300 K (130 K) was obtained. The improvement by the above-mentioned treatment is also due to the increase of the Josephson coupling among superconducting grains, which is clearly seen in Fig. 2(c).

From the above results, it can be said that the zero-field complex magnetic susceptibility measurement is useful to characterize the nature of grain boundaries. Although resistivity also reflects the superconducting characteristics at grain boundaries, it will give no further information once it drops to zero. On the other hand, complex susceptibility can measure the degree of strength of the intergrain coupling continuously, even in zero resistance state. Thus, it will become a simple, but useful tool for the study of the transport critical current density of ceramic superconductors, or superconducting wires.

#### REFERENCES

- [1] For example, T. Ishida et al., Jpn. J. Appl. Phys. 26, L1296 (1987).
- [2] A. Maeda et al., J. Appl. Phys. 64, 4095 (1988).
- [3] A. Maeda et al., to be submitted.
- [4] M. K. Wu et al., Phys. Rev. Lett. 58, 908 (1987).
- [5] A. Maeda et al., Jpn. J. Appl. Phys. 26, L1368 (1987).
- [6] For example, K. Kishio et al., in Materials Research Society Symposium Proceedings Vol. 99, High-Temperature Superconductors Symposium, Nov. 30-Dec. 4, 1987, Boston, ed. by M. B. Brodsky, R. C. Dynes, K. Kitazawa, and H. L. Tuller (Materials Research Society, Pittsburg, PA), p33.
- [7] T. Wada et al., Appl. Phys. Lett. 52, 1989 (1988).
- [8] H. Maeda et al., Jpn. J. Appl. Phys. 27, L209 (1988).
- [9] E. Takayama-Muromachi et al., Jpn. J. Appl. Phys. 27, L556 (1988).
- [10] M. Takano et al., Jpn. J. Appl. Phys. 27, L1041 (1988).
- [11] U. Endo et al., Jpn. J. Appl. Phys. 27, L1476 (1988).

## MAGNETIZATION AND CRITICAL CURRENT OF YBCO AND BSCCO MATERIALS

D. ITO, E. SHIMIZU and M. KOIZUMI  
TOSHIBA R&D CENTER, TOSHIBA CORPORATION,  
4-1. Ōkushima-cho, Kawasaki-ku, Kawasaki, 210, Japan

### ABSTRACT

Magnetization properties have been measured for YBCO powders and BSCCO single crystals. Current flows in YBCO are limited by grain boundaries for both Meissner current and bulk current. Critical current in BSCCO single crystals, in a temperature region above 20K, has a strong inverse anisotropy compared with that for YBCO. This result suggests that the pinning centers in BSCCO are different from those in YBCO.

### INTRODUCTION

Important superconducting parameters  $T_c$  and  $B_{c2}$  are both determined by 'chemistry' of a materials, whereas  $J_c$  is determined by its microstructure.

In order to reveal current flow performance in high  $T_c$  superconductor, magnetization properties have been measured for YBaCuO powders and BiSrCaCuO single crystals.

### EXPERIMENTAL

$YBa_2Cu_3O_{7-\delta}$  powders calcined in air, with average particle diameters ranging from 3 to 53  $\mu m$ , were used as YBCO sample. Raw material was made using a coprecipitated method.

Temperature dependence of magnetization for YBCO powders was obtained with a SQUID magnetometer. Most magnetization measurements for powder samples were carried out with D.C. magnetization measurement systems, which have two coaxial search coils in a back up field coil. The powder samples were packed in the form of a hollow cylinder.

Single crystals of  $Bi_2(Sr,Ca)_2Cu_2O_{10}$  were grown by a self-flux method, as described previously[1]. A plate-like crystal, with 0.3 x 1.25 x 1.5 mm average dimensions, was used in the present study. The magnetization measurements for BSCCO single crystals were performed using the SQUID magnetometer in the temperature range from 5K to near  $T_c$ , in an up to 5T magnetic field with the field direction parallel or perpendicular to the a-b plane for the single crystal sample.

### RESULTS AND DISCUSSION

#### Magnetization of YBCO powders

##### 1. $B < B_{c1}$

Figure 1 shows the temperature dependence of magnetization for different sizes of YBCO powders. These data were obtained in a 20 gauss field under zero field cooling condition.

This result indicates that the critical temperature,  $T_c$ , value for these samples is 93 K. However, a small amount of low  $T_c$  phase magnetization, ortho II phase, whose  $T_c$  is approximately 60K[2], is superimposed on the curves. Therefore, 93K phase is covered by 60K phase.



Magnetization decreasing rate  $P(d,\lambda)$ , as a function of powder diameter  $d$  and penetration depth  $\lambda$ , can be explained as follows

$$P(d,\lambda) = 1 - \frac{2\lambda(T)}{d/2} \coth\left(\frac{d/2}{\lambda(T)}\right) + 3 \cdot \left(\frac{\lambda(T)}{d/2}\right)^2 \quad (1)$$

where the  $\lambda$  value depends on temperature, as follows.

$$\lambda(T) = \lambda_0 / (1 - t^4)^{1/2} \quad (2)$$

Temperature dependence of magnetization for the YBCO powders, normalized by 4.2 K magnetization and  $T_c$ , respectively, are shown in Fig. 2. Solid line curves indicate calculated values for  $d/2\lambda$ , where  $\lambda_0$  is a penetration depth at 0 K. The calculated magnetizations, in the  $T/T_c > 0$  temperature region, increase with increasing powder size. On the other hand, experimentally obtained magnetization saturate over  $19 \mu\text{m}$  powder size. These results indicate that the Meissner current flow in the YBCO powder is limited by some barriers in the region whose dimensions are approximately  $20 \mu\text{m}$ . It will be shown, in the following, that these barriers are caused by grain boundaries.

## 2. B>Bc1

Magnetization loop width  $\Delta M$  can be explained, based on the Bean model, as follows.

$$\Delta M = \frac{\mu_0 d J_c}{2} \quad (3)$$

where  $\mu_0$  is permeability in a vacuum and  $d$  is the mean diameter, for individual powder particles. Average  $J_c$  values for individual particles can be derived from the slope of the  $\Delta M$  versus the powder diameter relationship.

Figure 3 shows the  $\Delta M$  dependence on powder size at 4.2 K for 0.3 T, 0.5 T and 0.8 T. The magnetization at 4.2 K for every field measured is in linear proportion to particle size over the  $1\text{--}20 \mu\text{m}$  range and saturates at above  $20 \mu\text{m}$ . The  $J_c$  value, derived from Eq. (1), is approximately  $2 \times 10^6 \text{ A/cm}^2$  at 4.2 K, 0.3 T from the slope in the linear relationship.

Figure 4 shows the  $\Delta M$  dependence on powder size at 77 K for 0.03 T, 0.1 T and 0.3 T. The magnetization at 77 K for every field measured is also in linear proportion to the powder size over the  $1\text{--}20 \mu\text{m}$  range and saturates at above  $20 \mu\text{m}$ .  $J_c$  at 77 K is obtained as approximately  $7 \times 10^5 \text{ A/cm}^2$  at 0.03 T.

These  $J_c$  values are almost the same or somewhat larger, compared with  $J_c$  values for the single crystal [3].

The magnetization saturation indicates that major magnetization current cannot flow through boundaries on a  $20 \mu\text{m}$  wide region.

Estimated grain size in YBCO suggests that individual particles, whose average powder sizes are smaller than  $20 \mu\text{m}$ , are made of a single crystal or its fragment. On the other hand, each particle, whose powder size is larger than  $20 \mu\text{m}$ , seems to be made of several grains. Therefore, the magnetization saturation can be explained with a model wherein current flow over the  $20 \mu\text{m}$  range is limited by grain boundaries.

## Magnetization of BSCCO single crystals

Figure 5 show the Meissner effect for single crystal  $\text{Bi}_{2.2}(\text{Sr,Ca})_{2.6}\text{Cu}_2\text{O}_y$  in low perpendicular magnetic field. A superconducting transition was observed at 80 K. The same transition temperature was obtained under the parallel magnetic field.

Figures 6(a) and 6(b) show typical magnetization curves for the BSCCO single crystal at 5K temperature in parallel and perpendicular fields, respectively. In comparison with the two curves, no strong anisotropy in the magnetization curves to field direction was observed at this temperature. A similar result was also obtained by Lin, et al[4]. However, in a higher temperature region above 20K, the anisotropy appeared in the critical current densities, as shown in Fig.7.

Critical current density  $J_c$  values were determined from the magnetization curves, using a simple relation between  $J_c$  and magnetization,  $J_c = 30 \Delta M / r$  ( $J_c$  in  $A/cm^2$ ,  $\Delta M$  in  $emu/cm^3$ ,  $r$  in  $cm$ ), where  $\Delta M$  is the width of a magnetization curve, and  $r$  is the radius of a disk sample.

The anisotropy in Fig.7 shows that the  $J_c$  value, obtained under a field parallel to the a-b plane of the single crystal, is higher than that for the perpendicular field. This result is contrary to the anisotropic behavior for YBaCuO [3].

Inverse anisotropy in critical current suggests that pinning centers are different between YBCO and BSCCO. The pinning center in BSCCO might be due to micro-cleavage surface along the a-b plane.

## CONCLUSION

In summary, Meissner and bulk current flows, which are responsible to magnetization, are limited in the  $20 \mu m$  range by grain boundaries in YBCO.

Critical current values for YBCO, obtained from the slope in the linear relationship between magnetization and powder size, are approximately  $2 \times 10^6 A/cm^2$  at 4.2 K and 0.3 T, and approximately  $7 \times 10^4 A/cm^2$  at 77 K and 0.03 T.

Critical current in a BSCCO single crystal has strong anisotropy. The anisotropy is opposite to the anisotropy for YBCO. These results indicate important information concerning the origin of the pinning centers in high  $T_c$  superconductors.

## REFERENCES

- [1] S. Nomura, T. Yamashita, H. Yoshino, and K. Ando, Proc. Int. Supercon. Soc., Nagoya, (1988).
- [2] M. Tokumoto, H. Ihara, T. Matubara, Jpn. J. Appl. Phys. 26, L1565 (1987).
- [3] T.R. Dinger, T.K. Worthington, W.J. Gallagher and R.J. Sandstrom, Phys. Rev. Lett. 58, 2687 (1987).
- [4] J.J. Lin, E.L. Benitez, S.J. Poon, M.A. Subramanian, J. Gopalakrishnan, and A.W. Sleight, Phys. Rev. B38, (7), 5095 (1988).

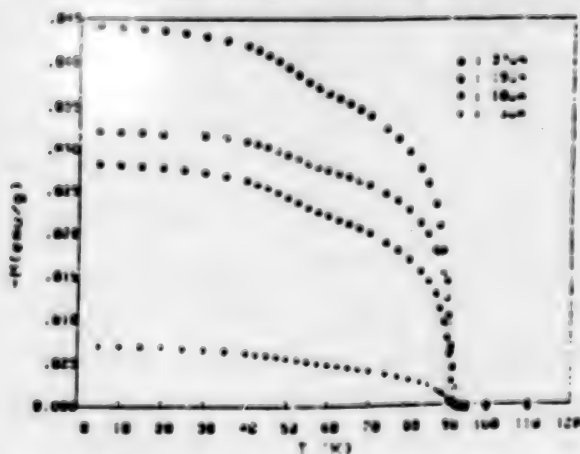


Fig.1 Magnetization temperature dependence for YBCO powders.

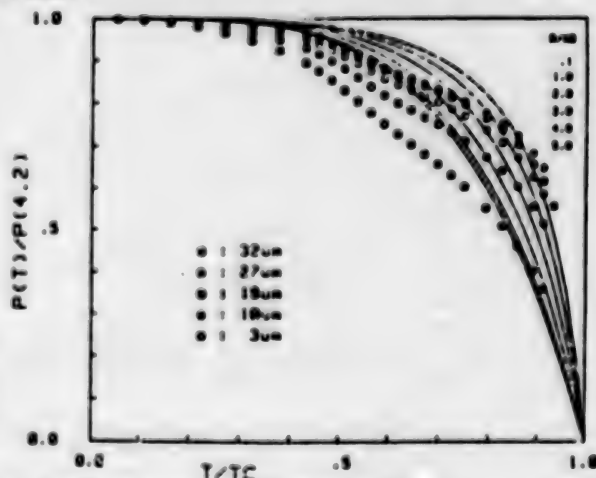


Fig.2 Normalized magnetization temperature dependence for YBCO powders.

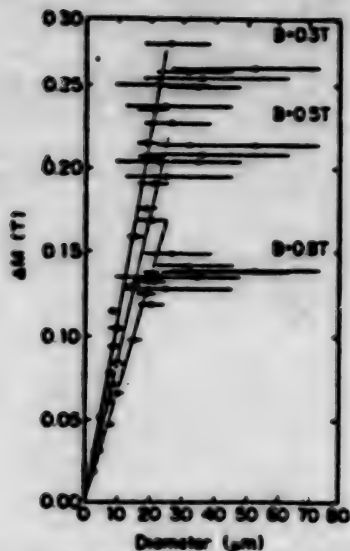


FIG. 3. Magnetization powder diameter dependence at 4.2 K. Horizontal bar cover diameter distribution from  $D^{25}$  to  $D^{75}$  and central points show  $D^{50}$ .

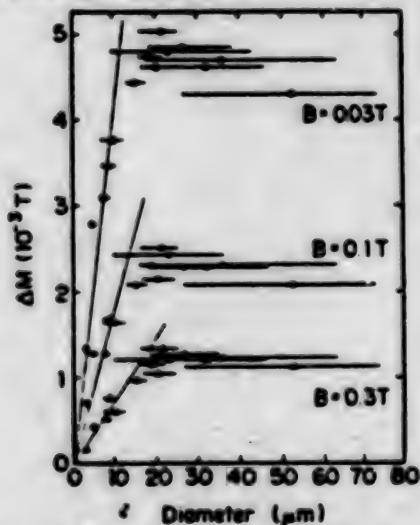


FIG. 4. Magnetization powder diameter dependence at 77 K. Horizontal bars cover diameter distribution, from  $D^{25}$  to  $D^{75}$ , and central points show  $D^{50}$ .

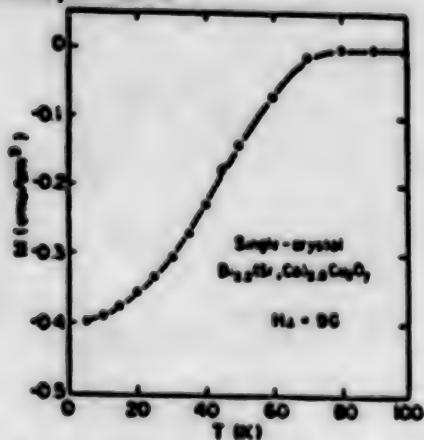


Fig. 5 Meissner effect for single-crystal  $\text{Bi}_{2.2}(\text{Sr},\text{Ca})_{2.6}\text{Cu}_2\text{O}_y$  in low perpendicular field.

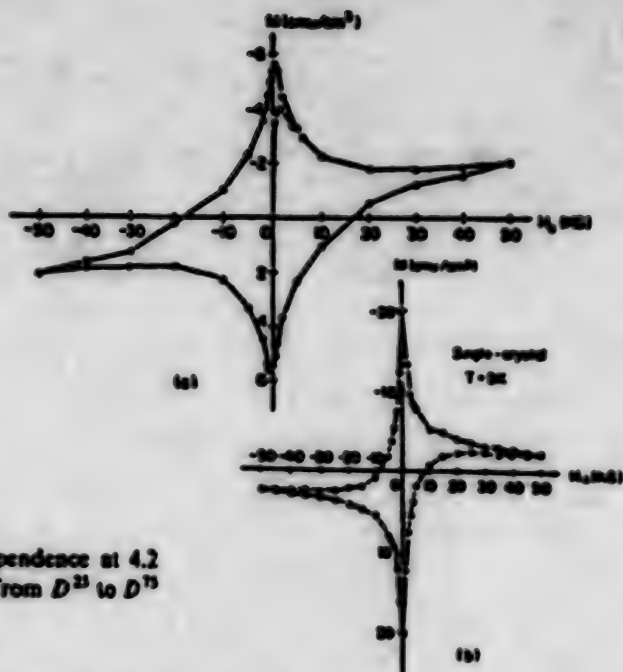


Fig. 6 Typical magnetization curves for single crystal BSCCO at 5K. (a) In a parallel field. (b) In a perpendicular field.

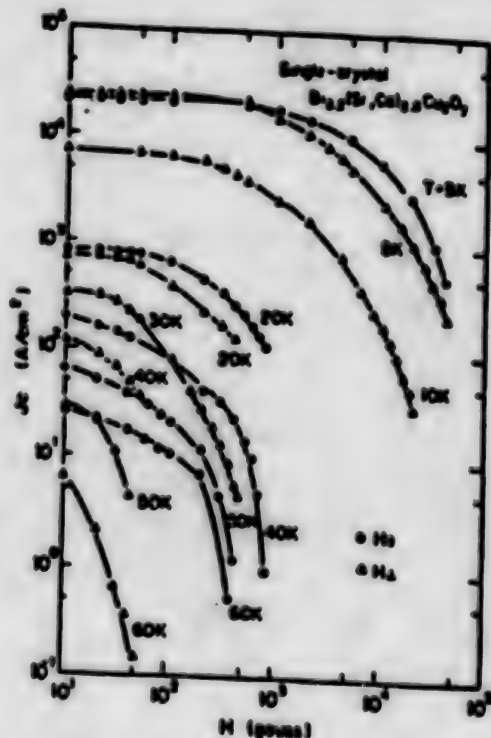


Fig. 7 Magnetic field dependence of critical current for single-crystal  $\text{Bi}_{2.2}(\text{Sr},\text{Ca})_{2.6}\text{Cu}_2\text{O}_y$ .

# CRITICAL CURRENT AND FLUX CREEP IN YBaCuO PREPARED BY THE QUENCH AND MELT GROWTH TECHNIQUE

Masato MURAKAMI, Mitsuru MORITA, and Katsuyoshi MIYAMOTO

R & D Laboratories-I, Nippon Steel Corporation  
1618 Ida, Nakahara-ku, Kawasaki 211 Japan

## ABSTRACT

Critical current density ( $J_c$ ) of bulk sintered oxide superconductors is fairly small due to the presence of weak-link networks along grain boundaries. The quench and melt growth (QMG) process, which consists of quenching from molten oxide region and subsequent reheating and slow cooling, enables unidirectional growth of a superconducting phase and elimination of weak-links from bulk samples and transport  $J_c$  exceeding  $10^5$  A/cm<sup>2</sup> is attained at 77K and 10T. Magnetization measurements revealed that the QMG processed samples obey Bean critical state model and yield  $J_c$  value exceeding  $10^5$  A/cm<sup>2</sup> at 77K and 1T. Flux creep measurements on such samples also revealed that giant flux creep is not inherent to oxide superconductors even when they are used at 77K.

## INTRODUCTION

Critical current density ( $J_c$ ) is the most important property for practical applications of the superconductors. Unfortunately, in spite of tremendous efforts,  $J_c$  values of bulk sintered oxide superconductors remain low presumably due to the presence of weak-links and a strong anisotropy in  $J_c$ .

The first breakthrough has been accomplished by Jin et al.[1] who employed so-called melt-textured growth process to fabricate YBaCuO with highly oriented structure and achieved  $J_c$  value of 4000 A/cm<sup>2</sup> at 77K and 1T.

Recently we have also developed the quench and melt growth (QMG) process which enables elimination of weak-links from bulk samples[2]. The QMG process consists of quenching from  $Y_2O_3$  + liquid region and subsequent reheating to  $Y_2BaCuO_5$  + liquid region followed by slow cooling in flowing oxygen. If thermal gradient technique is used in the last step, unidirectional growth of the superconducting phase takes place. In the samples fabricated by the QMG process, fairly high  $J_c$  values are attainable even in the presence of a significant magnetic field.

In this paper, we summarize the QMG process and then report some results of magnetization and flux creep measurements for the QMG processed YBaCuO samples.

## THE QMG PROCESS

In order to reduce the weak-links in bulk oxide superconductors, it is desirable to fabricate YBaCuO with large elongated grains aligned perpendicular to the C axis. A solidification process seems to be best for achieving this. However, microstructural observation[3] revealed that the connectivity of superconducting phases is quite poor in solidified samples. It is known[4] that a  $(Ba_2Cu_3O_{7-x})$  phase (123) is produced by peritectic solidification of a  $(Y_2BaCuO_5 + 211)$  phase. Therefore how the 211 phases are distributed in a liquid is a key parameter to determine the connectivity of the 123 phases. The desired precursor microstructure is the





Fig. 1 Optical micrograph of microstructure of the QMG processed sample.

one with the 211 phases finely and homogeneously dispersed in the liquid. However, it becomes clear that it is difficult to refine the 211 phases within 211 + L region. It also becomes clear[5] that the 211 phases are not stable above 1200 C and melt incongruently into  $Y_2O_3$  and liquid. To obtain the microstructure with finely distributed 211 phases, we have to start from  $Y_2O_3$  + L region. However, in this region  $Y_2O_3$  tends to agglomerate resulting in inhomogeneous distribution of the 211 phases. The reaction of the melt with crucible materials is also severe. To overcome these problems we employed rapid heating to  $Y_2O_3$  + L region and subsequent quenching which is effective to avoid coarsening of  $Y_2O_3$  and to minimize the contamination from crucible materials. By reheating the quenched materials in 211 + L region, the 211 phases are produced by peritectic solidification. It is also possible to connect precursor quenched materials and to fabricate desired shapes at this stage. If we slow cool the material with thermal gradient in flowing oxygen, we can obtain the specimen oriented to a-b direction as shown in Fig. 1.

## CRITICAL CURRENT

### Transport $J_c$

First we measured  $J_c$  of the QMG processed samples by the standard four probe method using  $1 \mu V/cm$  criterion. Electric currents were applied along growth direction. Typical results are presented in Fig. 2.  $J_c$  exceeding  $1000 A/cm^2$  was obtained at 77K and 10T, which is dramatically high compared to those of sintered bulk samples. However, we noticed that the sample becomes normal due to heat generation from electric contacts[2]. Small dependence of  $J_c$  on magnetic field is also evidence for this. Therefore we need reduce contact resistance to obtain real  $J_c$ . This result also suggests that even higher  $J_c$  is obtainable in the QMG processed samples.

### Magnetic $J_c$

It is also possible to determine  $J_c$  through magnetization measurements. The contact resistance problem can be neglected in this method. However, in bulk sintered material where the difference in magnetization( $\Delta M$ ) is almost independent of sample size,  $J_c$  cannot be estimated from  $\Delta M$ . Fig. 3 shows the relationships between  $\Delta M$  and sample thickness( $d$ ) at various magnetic fields for the QMG processed sample. Straight lines can be obtained, indicating that the sample obeys Bean critical state model. Under such a condition,  $J_c$  can be related to  $\Delta M$ . In the case of flat long sheet with thickness  $d$  in parallel magnetic field,

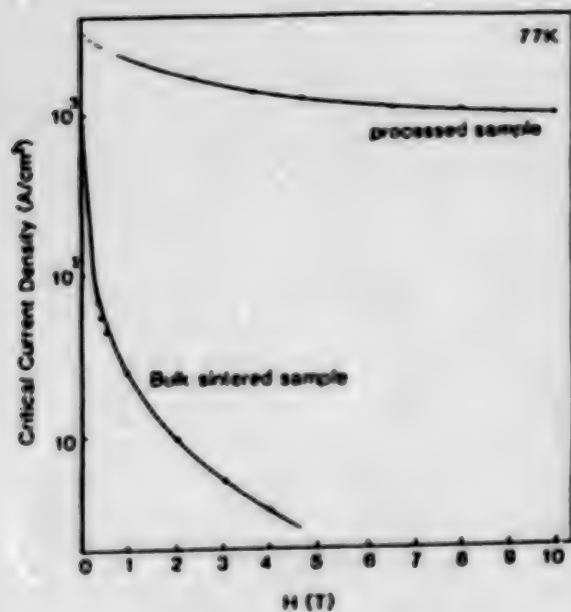


Fig. 2. Magnetic field dependence of  $J_c$  for the QMG processed sample.

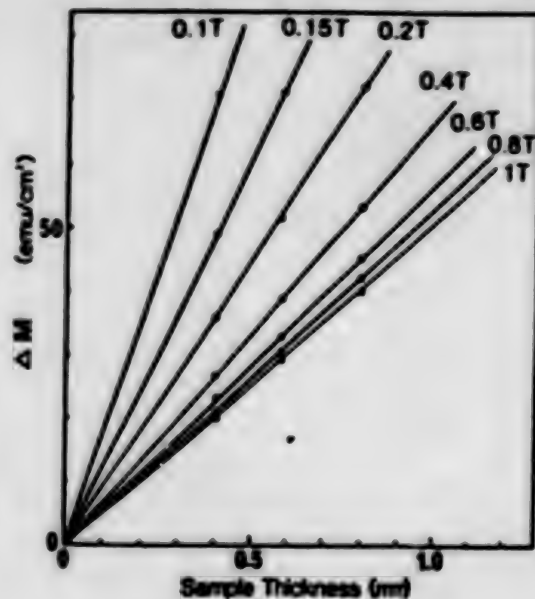


Fig. 3. Relationship between  $\Delta M$  and  $d$  for the QMG processed sample.

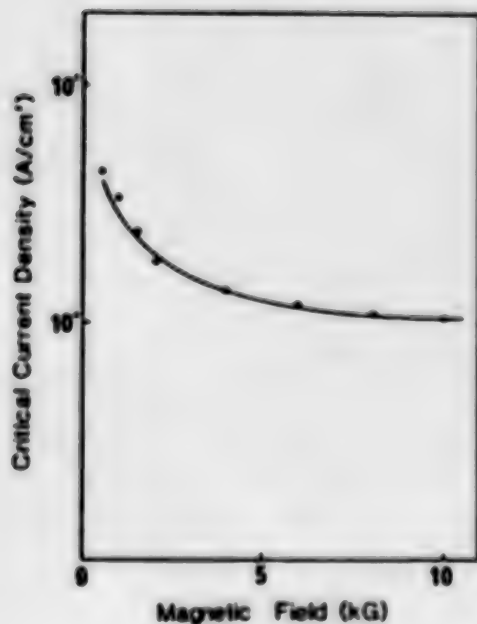


Fig. 4. Magnetic field dependence of  $J_c$  estimated from  $\Delta M$ .

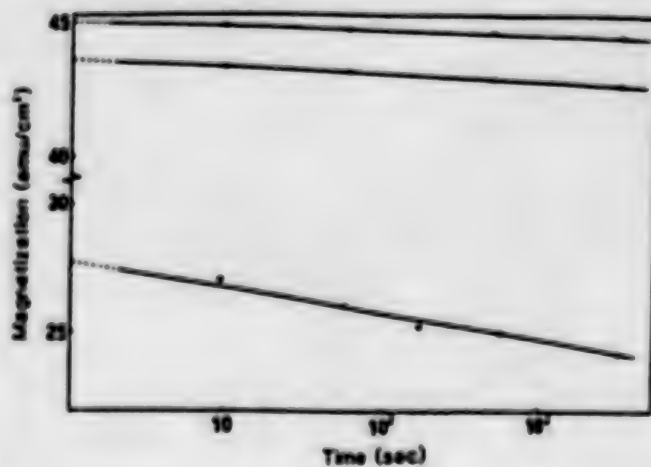


Fig. 5. Relaxation of the remnant magnetization as a function of time.

the following equation can be obtained to a first approximation(in cgs units):

$$4\pi (M^+ - M^-) = (8\pi/c) (4/d) J_c$$

If we take the unit as  $M$  in  $\text{emu/cm}^3$ ,  $d$  in  $\text{cm}$ , and  $J_c$  in  $\text{A/cm}^2$ ,  $J_c$  can be estimated from the following equation:

$$J_c = 20 (\Delta M / d)$$

Magnetic field dependence of  $J_c$  thus estimated is presented in Fig. 4.  $J_c$  exceeding  $10^4 \text{ A/cm}^2$  is achievable at 77K and 1T, which poses a strong potentiality of oxide superconductors for applications at 77K.

### FLUX CREEP

Recently flux creep has been considered to be a serious problem when oxide superconductors are used at 77K[6]. In type II superconductors, magnetic fluxoids are trapped in pinning sites, however, at temperature  $T(K)$  fluxoids diffuse by thermal activation with the diffusivity proportional to  $\exp(-U_0/kT)$ , where  $U_0$  is the pinning potential. In the conventional superconductors, the effect of flux creep can be neglected because they are used at fairly low temperature(4.2K). On the other hand at 77K, where oxides are to be used, thermal component  $kT$  becomes fairly large(0.006eV). Along with large  $kT$ ,  $U_0$  of oxide superconductors seems to be small due to small coherence length, which results in small  $U_0/kT$  thereby giant flux creep[6].

However, it is also true that  $U_0$  can be enhanced by the introduction of pinning points[7]. The QMG processed YBaCuO samples exhibit high  $J_c$  in magnetic field indicating that strong pinning points exist. Therefore we conducted flux creep measurements using a vibrating sample magnetometer. External field was increased up to 1000G and then rapidly reduced to zero and then relaxation of the remnant magnetization was monitored. Typical results for three samples with different  $J_c$ 's are shown in Fig. 5. The sample with higher  $J_c$  exhibited smaller relaxation. In the best sample, flux creep rate is fairly slow indicating that giant flux creep is not inherent to oxide superconductors.

### CONCLUSIONS

The QMG process is effective to fabricate YBaCuO with high  $J_c$ , in which Bean critical state is established. Magnetization measurements revealed that  $J_c$  values exceeding  $10^4 \text{ A/cm}^2$  are achievable in the QMG processed samples at 77K and 1T. Giant flux creep is not observed in such samples.

### REFERENCES

- [1] S. Jin, T. H. Tiefel, R. C. Sherwood, R. B. van Dover, M. E. Davis, G. W. Kammlott, and R. A. Fastnacht: *Phys. Rev. B.*, 37 (1988) 7850.
- [2] M. Murakami, M. Morita, and K. Miyamoto: *Proc. of Osaka University International Symposium*, Osaka, 1988, to be published.
- [3] M. Murakami and M. Morita: *Proc. of MRS meeting*, Tokyo, 1988, to be published.
- [4] e. g. S. Takekawa and N. Iyi: *Jpn. J. Appl. Phys.* 26 (1988) L 851.
- [5] M. Murakami, M. Morita, K. Doi, K. Miyamoto and H. Hamada: submitted to *Jpn. J. Appl. Phys.*
- [6] Y. Yeshurun and A. P. Malozemoff: *Phys. Rev. Lett.*, 60 (1988) 2202.
- [7] M. Suenaga: *Proc. of MRS Meeting*, Tokyo, 1988, to be published.

## HIGH $J_c$ BiSrCaCuO AND TlBaCaCuO SUPERCONDUCTING THIN FILM

H. ITOZAKI, S. TANAKA, K. HIGAKI, & HARADA, S. YAZU and K. TADA  
Sumitomo Electric Industries Ltd.  
1-1 Koyakita 1-Chome Itami 664 JAPAN

### ABSTRACT

BiSrCaCuO and TlBaCaCuO thin film were grown on MgO substrate by an RF magnetron sputtering. Their  $J_c$  were 3.4 MA/cm<sup>2</sup> and 3.2 MA/cm<sup>2</sup>, respectively. Anisotropic degradation of  $J_c$  by magnetic field was observed. X-ray, RHEED and SEM observation showed that these high  $J_c$  thin film were c-axis oriented poly-crystalline. Grain boundaries and stacking faults may act as pinning places of a magnetic flux.

### INTRODUCTION

Since the discovery of high  $T_c$  superconducting materials(1,2), many studies have been done in the field of thin film. High  $T_c$  superconducting thin film has a big potential in electronics, for sensors(3) or high speed devices(4). The authors have studied epitaxial growth of a HoBaCuO thin film, and have gotten a single crystal thin film which had  $J_c$  of 3.5 MA/cm<sup>2</sup>(5,6). Recently BiSrCaCuO and TlBaCaCuO which have higher  $T_c$  than LnBaCuO were reported(7,8). The authors have obtained high  $J_c$  superconducting thin films of BiSrCaCuO and TlBaCaCuO. Here we will report the preparation conditions of these high  $J_c$  superconducting thin films and their properties.

### EXPERIMENTAL

Films have been prepared by rf magnetron sputtering with a single target. The target was prepared by sintering mixed power of BaCO<sub>3</sub>, CaO, Bi<sub>2</sub>O<sub>3</sub>, Tl<sub>2</sub>O<sub>3</sub> and CuO for each system. A substrate was MgO single crystal. The glow discharge was radio-frequency excited (13.56 MHz) under 80% Ar and 20% oxygen atmosphere. The substrates were heated at 350 to 800°C. The films were annealed at 800 to 950°C. In the case of TlBaCaCuO films, the substrate temperature were kept at 350°C and the films were annealed in a sealed tube containing Tl<sub>2</sub>O<sub>3</sub>, because of a high vapor pressure of Tl compound. The temperature dependence of the film resistivity and the critical current densities were measured by a four-probe method in a cryostat. For these measurements, an annealed thin film was etched with a diluted HCl (0.5 vol%) solution to form a narrow region with an area of about 20  $\mu$ m in length and 20  $\mu$ m in width. The structure and morphology were analyzed by X-ray diffraction (XRD), reflection high-energy electron diffraction (RHEED), scanning electron microscopy (SEM).

### EXPERIMENTAL RESULTS AND DISCUSSIONS

#### 1. BiSrCaCuO Thin Film

A BiSrCaCuO thin film was prepared by the rf magnetron sputtering with a single target(9). An X-ray diffraction pattern of the BiSrCaCuO



thin film is shown Fig.1. It indicates that the film is c-axis textured and is composed of a single 2223 high  $T_c$  phase with  $c=37.2\text{\AA}$ . As a RHEED pattern shows fine rings, this thin film is c-axis textured polycrystalline.

The temperature dependence of critical current density is shown in Fig.2. One film has the  $J_c$  of  $1.9\text{ MA/cm}^2$  at  $77.3\text{K}$  and that of  $21\text{ MA/cm}^2$  at  $40\text{K}$ . The another film has  $3.4\text{ MA/cm}^2$  at  $77.3\text{K}$ .

The magnetic field dependence of critical current density at  $77.3\text{K}$  was also investigated. As the applied magnetic field increases, the  $J_c$  decreases as shown in Fig. 3. Degradation of  $J_c$  depends on the direction of the applied field to the substrate and to the direction of the current flow. If the current flows parallel to the magnetic field, no Lorentz force comes out and  $J_c$  should not be affected by the magnetic field. But Fig. 3 shows that degradation in this case has occurred. This indicates that the film has many obstacles to current flow and the actual current passes in a zigzag pattern. Therefore the magnetic flux accumulates force and degradation of the  $J_c$  occurs. As this film is polycrystalline, many grain boundaries may act as obstacles. In the other cases where the current and the magnetic field are perpendicular to each other, degradation is larger than the above case. Comparing the two cases (b) and (c) in the fig. 3, degradation of (c) is larger than that of (b). Magnetic flux which is parallel to the surface is pinned stronger than those which are perpendicular to the surface. The magnetic flux may be pinned at grain boundaries or stacking faults, which are mainly located parallel to the surface.  $J_c$  becomes  $0.26\text{ MA/cm}^2$  under the magnetic field of even  $0.5\text{ tesla}$  at  $77.3\text{K}$ . This degradation is much larger than that of a  $\text{HoBaCuO}$  thin film which can sustain more than  $1.5\text{ MA/cm}^2$  under the magnetic field of  $1\text{ tesla}$ .

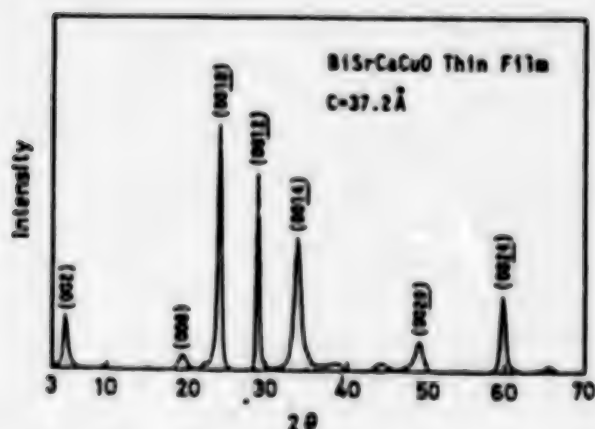


Fig.1 X-ray diffraction of BiSrCaCuO thin film

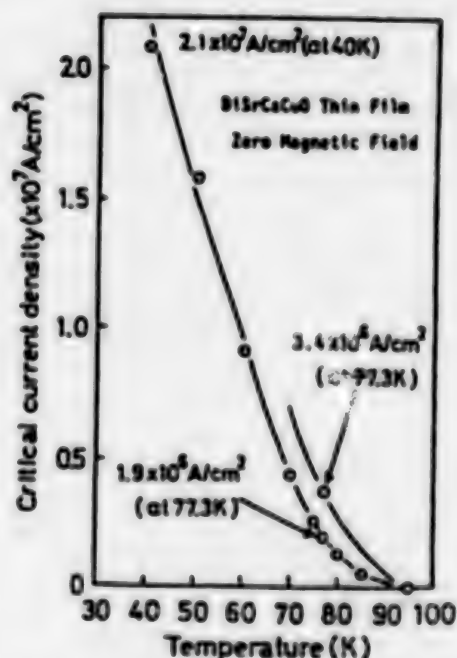


Fig.2 Temperature dependence of  $J_c$  for BiSrCaCuO thin film

## 2. TlBaCaCuO Thin Film

A TlBaCaCuO thin film was also prepared by the sputtering(10). As thallium is volatile, the film is deposited without heating the substrate. This film was post-annealed around 900°C in oxygen and thallium vapor. X-ray patterns of the as-grown film and the post annealed film are shown in Fig.4. The as-grown film is amorphous, and the post annealed film is c-axis textured polycrystalline. The superconducting transition of

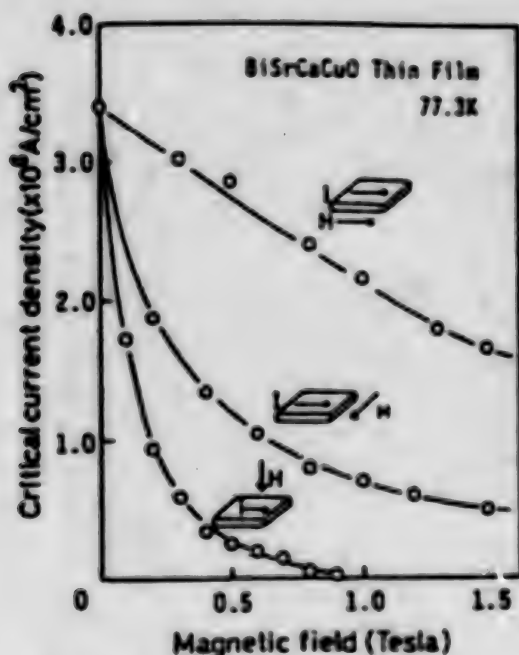


Fig.3 Magnetic field dependence of  $J_c$  for BiSrCaCuO thin film

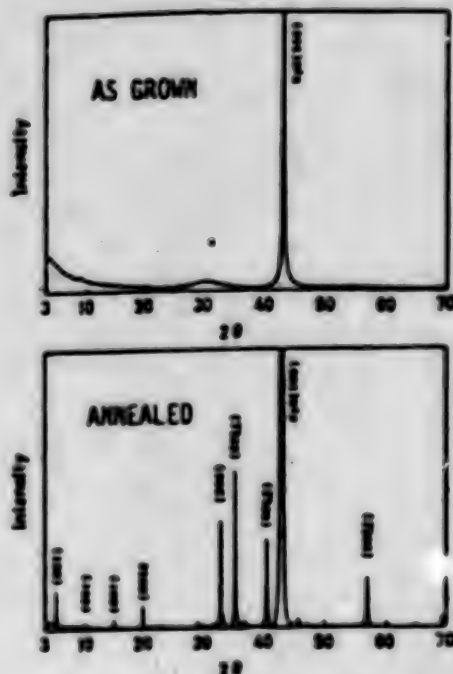


Fig.4 X-ray diffraction of TlBaCaCuO thin film

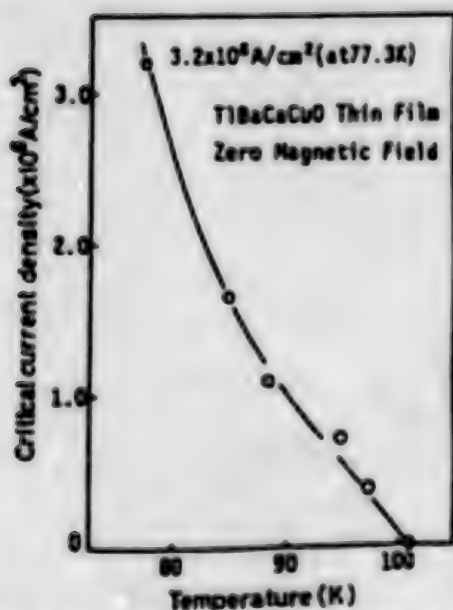


Fig.5 Temperature dependence of  $J_c$  for TlBaCaCuO thin film

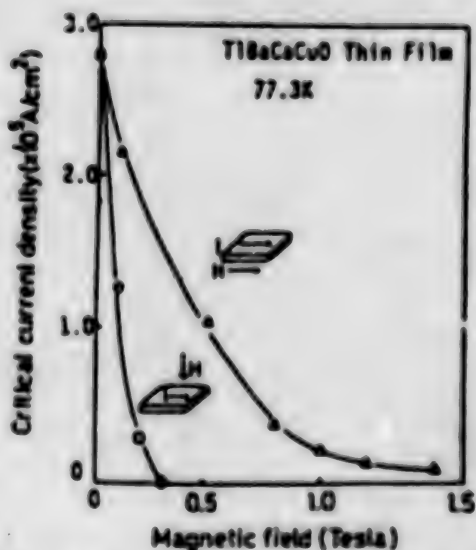


Fig.6 Magnetic field dependence of  $J_c$  for TlBaCaCuO thin film

zero resistance of this film is 115K. We also obtained a 2212 phase TlBaCaCuO thin film, whose  $T_c$  was 102K. The temperature dependence of  $J_c$  of this 2212 phase film is shown in Fig.5. The  $J_c$  of 3.2 MA/cm<sup>2</sup> was obtained at 77.3K under zero magnetic field. Applied magnetic field strongly suppress the critical current densities(Fig.6). We found many tiny pores which is probably caused by evaporation of Tl compound. These defects of the film and the grain boundaries will be the cause of rapid degradation of the critical current density by the applied magnetic field.

## CONCLUSION

Experimental results are summarized in Table 1. This include the results of high  $J_c$  LnBaCuO thin film, too. We obtained high  $J_c$  superconducting LnBaCuO (Ln: Ho,Er,Y), BiSrCaCuO and TlBaCaCuO thin films. These films have more than 3MA/cm<sup>2</sup> at 77.3K under zero magnetic field. Applied magnetic field strongly suppress the  $J_c$  in poly-crystalline BiSrCaCuO and TlBaCaCuO films compared with in the case of the single crystal LnBaCuO film.

Table1 Characteristics of high  $J_c$  superconducting thin film

	HoBaCuO	BiSrCaCuO	TlBaCaCuO
$T_c(R=0)$	90K	105K	115K
$J_c(77.3K)$	$3.5 \times 10^4 A/cm^2$	$3.4 \times 10^4 A/cm^2$	$3.2 \times 10^4 A/cm^2$
CRYSTALLINITY	SINGLE	POLY	POLY
MORPHOLOGY	FLAT	ROUGH	ROUGH
$J_c$ UNDER MAG. FIELD	$1.5 \times 10^4 A/cm^2$ (at 1.0T)	$2.6 \times 10^3 A/cm^2$ (at 0.5T)	$1.2 \times 10^3 A/cm^2$ (at 0.1T)

## REFERENCES

- 1) J.G.Bednorz and Muller, Z.Phys.B64,189(1986).
- 2) M.K.Wu, J.R.Ashburn, C.W.Chu, Phys.Rev.Lett.58,908(1987).
- 3) Y.Enomoto, T.Murakami and M.Suzuki, in Proc.5th.Int.Workshop on Future Electron Devices, Miyagi-Zao, June 1988, p325.
- 4) S.Takada, in Proc.5th.Int.Workshop on Future Electron Devices, Miyagi-Zao, June 1988, p305.
- 5) S.Tanaka and H.Itozaki, Jpn.J.Appl.Phys.27,L622(1988).
- 6) H.Itozaki, S.Tanaka, K.Higaki, and S.Yazu, Physica C153-155, 1155 (1988).
- 7) H.Maeda, Y.Tanaka, M.Fukutomi, and T.Asano, Jpn.J.Appl.Phys.27, L209(1988)
- 8) Z.Z.Sheng and A.M.Hermann: Nature 332 (1988) 138.
- 9) H.Itozaki, K.Higaki, K.Harada, S.Tanaka, N.Fujimori and S.Yazu, in Proc.1st. Int. Symp. on Superconductivity, Nagoya, Japan, August 1988.
- 10) S.Yazu, in Proc.1st Int Symp.on Superconductivity, Nagoya, Japan, August 1988.

# EFFECTS OF BOUNDARY DEFECTS ON CRITICAL CURRENT DENSITIES OF $\text{ErBa}_2\text{Cu}_3\text{O}_{7-x}$ THIN FILMS

K. TAKAGI, T. AIDA, K. NIYAUCHI, T. ICHIGUCHI,  
Y. KAMANAMI, and Y. MADOKORO

CENTRAL RESEARCH LABORATORY, HITACHI LTD.  
1-280, HIGASHIKOIGAKUBO, KOKUBUNJI, TOKYO 185, JAPAN

## **ABSTRACT**

In order to discuss the effects of boundaries on  $J_c$ , two experimental results are presented. The microstructure of  $\text{ErBa}_2\text{Cu}_3\text{O}_{7-x}$  films prepared by sputtering are examined by a TEM. Many subgrains are observed in the film with a low  $J_c$ , and  $J_c$  is considered to be affected by the sub-boundaries rather than by the twin boundaries. Artificial crystalline defects are formed in a epitaxial film using a focused ion beam technique. These defects show the properties of weak link junctions.

## **INTRODUCTION**

Since 1986, superconducting oxides with high critical temperature ( $T_c$ ) have been discovered in succession [1-4]. These superconductors are expected to create new electronic devices which make better use of their properties. When new superconducting oxides are used for electronic devices, thin films with high critical current densities ( $J_c$ ) must be grown on various substrates such as semiconductors and oxides. And controllable Josephson junctions must be fabricated in these films, too. Though high  $J_c$  of  $10^4 \text{ A/cm}^2$  at 77K has been achieved in films prepared by sputtering and reactive evaporation [5-7], the essential factors which determine the  $J_c$  of the oxide superconductors are not clear. Weak link junctions have been fabricated using grain boundaries of polycrystalline films and have been applied to make SQUID's [8, 9]. However, it is difficult to control the properties of junctions as far as polycrystalline films are utilized. These problems come from the lack of knowledge of  $J_c$  in oxide superconductors. In this presentation, we show our results of the preparation and characterization of thin films, and of the fabrication of weak link junctions for fruitful discussions.

## **CHARACTERIZATION OF MICROSTRUCTURE OF THIN FILMS**

### Film preparation

$\text{ErBa}_2\text{Cu}_3\text{O}_{7-x}$  films were prepared by sputtering onto the heated substrate (600°C) in a gas pressure of 4 Pa. The sputtering gas was a mixture of Ar and  $\text{O}_2$  (1:1). Substrates used were  $\text{MgO}$  (100) and  $\text{SrTiO}_3$  (110). After deposition, the films were post-annealed at 800-900°C for 2-40 h in  $\text{O}_2$  at 1 atm. Film thickness was 0.7  $\mu\text{m}$ . The microstructures of the films were examined by using a transmission electron microscope. Electrical properties are measured by a conventional four-point probe technique. Magnetic field dependence of  $J_c$  was measured in external magnetic field of 1T in maximum.



Deposited films had smooth surfaces. The X-ray diffraction analysis showed that the film on MgO substrate was highly oriented in c-axis. High resolution TEM image of the cross-section of the film deposited on MgO (001) showed that the a-b basal plane of the film was parallel to substrate surface and that continues in a wide range. The  $J_c$  along a [100] direction of the film was as high as  $10^9$ – $10^8$  A/cm<sup>2</sup>. This high value may be the result of the continuation of the basal plane where superconducting current flows. However, the samples with low  $J_c$ 's were sometimes prepared even when they were grown under the same conditions. The TEM images and diffraction patterns of the films which have different values of  $J_c$  are shown in Fig. 1. These bright field images were taken with electron incidences of the [001]. The twin lamellas which lie on (110) planes are clearly observed. And there are many domains. The number and the spacing of twins are almost the same in these images. Feature of the TEM image of the low  $J_c$  film is the existence of subgrains. Misorientation between each subgrain can be estimated from the angle difference of twin directions, the contrast of subgrains and electron diffraction patterns. There are many subgrains in the film with low  $J_c$  and the misorientation of these subgrains are large.  $J_c$  is considered to be affected by the sub-boundary rather than by the twin boundaries. Sub-boundaries

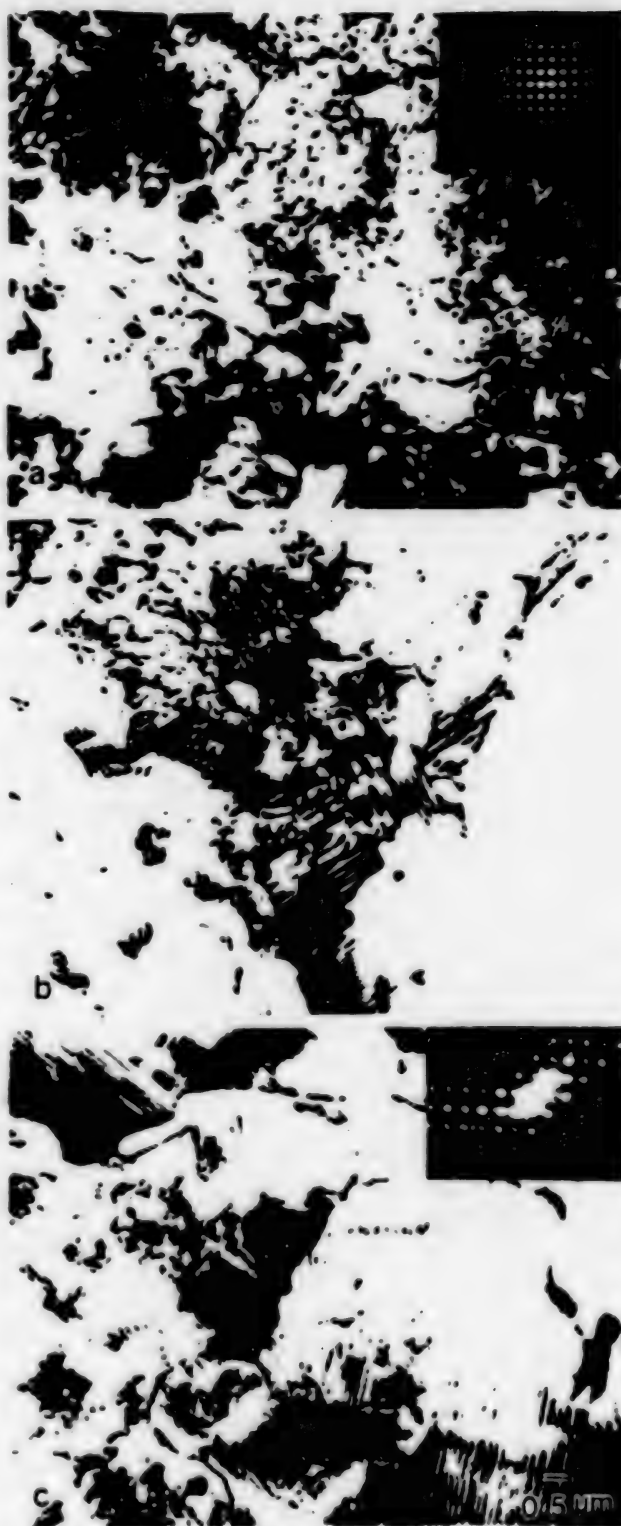


Fig. 1 TEM images of  $\text{ErBa}_2\text{Cu}_3\text{O}_{7-x}$  films prepared on MgO (100) substrates. (a)  $J_c = 10^9$  A/cm<sup>2</sup>, (b)  $J_c = 10^8$  A/cm<sup>2</sup> and (c)  $J_c = 10^7$  A/cm<sup>2</sup>

act as weak link junctions and lower the  $J_c$  because of the quite short coherent length of the oxide superconductors [10]. The measurement of external magnetic field dependence of  $J_c$  also showed that the twin boundary has little role in pinning the magnetic flux motion [7].

## FABRICATION OF A WEAK LINK JUNCTION

### Fabrication process

$\text{SrTiO}_3$  (110) substrates were used for epitaxial growth of superconducting films. Gallium (Ga) ions were irradiated on the substrate by sweeping a focused ion beam (FIB) at a energy of 30kV and dose of  $4 \times 10^{11} \sim 4 \times 10^{12} / \text{cm}^2$ . The length of sweeping beam lines was 0.5mm. The superconducting film was prepared by sputtering onto the substrate. Growth conditions were the same as mentioned above. The damaged region obstructed the epitaxial growth and this caused a crystalline defect in the film.

### Characterization of artificial defects

When the ion dose was more than  $4 \times 10^{11} / \text{cm}^2$ , dark lines were observed on the substrate by an optical microscope. Contrast of these lines was clear with their dose. Epitaxial growth was confirmed by X-ray diffraction after deposition of the film. Line defect was formed on the film where dose was more than  $10^{12} / \text{cm}^2$  as shown in Fig. 2.

The generated voltage when a bias current ( $I$ ) was swept at 4 Hz across this line defect was measured. In this measurement, a neck was formed by removing the film mechanically as shown in Fig. 2. The current-voltage characteristics were measured at 4.2K with a conventional four-point probe method. The typical curves for the circuit crossing the defect and for one in a blank region are shown in Fig. 3. At 4.2K, an critical current density of this film was too high to generate

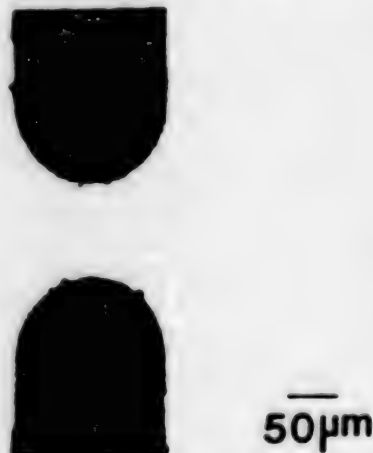


Fig. 2 Photograph of a patterned specimen for measurement of I-V properties. A line defect is located at the neck region.

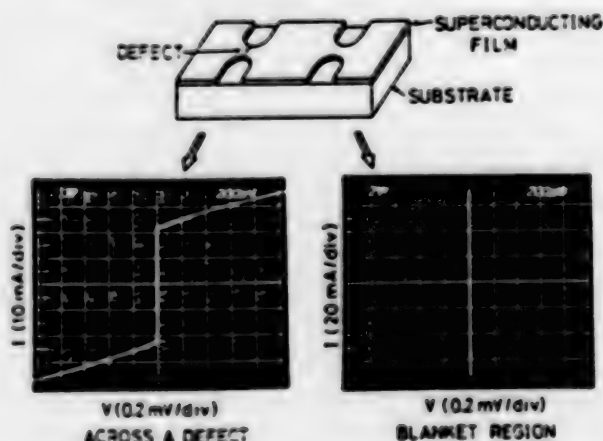


Fig. 3 I-V characteristics of a circuit straddling the defect and one in a blank region

voltage. On the other hand, critical current crossing the defect was low and voltage was detected. At 77K, critical currents for both circuits decreased, and I-V curves show gradual change. Temperature dependence of  $I_c$  for the circuit straddling the defect was of form  $I_c \propto (1-T/T_c)^{1/2}$ . Here  $T_c$  is a critical temperature 83K. This is similar to the result obtained for dc SQUID which utilizes grain boundaries for junction[9]. These results indicate that this artificial defect acts as a weak link junction.

## SUMMARY

$\text{ErBa}_2\text{Cu}_3\text{O}_{7-x}$  films were prepared onto  $\text{MgO}$  and  $\text{SrTiO}_3$  substrates by sputtering and their micro-structures were examined by TEM. The observation indicated that sub-boundaries caused the decrease of  $J_c$ . In order to control the  $J_c$ , artificial crystalline defects were fabricated in a epitaxial film using a focused ion beam technique. These defects showed the properties of weak link junctions.

## ACKNOWLEDGMENTS

The authors are grateful to Dr. T. Suganuma for his useful discussions. Thanks are also extended to Mr. T. Fukazawa, A. Tsukamoto and T. Shimotsu for the film preparation and TEM observations.

## REFERENCES

- 1) J. G. Bednorz and K. A. Muller: *Z. Phys.* B64 (1986) 189.
- 2) M. K. Wu, J. R. Ashburn, C. J. Torng, P. H. Hor, R. L. Meng, L. Gao, Z. J. Huang, Y. Q. Wang and C. W. Chu: *Phys. Rev. Lett.* 58 (1987) 908.
- 3) H. Maeda, Y. Tanaka, M. Fujitomi and T. Asano: *Jpn. J. Appl. Phys.* 27 (1988) L209.
- 4) Z. Z. Sheng and A. M. Herman: *Nature* 332 (1988) 138.
- 5) S. Tanaka and H. Itozaki: *Jpn. J. Appl. Phys.* 27 (1988) L622.
- 6) Y. Enomoto, T. Murakami, M. Suzuki and K. Moriwaki: *Jpn. J. Appl. Phys.* 26 (1987) L1248.
- 7) T. Aida, T. Fukazawa, A. Tsukamoto, K. Takagi, T. Shimotu and T. Ichiguchi: submitted to *Proc. of ISS'88*.
- 8) H. Nakane, Y. Tarutani, T. Nishino, H. Yamada and U. Kawabe: *Jpn. J. Appl. Phys.* 26 (1987) L1925.
- 9) R. H. Koch, C. P. Umbach, G. J. Clark, P. Chaudhari and R. B. Laibowitz: *Appl. Phys. Lett.* 51 (1987) 200.
- 10) M. Suenaga: *Mat. Res. Soc. Symp. Proc.*, to be published.

# IN-SITU GROWTH OF $\text{YBa}_2\text{Cu}_3\text{O}_{7-x}$ THIN FILMS BY ACTIVATED REACTIVE EVAPORATION

T. TERASHIMA, K. IIJIMA<sup>+</sup>, K. YAMAMOTO<sup>+</sup>, K. HIRATA<sup>+</sup> and Y. BANDO  
INSTITUTE FOR CHEMICAL RESEARCH, KYOTO UNIVERSITY, UJI 611, JAPAN  
<sup>+</sup>RESEARCH INSTITUTE FOR PRODUCTION DEVELOPMENT, KYOTO 606, JAPAN

## ABSTRACT

Epitaxial growth of (001) oriented  $\text{YBa}_2\text{Cu}_3\text{O}_{7-x}$  on (100)  $\text{SrTiO}_3$  and (100)  $\text{MgO}$  by activated reactive evaporation was investigated by in-situ reflection high energy electron diffraction. Formation of the perovskite structure was observed for the first atomic layer on the substrates, and the subsequent layers exhibited a layer by layer growth. The lattice spacing in the (001) plane of the film on the (100)  $\text{MgO}$  had converted from that of  $\text{MgO}$  to  $\text{YBa}_2\text{Cu}_3\text{O}_{7-x}$  when the thickness of the film came to a few unit cell length of 1:2:3 structure.

## INTRODUCTION

High temperature superconducting oxides thin films with excellent characteristics, such as good crystallinity, smooth surface and high critical current density were strongly required for the wide applications of the high temperature superconductivity. Recent trend of the preparation of the high- $T_c$  films has been directed toward "in-situ" growth of the superconducting phase at relatively low temperatures to attain a smooth film surface which is suitable for the fabricating of the film devices. Several methods, including reactive evaporation with an activated oxygen source [1,2], reactive sputtering [3,4] and pulsed laser evaporation [5], have been successfully applied to "in-situ" growth.

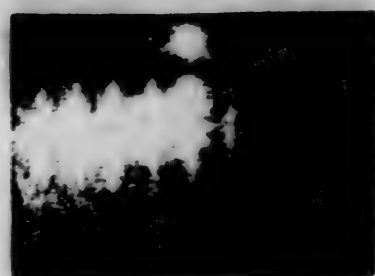
We have already demonstrated that a good quality single-crystal  $\text{YBa}_2\text{Cu}_3\text{O}_{7-x}$  (hereafter referred to as YBCO) thin films with large critical current density ( $4 \times 10^6$  A/cm<sup>2</sup> at 77K) can be prepared by activated reactive evaporation [6]. In order to make progress in the formation of the high quality superconducting films, it is of significant importance to investigate the growth mode of the films from the first stage.

Here we report the in-situ observation of the reflection high energy electron diffraction (RHEED) during the growth of YBCO thin films. The substrates used in this study were (100)  $\text{SrTiO}_3$  and (100)  $\text{MgO}$ .  $\text{SrTiO}_3$  has a perovskite structure and good lattice matching with the YBCO (lattice misfit is less than 2%), while  $\text{MgO}$  has the NaCl structure and large misfit of 9%. Especially, in the last case, it is interesting to investigate when the perovskite structure of 1:2:3 compound is formed and how the lattice spacing varies.

## EXPERIMENT

The YBCO films were prepared in a ARE system, assorted with the in-situ RHEED observation system and cold cathode type ion beam sources which is used for the pre-cleaning of the substrate surface. The Y and Ba metals were evaporated from the two





0 Å



12 Å



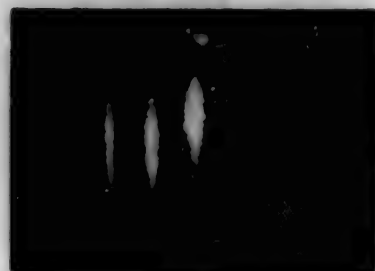
3 Å



24 Å



6 Å



200 Å

Fig.1 In-situ RHEED patterns observed during growth of YBCO on (100)  $\text{SrTiO}_3$ .

electron-beam heated sources, and the Cu metal was from the alumina crucible heated by a tungsten wire. Each source had a its own quartz oscillating rate monitor and the source power was controlled by the feedback from the rate monitor to maintain a constant evaporation rate for the film stoichiometry. The total overall growth rate was 0.8 Å/sec.

The oxygen incorporation was made by a oxygen gas flow from the both side of the substrate. The local oxygen pressure near the substrate surface was made to be  $10^{-2} \sim 10^{-1}$  Torr, while the back ground pressure was kept at  $10^{-5}$  Torr during the deposition. And a oxygen plasma was produced in the chamber by RF power supply (100W) to activate the oxidation of Cu.

## RESULTS AND DISCUSSION

In the first place, we mention about the result on the (100)  $\text{SrTiO}_3$ .  $\text{SrTiO}_3$  wafer used was sliced from the single crystal ingot which was prepared by Verneuil method, and then

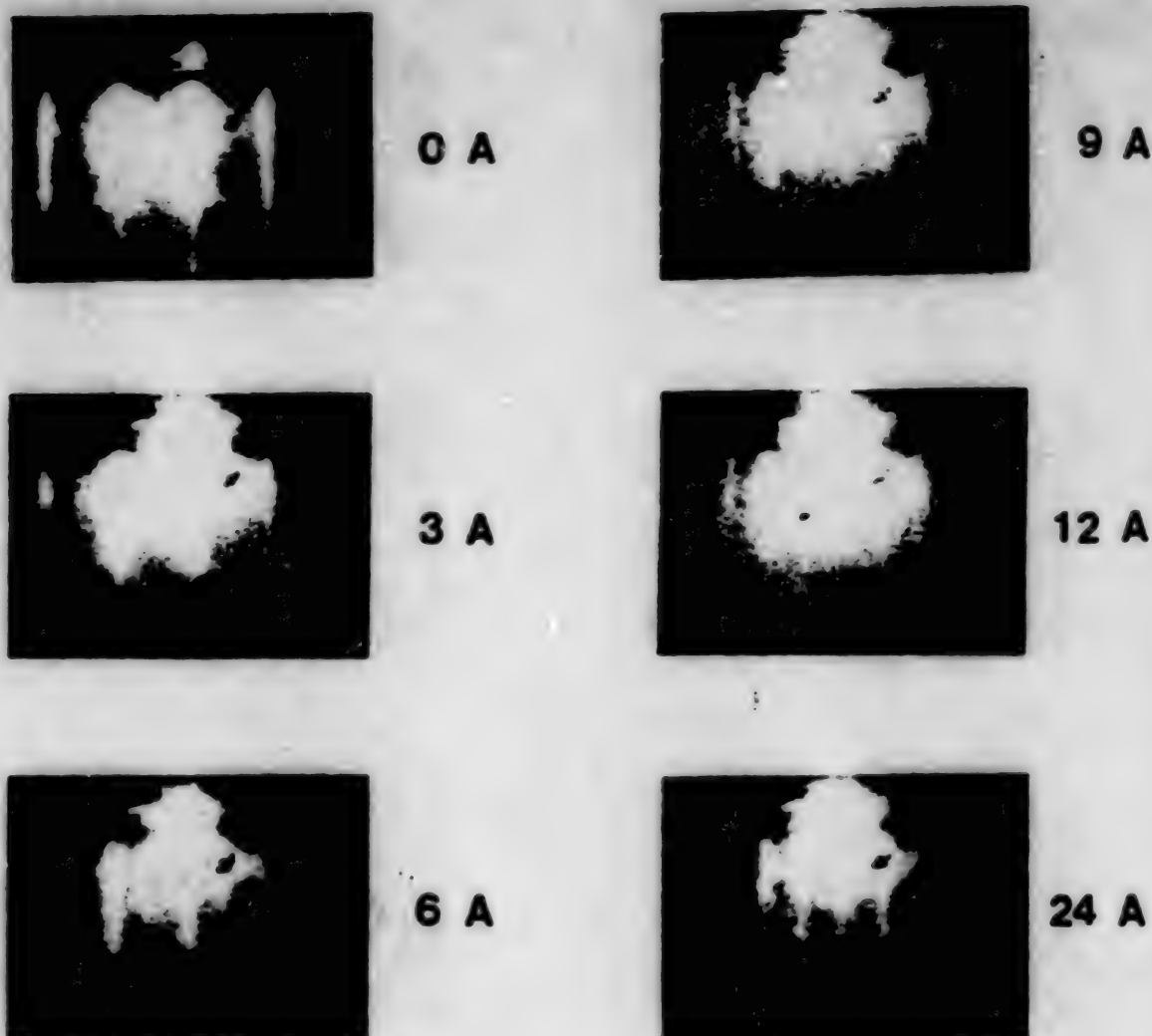


Fig.2 In-situ RHEED patterns observed during growth of YBCO on (100) MgO.

mechanically polished. The streaky RHEED pattern was observed for as-prepared substrate surface, however, the background level was relatively high and the streak was not so sharp. We made the cleaning of the surface of the  $\text{SrTiO}_3$  by  $\text{Ar}^+$  ion bombardment ( acceleration voltage : 600 eV ) at 650 °C for 1 min. After this treatment the back ground level became very weak and the streaks became very sharp. Then the YBCO film was grown on this substrate at 650 °C.

Figure 1 shows in-situ RHEED patterns during the growth of the YBCO film on the (100)  $\text{SrTiO}_3$ . In this case, the in-plane epitaxial relation between the YBCO and  $\text{SrTiO}_3$  was  $[100]\text{YBCO} // [100]\text{SrTiO}_3$  and  $[110]\text{YBCO} // [110]\text{SrTiO}_3$ . The thickness indicated at the RHEED pattern was the monitored value by a quartz oscillating sensor located at near the substrate. It is clear from this result that the perovskite structure of the film was formed from the first atomic layer and no three dimensional nucleation occurred. The streaky RHEED patterns of the perovskite structure during the film growth suggest that the YBCO showed a layer by layer growth and the film surface was atomically smooth.

From the beginning of the film growth, extra streak pattern corresponding to the  $2a_0$  ( $a_0$  is a lattice constant of the YBCO) appeared. This extra pattern remained after the substrate was cooled to room temperature. The streak pattern corresponding to  $2a_0$  was also observed for the [110] incidence of the electron beam. This superstructure along the a-axis was confirmed by the [h00] scanning of the X-ray diffraction. Oxygen content of the as-grown film was found to be insufficient because the lattice spacing  $c_0$  was rather large ( $c_0=11.75\text{\AA}$ ) and the resistive superconducting transition was  $T_c(\text{onset})=60\text{K}$ , and  $T_c(R=0)=45\text{K}$ . In order to make a optimum oxygen content, after the deposition the film was successively oxidized in the chamber below the growth temperature under the relatively high oxygen pressure (200Torr). After the oxidation, the extra streak disappeared. We assume the  $2\times 2$  superstructure would be originated from the oxygen vacancy ordering in the grown film.

Figure 2 shows in-situ RHEED patterns during the growth of YBCO on the (100) MgO. The (100) MgO substrate was mechanically polished and then chemically etched by a nitric acid. The substrate was also etched in the chamber by  $\text{Ar}^+$  ion beam as the same with the case of  $\text{SrTiO}_3$ . On the (100) MgO the YBCO shows the in-plane epitaxial relation as  $[100]\text{YBCO} // [100]\text{MgO}$  and  $[110]\text{YBCO} // [110]\text{MgO}$ .

As the MgO has the NaCl structure, the RHEED pattern of the substrate was made from the streaks corresponding to the lattice spacing of  $a_0/2$ . When the thickness of overgrown YBCO came to  $3\sim 6\text{\AA}$ , which means the  $1\sim 2$  atomic layers of the perovskite structure, the distinct streaks corresponding to the lattice spacing of  $a_0$  which is characteristic for the perovskite structure appeared and its intensity increased with the increase of the thickness. The lattice constant  $a_0$  of the MgO at  $650^\circ\text{C}$  can be calculated to be  $4.25\text{\AA}$  using the thermal expansion coefficient and we regard the distance of the streaks of the substrate to correspond with this value. The lattice spacing of the YBCO calculated from the distance of the streaks had a very near value with MgO until the thickness came to  $12\text{\AA}$ . However, when the thickness came to  $24\text{\AA}$ , the lattice spacing of the YBCO drastically converted to  $3.9\text{\AA}$ , which is really the one of the YBCO itself.

In conclusion, we have demonstrated that the YBCO showed a layer by layer growth on the (100)  $\text{SrTiO}_3$  and (100) MgO. This result gives a hopeful prospect to attain a highly perfect film surface for fabricating a junction structure.

## REFERENCES

- <sup>1</sup> K.Moriwaki, Y.Enomoto, S.Kubo and T.Murakami, Jpn.J.Appl.Phys. 27, L2075 (1988).
- <sup>2</sup> J.Kwo, M.Hong, D.J.Trevor, R.M.Fleming, A.E.White, R.C.Farrow, A.R.Kortan and K.T.Short, to be appeared in Appl.Phys.Lett.
- <sup>3</sup> Y.Enomoto, T.Murakami, M.Suzuki and K.Moriwaki, Jpn.J.Appl.Phys. 26, L1248 (1987).
- <sup>4</sup> S.Tanaka and H.Itozaki, Jpn.J.Appl.Phys. 27, L622 (1988).
- <sup>5</sup> X.D.Wu, A.Inam, T.Venkatesan, C.C.Chang, E.W.Chase, P.Barboux, J.M.Tarascon and B.Wilkens, Appl.Phys.Lett. 52, 754 (1988).
- <sup>6</sup> T.Terashima, K.Iijima, K.Yamamoto, Y.Bando and H.Mazaki, Jpn.J.Appl.Phys. 27, L91 (1988).

# Ba<sub>1-x</sub>K<sub>x</sub>BiO<sub>3</sub> THIN FILMS PREPARATION WITH ECR ION BEAM OXIDATION AND THEIR PROPERTIES

Y. ENOMOTO, T. MURAKAMI and K. MORIWAKI  
NTT OPTO-ELECTRONICS LABORATORIES  
TOKAI-MURA, IBARAKI-KEN 319-11, JAPAN

## ABSTRACT

Ba<sub>1-x</sub>K<sub>x</sub>BiO<sub>3</sub> thin films were epitaxially deposited on MgO substrates by using an oxygen ion source of ECR-type. As-grown films showed superconductivity, when substrate temperature was about 500°C and x values 0.3 to 0.4. Measurements on their lattice constants, superconductivity, and optical reflection were carried out.

## INTRODUCTION

All the Cu-based high T<sub>c</sub> oxide superconductors have a Cu-O layered crystal structure and many researchers attribute the high T<sub>c</sub> to those structures. Because of the layered structures, oxide superconductors have large anisotropy and very small coherence length along the c-axis. On the contrary, Ba<sub>1-x</sub>K<sub>x</sub>BiO<sub>3</sub> (BKBO) exhibits a maximum T<sub>c</sub> of 30 K in spite of having a cubic symmetry<sup>(1-4)</sup>. This fact brings about another possibility in the development of high T<sub>c</sub> materials. Further, the coherence length will become isotropic and this will be effective in the device application.

However, the preparation of BKBO samples needs complicated processes involving sintering at high temperature in a reduced atmosphere and a short time oxidation at a low temperature. Those processes leave oxygen defects and non-uniformity of K-ions distribution in those samples and such structural imperfection impairs their electrical properties.

This paper describes preparation and properties of BKBO thin films by using the reactive evaporation method assisted with ECR ion beam oxidation. This method makes it easy for K ions to be introduced into films together with other constituents. We have succeeded in obtaining superconducting as-grown BKBO films.

## EXPERIMENTS AND RESULTS

The system involves three K-cells for metal sources and an ECR (Electron Cyclotron Resonance) ion source, which was related in our previous paper<sup>(5)</sup>. Based pressure in the vacuum chamber was reduced to 10<sup>-4</sup> Pa with a diffusion pump. The oxygen beam was bombarded onto a substrate simultaneously with three evaporated beams to form oxide films. The ECR ion beam was introduced through the outlet of 10 cm in diameter and was accelerated by bias voltage of 50V. The ion current density was monitored by Faraday cups. The maximum ion current density was 300 μA/cm<sup>2</sup> using oxygen gas flow of 3 SCCM and neutralized to be 50 μA/cm<sup>2</sup> with a filament heater. When the ion beam was not neutralized or the gas flow amount was less than the above value, as-grown films could not become superconducting. Granular metals of Ba, K and Bi were used as metal sources. Metal composition in the film was adjusted by controlling each evaporation rate. Typical preparation conditions are listed in Table 1 and 2.

BKBO thin films were deposited on (100) MgO and (110) SrTiO<sub>3</sub> substrates at 500°C. In both the cases, the films grew epitaxially on the substrates. However, when the



composition was near at  $x = 0.2$ , cracks often arised in films. The reason is not clear at present.

Figure 1 shows the x-ray pattern of a BKBO film on a (001) MgO. Small peaks of other orientations were recognized, although the misfit of the lattice constants is small(1.2%). In the case of SrTiO<sub>3</sub>, no such peaks were detected in spite of a large lattice constant misfit of 11% against the substrates, because both are of perovskite-type.

Figure 2 shows K/Bi dependence of the lattice constant. The lattice constant decreases with increase of K/Bi ratio below about 0.4 similarly to the result of Hinks and others<sup>(3)</sup>, but it increases above 0.4. The films of  $x = 0.25$  to 0.4 became superconducting.

Figure 3 indicates temperature dependences of the magnetic moment at 40 G of an as-grown film whose K/Bi ratio is about 0.35. The sample thickness was about 500 nm and the area  $2 \times 3 \text{ mm}^2$ . The moment was rather reduced by annealing at 400 °C in an oxygen flow for 2 hours.

In Fig.4, the change of  $H_{c1}$  of the same sample as in Fig.3 is plotted against temperature, compared with the data of Batlogg and others<sup>(2)</sup>. Both the data agree with each other.

In Fig.5, the optical reflection of a BKBO film is shown together with the data of a BPBO (by Tajima and others<sup>(6)</sup>). The theoretical curve of the BKBO film was calculated by using the same value as in the case of the BPBO sample. The plasma frequency of the BKBO film is about 700 nm, while that of the BPBO sample is about 880 nm. The shorter wavelength may indicate the increase of the carrier density.

## CONCLUSION

BKBO thin films grew epitaxially on (001) MgO and (110) SrTiO<sub>3</sub> substrates by using a reactive deposition system with a oxygen ion source of ECR-type. The lattice constant agreed with the data reported, but showed an increase above  $x = 0.4$ . The superconducting properties agreed with the data reported so far. The optical reflection showed a plasma wavelength of about 700 nm. The shorter wavelength may indicate the increase of the carrier density.

## ACKNOWLEDGEMENT

The authors wish to thank Y. Katayama, T. Inamura for encouragement and also to present thanks to A. Yamaji for helpful discussion.

## REFERENCE

1. L. F. Mattheiss, E. M. Gyorgy, and D. W. Johnson, Jr., Phys. Rev. **B 37**, 3745 (1988).
2. B. Batlogg, R. J. Cava, L. W. Rupp, Jr., A. M. Muzsce, J. J. Krajewski, J. P. Remick, W. F. Peck, Jr., A. S. Cooper, and G. P. Espinosa, Phys. Rev. Lett. **61**, 1670 (1988).
3. D. G. Hinks, B. Dabrowski, J. Jorgensen, A. W. Mitchell, D. R. Richards, Shiyou pei and Donglu Shi, Nature **333**, 836 (1988).
4. S. Jin, T. H. Tiefel, R. C. Sherwood, A. P. Ramirez, E. M. Gyogy, G. W. Kammlott, and R. A. Fastnacht, Appl. Phys. Lett. **53**, 1116 (1988).
5. K. Moriwaki, Y. Enomoto, S. Kubo, and T. Murakami, Jpn. J. Appl. Phys. **27**, L2075 (1988).
6. S. Tajima, S. Uchida, A. Masaki, H. Takagi, K. Kitazawa and S. Tanaka, Phys. Rev. B **32**, 6302 (1985).

**Table 1 Typical evaporation conditions**

	deposition rate	k-cell Temp.
K	10 Å/sec	150 °C
Ba	3	650
Bi	5	500
BKBO	3 Å/sec	

**Table 2 Typical oxydation conditions**

Ion energy	50 eV
Ion current density	150 $\mu\text{A}/\text{cm}^2$ (before neutralization)
	50 $\mu\text{A}/\text{cm}^2$ (after neutralization)
Substrate temp.	500 °C .

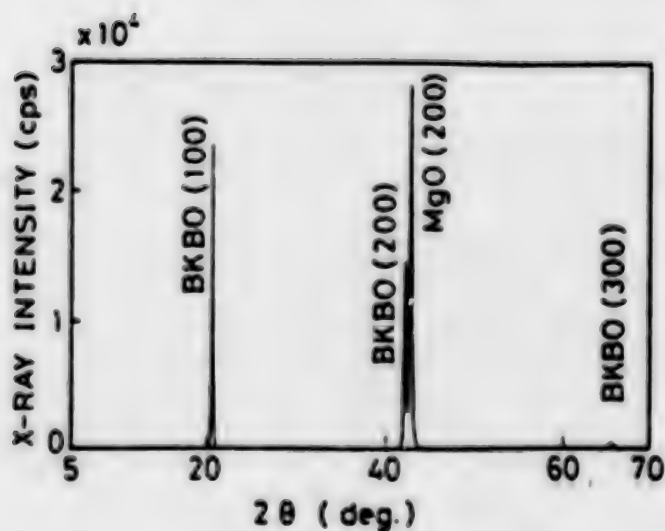


**Fig.1 x-ray diffraction pattern of a BKBO film on (100) MgO.**

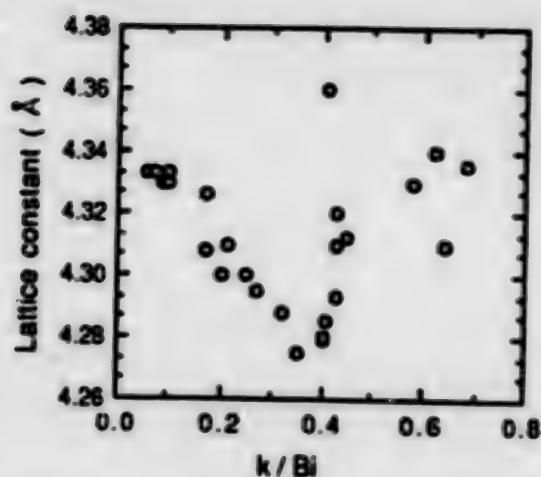


Fig.2 Lattice constant change due to K/Bi ratio.

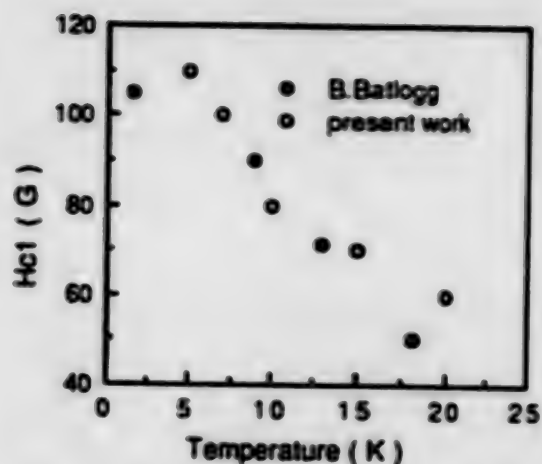


Fig.4 Temperature change of  $H_{c1}$ . The film is the same as that in Fig.3.

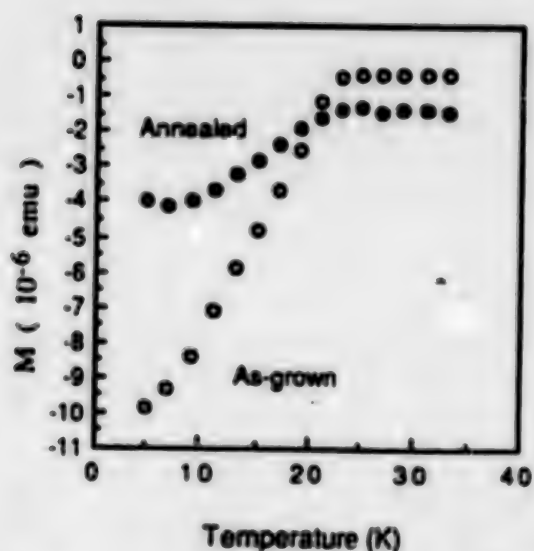


Fig.3 Temperature dependence of the magnetic moment of a BKBO film. The K/Bi ratio is 0.35, the thickness about 500 nm, and the area  $2 \times 3 \text{ mm}^2$ .

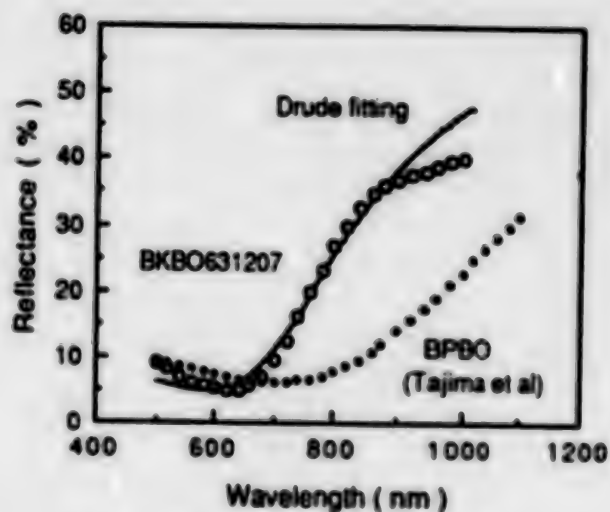


Fig.5 Optical reflectance of a BKBO film, compared with a BPBO film ( by Tajima et al )

# LOW TEMPERATURE FORMATION OF Bi(Pb)-Sr-Ca-Cu-O THIN FILMS BY A SUCCESSIVE DEPOSITION METHOD WITH EXCIMER LASER

TOMOJI KAWAI, MASAKI KANAI AND SHICHIO KAWAI  
THE INSTITUTE OF SCIENTIFIC AND INDUSTRIAL RESEARCH,  
OSAKA UNIVERSITY, MIHOGAOKA, IBARAKI, OSAKA 567 JAPAN

## ABSTRACT

Crystallized as-grown Bi(Pb)-Sr-Ca-Cu-O thin films are formed by laser ablation method at the substrate temperature as low as 480 °C under N<sub>2</sub>O gas flow. The as-grown thin film which has a crystal structure consisting of four or five Cu-O<sub>2</sub> layers between adjacent Bi<sub>2</sub>O<sub>2</sub> layers can be formed by combination of N<sub>2</sub>O gas flow and "successive deposition method" with excimer laser pulses.

## INTRODUCTION

We have prepared thin films of Bi-Sr-Ca-Cu-O (BSCCO) and Bi(Pb)-Sr-Ca-Cu-O(BPSCCO) by laser ablation[1,2] under N<sub>2</sub>O gas flow, and have succeeded in the formation of crystallized as-grown thin films at the substrate temperature as low as 480 °C. The films were prepared by a "successive deposition method" (Fig.1) using multi-targets. The application of the successive deposition method to the controlling of the number of Cu-O<sub>2</sub> layers in the BSCCO film was tried with a multi-target magnetron sputtering method[3] at 650 °C. We have tried to control the structure of the Bi based superconducting film; by the successive deposition method at lower substrate temperatures with laser ablation using activated oxygen from N<sub>2</sub>O. By this technique, we have formed as-grown Bi(Pb)-Sr-Ca-Cu-O film containing one to five Cu-O<sub>2</sub> layers at 480 °C.

## EXPERIMENTAL

The films are formed on a MgO(100) substrate using pulses of ArF excimer laser(193nm) focused on the target placed on the opposite side of the substrate. Pellets of Bi<sub>2</sub>O<sub>3</sub>, SrCuO<sub>y</sub> and CaCuO<sub>y</sub> were used as targets for BSCCO films, and those of Bi<sub>7</sub>Pb<sub>3</sub>O<sub>y</sub>, SrCuO<sub>y</sub> and CaCuO<sub>y</sub> for BPSCCO films. Film deposition was carried out successively from Bi<sub>2</sub>O<sub>3</sub> or Bi<sub>7</sub>Pb<sub>3</sub>O<sub>y</sub> for 20 sec with 7 Hz repetition rate, SrCuO<sub>y</sub> for 10sec,

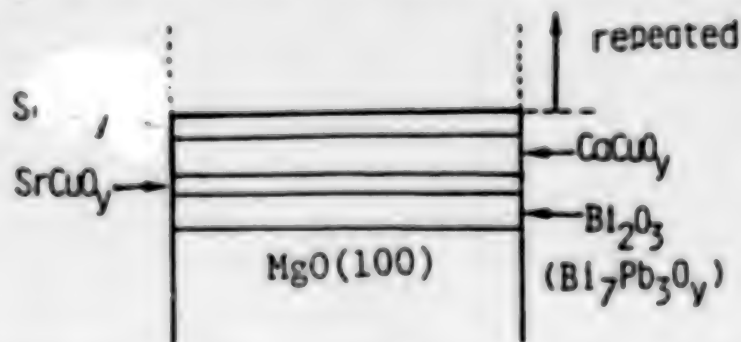


Fig.1 A schematic representation of multi-target successive deposition for Bi(Pb)-Sr-Ca-Cu-O film.



$\text{CaCuO}_y$  varying length of time and  $\text{SrCuO}_y$  for 10 sec that consist of one cycle. The deposition time for  $\text{CaCuO}_y$  was changed between 50 sec and 90 sec (Fig.1) in order to prepare the films with different numbers of  $\text{Cu-O}_2$  layers. The samples were prepared with 20 - 30 cycles to form 600 - 800Å thickness under oxygen or  $\text{N}_2\text{O}$  gas flow maintaining pressure of  $10^{-1}$  to 1 torr.

## RESULTS AND DISCUSSION

As-grown films of BSCCO with 700Å thickness as obtained from 20-cycle deposition under  $\text{O}_2$  atmosphere had very weak and broad X-ray diffraction peaks when the substrate temperature was 600 C. The films formed at lower substrate temperature were amorphous. These results indicated that the crystallization of the as-grown film did not occur or hardly proceeded in those temperature regions under oxygen atmosphere. At higher substrate temperatures (>600 C), the diffraction peaks of impurity phase attributable to  $\text{Bi}(\text{Sr,Ca})\text{O}_y$  grew and the peaks of BSCCO phase did not become larger. Therefore, a crystallized as-grown film was not obtained under these conditions. A weak and wide diffraction peak at  $2\theta = 4^\circ - 6^\circ$  corresponding to 002 of BSCCO system, however, was shifted towards lower angles with increase in the deposition time of  $\text{CaCuO}_y$  in the cycle. This shift of the peak position indicates that the precursor of BSCCO compound was already formed in the as-grown film and the lattice constant of the c-axis of that precursor became longer with increasing of the deposition time of  $\text{CaCuO}_y$ . Therefore,  $\text{O}_2$  atmosphere during deposition is not adequate enough to form a crystallized as-grown film below 600 C, but sintering procedure at high temperature is needed.

In order to obtain crystallized as-grown films at lower temperatures and to control the number of  $\text{Cu-O}_2$  layers in the structure, much stronger oxidizing agent of  $\text{N}_2\text{O}$  was used instead of  $\text{O}_2$  gas. As the Pb doping for this system is known to facilitate the formation of high  $T_c$  phase, BPSCCO films are prepared by the same successive deposition method using  $\text{Bi}_7\text{Pb}_3\text{O}_y$ ,  $\text{SrCuO}_y$ ,  $\text{CaCuO}_y$  targets at 520°C. Fig.2 shows the change of the X-ray diffraction patterns of these as-grown BPSCCO films against the deposition time of  $\text{CaCuO}_y$ . These films had a thickness of 600 - 800Å after 20 - 30 cycle deposition. The indication of the diffraction patterns in Fig.2 is that, when the deposition time of  $\text{CaCuO}_y$  was short, the film had diffraction peaks due to 80K phase (double  $\text{Cu-O}_2$  layers), its lattice constant c being 30.6Å (Fig.2 (a)). As the deposition time of  $\text{CaCuO}_y$  increases, the lattice constant c becomes longer and 110K phase with triple  $\text{Cu-O}_2$  layers appears whose c-axis length is 37.3Å (Fig.2 (b)). The phase having lattice constant larger than 37Å was obtained in the region of longer deposition time of  $\text{CaCuO}_y$  (Fig.2 (c,d)). The lattice constants c of these phases, calculated on the basis of the indices shown in Fig.2 (c,d) were 43.5Å and 50.0Å. These values correspond to the lattice constant of the structures having four  $\text{Cu-O}_2$  layers and five  $\text{Cu-O}_2$  layers, respectively, between adjacent  $\text{Bi}_2\text{O}_2$  layers. Thus, we believe that not only one to three  $\text{Cu-O}_2$  layer structures but also four and five  $\text{Cu-O}_2$  layer structures with the c-axis oriented perpendicular to the substrate surface was achieved in these films. These results show that the number of  $\text{Cu-O}_2$  layers even in the as-grown films made at 520 C could be controlled. The diffraction peaks of these phases, however,

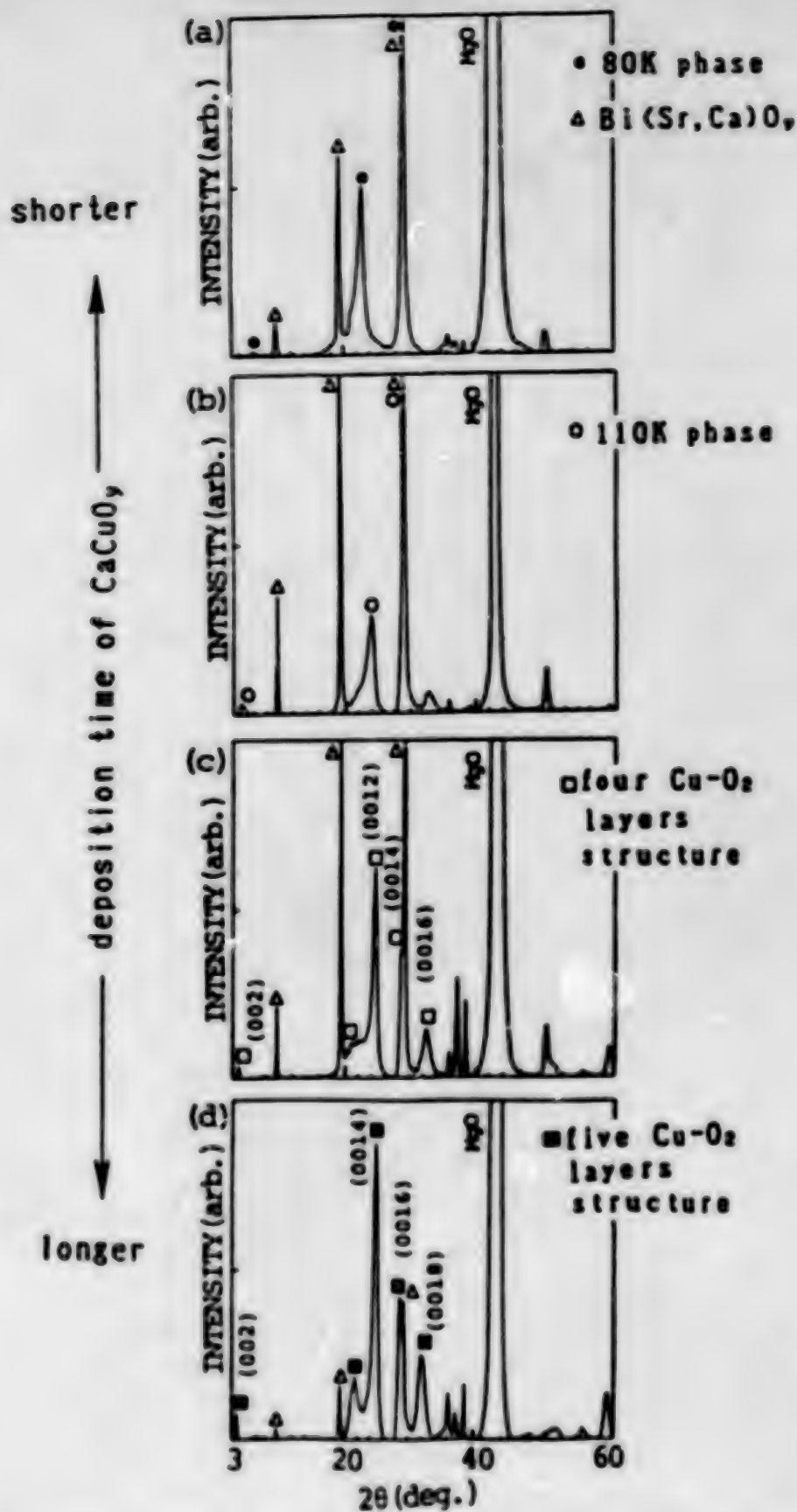


Fig.2 The change of the X-ray diffraction patterns of Bi-Pb-Sr- Ca-Cu-O as-grown films at  $520^\circ\text{C}$  under  $\text{N}_2\text{O}$  gas flow with the change of the deposition time of  $\text{CaCuO}_y$  in a cycle.

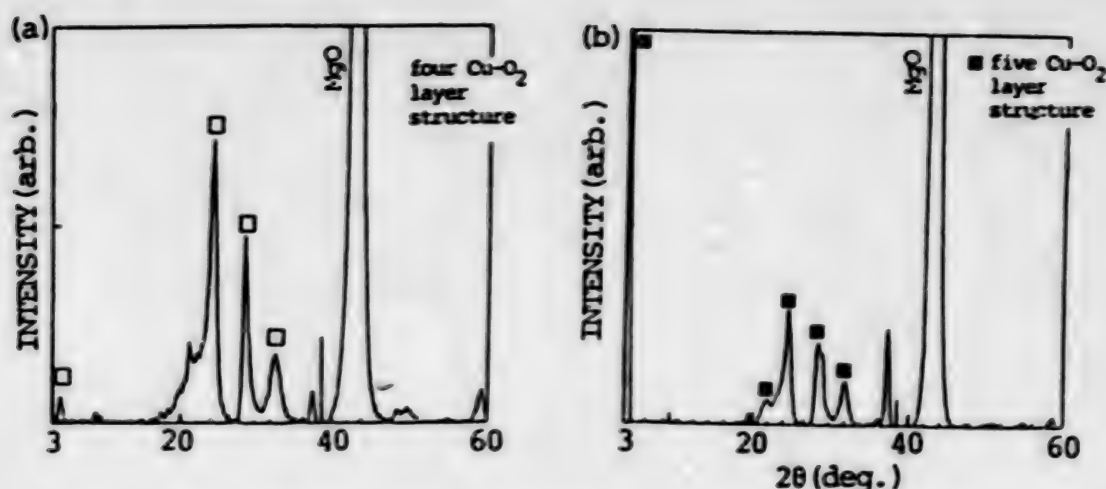


Fig.3 The X-ray diffraction patterns of Bi(Pb)-Sr-Ca-Cu-O as- grown films at 480 °C(a,b). (a) The lattice constant  $c$  is 43.5Å corresponding to four Cu- O<sub>2</sub> layer structure. (b) The lattice constant  $c$  is 50.0Å corresponding to five Cu-O<sub>2</sub> layer structure.

shows that the films contained some impurity phase, such as Bi(Sr,Ca)O<sub>y</sub>. The film formation at lower temperatures was quite effective in reducing the impurity phase. In the X-ray diffraction pattern of the film containing 4 and 5 Cu-O<sub>2</sub> layers as prepared at substrate temperature of 480 °C (Fig.3 (a,b)), the Bi(Sr,Ca)O<sub>y</sub> was not seen though the peaks of BPSCCO became a little bit weaker.

In summary, the numbers of Cu-O<sub>2</sub> layers in Bi(Pb)-Sr-Ca-Cu-O can be controlled by successive deposition method using a laser ablation of multi-target. In BPSCCO as-grown films, the structure having large lattice constant, of  $c$ -axis corresponding to four and five Cu-O<sub>2</sub> layer structure ( $c$ = 43Å, 50Å) can be formed even at 480 °C by this method. During the laser ablation, the introduction of dinitrogen monoxide(N<sub>2</sub>O) gas definitely enhances the crystallization of the as-grown films, allowing the diffraction peaks of BPSCCO phase to be seen in the as-grown films even at the substrate temperature of 480 °C. We expect that N<sub>2</sub>O gas may be effective in a film formation of other high-T<sub>c</sub> superconductors at lower temperature.

#### References

- 1) M.Kanai, T.Kawai, M.Kawai, and S.Kawai, Jpn.J.Appl.Phys. 27 (1988) L1293, 27,2001 (1988).
- 2) H.Tabata, T.Kawai, M.Kanai, O.Murata, and S.Kawai, Jpn.J.Appl.Phys, to be published
- 3) H.Adachi, S.Kohiki, K.Setsune, I.Mithuyu, and K.Wasa, Jpn.J.Appl.Phys, 27 (1988) L1883

AS-GROWN PREPARATION OF SUPERCONDUCTING EPITAXIAL  $\text{Ba}_2\text{YCu}_3\text{O}_x$  THIN FILMS  
SPUTTERED ON EPITAXIALLY GROWN  $\text{ZrO}_2/\text{Si}(100)$

H. MYOREN, Y. NISHIYAMA, H. FUKUMOTO, H. NASU AND Y. OSAKA  
HIROSHIMA UNIVERSITY, DEPT. OF ELECTRICAL ENGINEERING, FAC. OF ENGINEERING  
Saijo, Higashi-Hiroshima 724, Japan

## ABSTRACT

High- $T_c$  superconducting  $\text{Ba}_2\text{YCu}_3\text{O}_x$  thin films have been epitaxially grown on  $\text{Si}(100)$  substrate using the epitaxially grown tetragonal  $\text{ZrO}_2$  or cubic yttria-stabilized zirconia (YSZ) as a buffer layer. The thin films were prepared by rf magnetron sputtering of the stoichiometric  $\text{Ba}_2\text{YCu}_3\text{O}_x$  target below 700 °C. The adequate positive substrate bias was necessary to make surface smoothness and to show the superconducting transition above liquid nitrogen temperature without any post-treatment. The highest  $T_c(\text{onset})$  and  $T_c(\text{end})$  observed were 88 K and 84 K, respectively.

## INTRODUCTION

Since Bednorz and Müller have reported a possible high- $T_c$  superconducting La-Ba-Cu-O [1], many scientists all over the world intensify their efforts to apply the high- $T_c$  superconducting materials to a viable technology. Especially, the technique to fabricate thin films of the new materials is indispensable for electronic applications. In literature, these films have been only successfully deposited with smooth surface and good superconducting properties only on single crystalline substrates such as  $\text{SrTiO}_3$ ,  $\text{MgO}$ , or  $\text{ZrO}_2$ , so far. However, the use of these substrates brings disadvantage for the application of the high- $T_c$  superconducting oxide as a part of electronic devices using established VLSI technology based on Si. Although the direct deposition on Si substrate has been desired, the interdiffusion between substrate and film and cracks in the films result in poor superconducting qualities [2-5]. Therefore, it has been recently found that the buffer layers such as Pt,  $\text{MgO}$ ,  $\text{SiO}_2$  and  $\text{ZrO}_2$  [6-8], are quite useful for preparing good superconducting films on Si.

This paper reports successful as-grown preparation of superconducting epitaxial  $\text{Ba}_2\text{YCu}_3\text{O}_x$  thin films with  $T_c(\text{end})$  above 80 K on Si using  $\text{ZrO}_2$  or yttria-stabilized zirconia (YSZ) as the buffer layer, without any post-treatment by rf magnetron sputtering with the adequate positive substrate bias.

## EXPERIMENTAL

Epitaxial  $\text{ZrO}_2$  [9] or YSZ [10] ( $(\text{ZrO}_2)_{1-m}(\text{Y}_2\text{O}_3)_m$  :  $m=0.09$ ) films were deposited on p-type  $\text{Si}(100)$  substrate at 800 °C by electron beam evaporation of  $\text{ZrO}_2$  or YSZ pellets at a pressure of  $6.7 \times 10^{-3}$  Pa ( $5 \times 10^{-5}$  Torr). Before deposition, Si substrates were chemically and sequentially cleaned in a hot aqueous solution of HCl and  $\text{H}_2\text{O}_2$ , in an aqueous solution of  $\text{NH}_4\text{OH}$  and  $\text{H}_2\text{O}_2$ , in diluted hydrofluoric acid, and rinsed with deionized water. The Si substrate was electrically heated by the self-resistance. The deposition rate of  $\text{ZrO}_2$  films was about 10 nm/min and thickness was typically about 100 nm.



The films of  $\text{Ba}_2\text{YCu}_3\text{O}_x$  were deposited on  $\text{ZrO}_2/\text{Si}(100)$  or  $\text{YSZ}/\text{Si}(100)$  at  $\sim 700^\circ\text{C}$  by rf magnetron sputtering [8]. The target used was stoichiometric  $\text{Ba}_2\text{YCu}_3\text{O}_x$  powder which was made by sintering the mixture of  $\text{BaCO}_3$ ,  $\text{Y}_2\text{O}_3$  and  $\text{CuO}$  at  $900^\circ\text{C}$  for 8 h in  $\text{O}_2$  atmosphere. Sputtering carried out in ultrapure  $\text{Ar} + 50\sim 60\% \text{O}_2$  atmosphere with sputtering pressure of 0.67 to 4.0 Pa (5 to 30 mTorr). The applied rf power was 150 W for the target of 3 inch diameter. The Si substrate was electrically heated by the self-resistance and the substrate electrode was usually electrically grounded. The deposition rate was typically  $2\sim 4$  nm/min and the film thickness was 100 to 600 nm. The crystallographic properties of  $\text{Ba}_2\text{YCu}_3\text{O}_x$  films were investigated by X-ray diffraction (XRD) and reflection high-energy electron diffraction (RHEED). Stoichiometric and uniform formation of  $\text{Ba}_2\text{YCu}_3\text{O}_x$  films were investigated by X-ray photoelectron spectroscopy (XPS) and Rutherford back scattering (RBS) of 2 MeV  $\text{He}^+$  ion. The temperature dependence of dc resistance of the films was measured by the conventional four-probe method, with dc current. The surface morphology of the films was observed by scanning electron microscope (SEM).

In order to achieve stoichiometry of the films sputtered on the substrate, we put the substrate at off-centered position for the stoichiometric target [11,12]. The substrate position was more than 4 cm away from the anode center and the distance between target and substrates were about 2 cm. The obtained composition by RBS analysis for these films is rather close to the stoichiometry within several percent accuracy, with the wide range of sputtering condition.

## RESULTS AND DISCUSSION

XRD and RHEED pattern of as-grown  $\text{Ba}_2\text{YCu}_3\text{O}_x$  (100 nm thick) on  $\text{ZrO}_2/\text{Si}$  proves the epitaxial growth of tetragonal  $\text{Ba}_2\text{YCu}_3\text{O}_x$  with c-axis perpendicular to the  $\text{ZrO}_2$  layer. The lattice constant  $c_0$  calculated from the Bragg angle of (006) reflection line is  $c_0 = 11.789 \text{ \AA}$  and the oxygen content  $x$  is 6.2 [13]. However, no superconducting transition could be observed for the as-grown films above liquid nitrogen temperature.

To provide a suitable amount of oxygen into the deposited films and protect the films from the bombardment of the charged particles, a positive bias voltage was applied to the substrate since this seems to achieve the surface smoothness and to provide a suitable amount of oxygen to improve the superconducting properties. The applied bias voltage was the positive range from 0 to 50 V. Figure 1 and 2 show XRD and RHEED pattern of as-grown  $\text{Ba}_2\text{YCu}_3\text{O}_x$  (about 200 nm thick) prepared with bias voltage of 40 V for  $\text{YSZ}/\text{Si}(100)$ , respectively. These figures reveal the epitaxial growth of

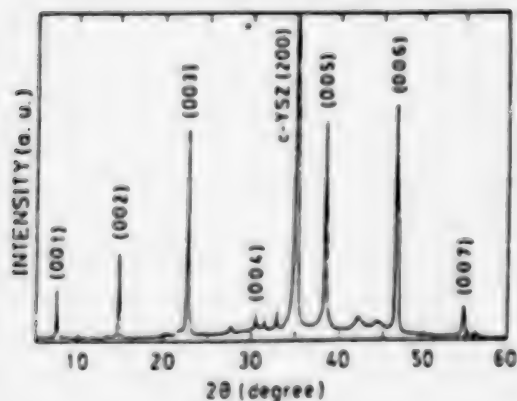


Figure 1  
XRD pattern of the as-grown  $\text{Ba}_2\text{YCu}_3\text{O}_x$  film (200 nm thick) prepared with the positive substrate bias on  $\text{YSZ}/\text{Si}(100)$ .



## CONCLUSIONS

High-Tc superconducting  $\text{Ba}_2\text{YCu}_3\text{O}_x$  thin films have been epitaxially grown on Si(100) substrate using the epitaxially grown tetragonal  $\text{ZrO}_2$  or cubic YSZ as a buffer layer. The films were prepared by rf magnetron sputtering of the target with the stoichiometric composition  $\text{Ba}_2\text{YCu}_3\text{O}_x$  below 700 °C. The as-grown  $\text{Ba}_2\text{YCu}_3\text{O}_x$  thin films prepared with positive substrate bias and with off-centered substrates have very smooth surface and show the superconducting transition above liquid nitrogen temperature without any post-treatment. The highest  $T_c(\text{onset})$  and  $T_c(\text{end})$  observed are 88 K and 84 K, respectively.

## ACKNOWLEDGMENTS

Authors are grateful to Prof. T. Fujita and Dr. Y. Maeno, Faculty of Science, Hiroshima University, for helping with measurements and stimulating discussions. They are also grateful to Prof. M. Hattori and Associate Prof. S. Yamanaka, Faculty of Engineering, Hiroshima University, for giving them chances to use rf magnetron sputtering apparatus.

## REFERENCES

1. J. G. Bednorz and K. A. Müller, Z. Phys. B64, 187 (1986).
2. M. Gurvitch and A. T. Fiory, Appl. Phys. Lett. 51, 1027 (1987).
3. C. Webb, S. L. Weng, J. N. Eckstein, K. Missert, K. Char, D. G. Schlom, E. S. Hellman, M. R. Beasley, A. Kapitulnik and J. S. Harris, Jr., Appl. Phys. Lett. 51, 1191 (1987).
4. C. L. Chien, G. Xiao, F. H. Streitz, A. Gavrin and M. Z. Cieplak, Appl. Phys. Lett. 51, 2155 (1987).
5. A. Mogro-Campero, B. D. Hunt, L. G. Turner, M. C. Barrell and W. E. Balz, Appl. Phys. Lett. 52, 584 (1988).
6. A. Mogro-Campero and L. G. Turner, Appl. Phys. Lett. 52, 1185 (1988).
7. K. Harada, N. Fujimori and S. Yazu, Jpn. J. Appl. Phys. 27, L1524 (1988).
8. H. Myoren, Y. Nishiyama, H. Nasu, T. Imura, Y. Osaka, S. Yamanaka, M. Hattori, Jpn. J. Appl. Phys. 27, L1068 (1988).
9. M. Morita, H. Fukumoto, T. Imura and Y. Osaka, J. Appl. Phys. 58, 2407 (1985).
10. H. Fukumoto, T. Imura and Y. Osaka, Jpn. J. Appl. Phys. 27, L1404 (1988).
11. S. I. Shah and P. F. Garcia, Appl. Phys. Lett. 51, 2146 (1987).
12. N. Terada, H. Ihara, M. Jo, M. Hirabayashi, Y. Kimura, K. Matsutani, K. Hirata, E. Ohno, R. Sugise and F. Kawashima, Jpn. J. Appl. Phys. 27, L639 (1988).
13. A. Ono, Jpn. J. Appl. Phys. 26, L1223 (1987).

# SYNTHESIS AND CHARACTERIZATION OF ARTIFICIALLY LAYERED Bi-Sr-Ca-Cu OXIDE FILMS

JUNICHI SATO\*, MASATSUGU KAISE, SHOZO IKEDA, KEIKICHI NAKAMURA  
AND KEIICHI OGAWA

NATIONAL RESEARCH INSTITUTE FOR METALS, 1-2-1 SENGUN TSUKUBA 305, JAPAN  
\*HITACHI CABLE LTD, 3-1-1 SUKEGAWACHO HITACHI 317, JAPAN

## ABSTRACT

The Bi-O/Sr-Ca-Cu-O multilayered films have been synthesized by two target reactive magnetron sputtering. It is shown that the modulation wave length  $\Lambda$ , corresponding to  $c/2$  of the crystal, can be simply controlled by varying the deposition time for one layer unit of Sr-Ca-Cu-O while that for Bi-O being kept constant. The resultant films have been found to have smooth surface and have  $\Lambda$  ranging from 12 to 26 Å which is almost equal to the lattice constant  $c/2$  found in the bulk Bi-Sr-Ca-Cu-O system. The layered structure has been confirmed by transmission microscopy. Their thermal stability will also be reported.

## INTRODUCTION

Soon after the discovery of multiphase oxide superconductors in the Bi-Sr-Ca-Cu-O system [1], it was realized that these phases can be distinguished by the number of  $\text{CuCaO}_2$  perovskite layers sandwiched by two  $\text{BiSrO}_{3/2}$  layers [2]. Frequent observations of many phases having different numbers of  $\text{CuCaO}_2$  layers, i.e.  $\text{Bi}_2\text{Sr}_2\text{Ca}_n\text{Cu}_{n+1}\text{O}_x$  ( $n=0-4$ ) [3] suggest that the free energy of these phases has no sharp minimum against the number of  $\text{CaCuO}_2$  layers. In contrast to the difficulty of obtaining a single phase by the conventional solid state reaction, it becomes recently clear that the multilayer deposition technique is one of the most promising methods to obtain a single phase having the desired layer thickness [4 and 5]. We have attempted to synthesize films with  $n=0$  to 4 using the two target multilayer deposition technique. We shall report some new results on the structure and superconducting property of these films.

## EXPERIMENTAL

The deposition technique used was two target reactive dc and rf magnetron sputtering. Targets were metallic Bi (dc) and sintered oxide Sr-Ca-Cu-O (rf) with a cationic ratio 2:2:2 in the above order. The reactive gas was Ar-10%O<sub>2</sub>, which was blown directly to the substrate through oxygen nozzles. The total pressure during the sputtering measured in the vicinity of the targets was 1 to 1.2 Pa. The substrate was cleaved (001) MgO and the substrate temperature ( $T_s$ ) was varied from RT to 700°C. The modulation wave length  $\Lambda$  was adjusted by changing the sequential deposition time for each layer, typically 5W x 9s for the Bi-O layer and 140W x 16 to 36s for the Sr-Ca-Cu-O layer; the sequence was repeated 100 times to obtain a multilayered film. To see the effect of annealing, the films were post-annealed in air at 660, 730, 810, 850 and 870°C for 1 to 3 h. The resultant films were characterized by the conventional  $\theta-2\theta$  Cu K $\alpha$  X-ray diffraction (XRD), and by taking EDAX analysis, high resolution SEM images (HRSEM) and high resolution transmission electron micrographs. The electrical resistivity was measured by the conventional four probe method.



## RESULTS AND DISCUSSION

In order to obtain a desired modulation wavelength  $\Lambda$  of a multilayered film deposited at a given substrate temperature, we have kept the deposition time for the Bi-O layer constant and varied that for the Sr-Ca-Cu-O layer. When the  $\text{Sr}_2\text{Ca}_2\text{Cu}_2$  oxide target alone was sputtered on to the substrate kept at room temperature, the composition became approximately 1:1:1, i.e.  $\text{Cu}/(\text{Ca}+\text{Sr})=0.5$ . When the Bi and oxide targets were sputtered alternately to form a multilayered film, the composition of the film, i.e.  $\text{Cu}/(\text{Ca}+\text{Sr})$  was found to depend significantly on the amount of Bi in the film. Figure 1 shows such a relation observed in the films deposited at various substrate temperatures. The Sr to Ca ratio in the films was almost independent of the sputtering conditions and was found to be around 0.8. The thick line in the figure shows a relation between the  $\text{Cu}/(\text{Sr}+\text{Ca})$  ratio and Bi concentration calculated from the ideal composition  $\text{Bi}_n\text{Sr}_2\text{Ca}_2\text{Cu}_{n+1}\text{O}_x$ . The observed dependence of the  $\text{Cu}/(\text{Sr}+\text{Ca})$  on the Bi concentration (and consequently on  $\Lambda$ ) tells us that the sticking coefficient of each component is not only the function of the substrate temperature but also of the relative concentration of each component. Any deviation from the ideal composition, i.e.  $n=0,1,2,\dots$ , indicates the presence of chemical disorder in the present film.

Figure 2 shows the X-ray diffraction patterns of the multilayered films deposited at  $T_s=650^\circ\text{C}$ . The index  $2.2.n.(n+1)$  in the figure shows that the produced film was attempted to simulate to  $\text{Bi}_n\text{Sr}_2\text{Ca}_2\text{Cu}_{n+1}\text{O}_x$  ( $n=0-4$ ). All the diffraction lines can be assigned to (00 $l$ ). Those patterns for  $n=0$  to 3 are nearly similar to the recently published results [4] except for the fact that the present patterns show no significant peaks arising from impurity phases such as CuO. Since the diffraction peaks observed at  $2\theta=29^\circ$  (Figure 2) arise from a single unit of stacking, the present as-deposited multilayered film must be crystalline.

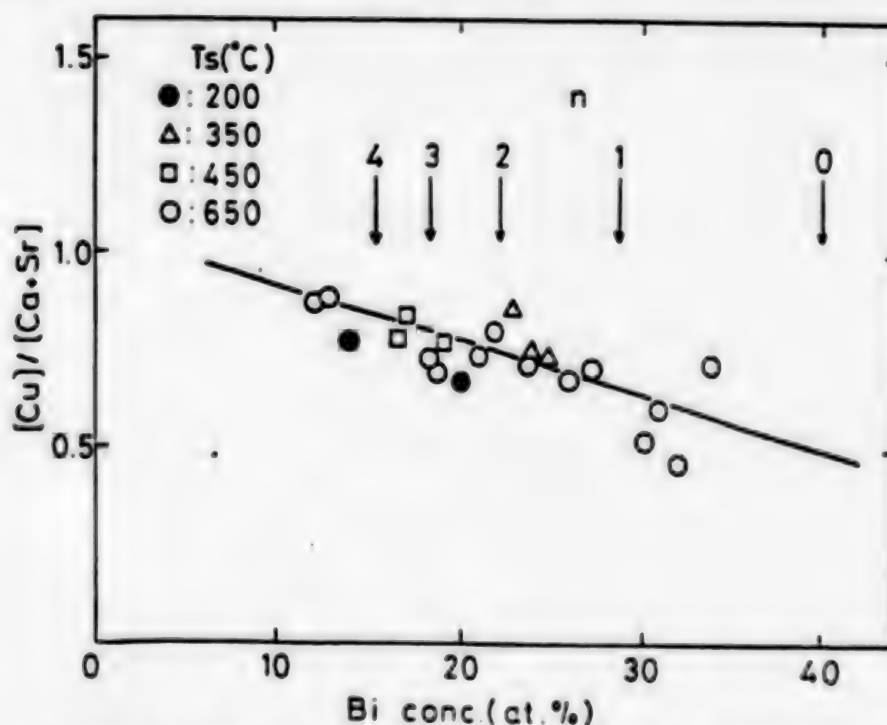


Figure 1 The molar ratio  $\text{Cu}/(\text{Ca}+\text{Sr})$  vs Bi concentration (atomic fraction of cationic ions) in as-deposited multilayered films.

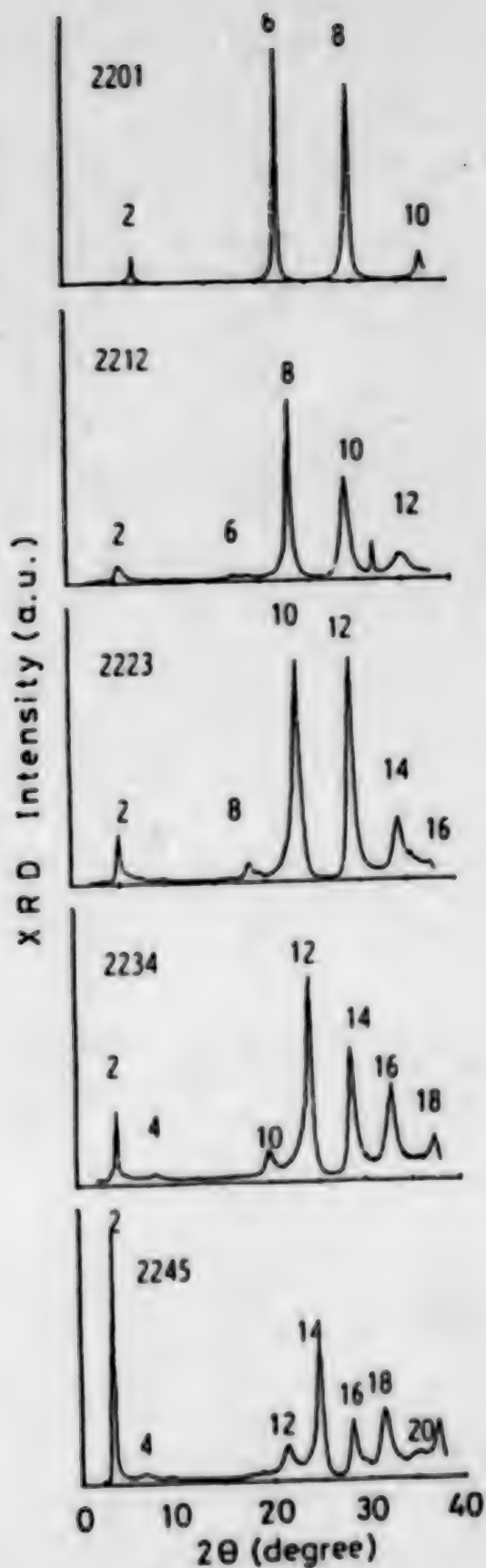


Figure 2 X-ray (Cu K $\alpha$ ) diffraction pattern of the as-deposited multilayered films (Ts=650°C), simulated to the 2201, 2212, 2223, 2234 and 2245 phases, respectively. The integer  $g$  marked on the diffraction lines represents the index  $g$  of the diffraction line arising from  $(00g)$  planes.

The HRSEM image shows that the surface of the present multilayered film is smooth indeed and neither grain boundaries nor precipitates are found in the figure. The smooth surface is in contrast with that of the films sputtered from a single composite target of Bi-Sr-Ca-Cu oxide onto the same substrate kept at 650°C, in which many fine grains were found to grow. The resistivity vs temperature curve of the as-deposited multilayered film was characteristic of semiconductor, unexpectedly from the layered superconducting perovskite structure. When the film was annealed above 810°C, it became superconducting except for the film of the shortest A, i.e. the one simulated to 2201.

Figure 3 shows a high resolution transmission electron micrograph of the cross section of the multilayered 2234 film which was annealed for 1 h at 810°C. Well developed layered structures are clearly seen in the figure. The lattice constant  $c$  is evaluated to be 43 Å which is in agreement with the expectation from the 2234 composition. In some portions of the figure the characteristic strain field modulation is also observed.

The X-ray and HRSEM studies, however, showed that the major phase 2234 decomposed into the 2212 and 2201 phases on the surface of the multilayered 2234 film when annealed for 1 h at 850°C. More detailed studies on the thermal stability will be reported in the conference.

Main parts of this report were based on the paper to appear in Jpn. J. Appl. Phys. Letter.



Figure 3 The high resolution transmission electron micrograph of the cross section for the multilayered 2234 film.

#### REFERENCES

- [1] H. Maeda, Y. Tanaka, M. Fukutomi and T. Asano, Jpn. J. Appl. Phys. 27(1988)L209.
- [2] R.M. Hazen, L.W. Finger, R.J. Angel, C.T. Prewitt, N.L. Ross, C.C. Hadjilacos, P.J. Heaney, D.R. Veblen, Z.Z. Sheng, A. El Ali, A.M. Herman, Phys. Rev. Lett. 60(1988)1657.
- [3] S. Ikeda, H. Tchinose, T. Kimura, T. Matsumoto, H. Maeda, Y. Ishida and K. Ogawa, Jpn. J. Appl. Phys. 27(1988)L999.
- [4] H. Adachi, S. Kohiki, K. Setsune, T. Mitsuya and K. Wasa, Jpn. J. Appl. Phys. 27(1988)L1883.
- [5] J. Sato, M. Kaise, K. Nakamura and K. Ogawa, to be published in Proceeding of the Conference on the Science and Technology of Thin Film Superconductors; Colorado Springs (Nov. 14-17th, 1988).

# EPITAXIAL FILM GROWTH OF ARTIFICIAL (BiO)(SrCaCuO) LAYERED STRUCTURE

J. FUJITA, \*T. TATSUMI, T. YOSHITAKE, AND H. IGARASHI  
FUNDAMENTAL RESEARCH LABORATORIES

\*MICROELECTRONICS RESEARCH LABORATORIES, NEC CORPORATION  
4-1-1 Miyazaki, Miyamae-ku, Kawasaki, 213, Japan

## ABSTRACT

Epitaxial film growth of artificial (BiO)(SrCaCuO) layered structures on MgO substrate was studied by using oxygen-gas-reactive dual ion beam sputtering and shuttering technique. Single phase films having periodicities of 12, 15, and 18Å (which are identical to bulk 24, 30, and 36Å phases) were selectively grown by adjusting the thickness of SrCaCuO layer sandwiched by BiO bi-planes. High  $T_c$  phase film with total thickness of about 300Å showed an onset  $T_c$  of 110K and a  $T_c$  end point of 45K without post-deposition annealing. The shuttering technique seems to enable the layer by layer film growth and it is very effective for the formation of smooth and perfect epitaxial structure.

## INTRODUCTION

Epitaxial film growth of the recent high  $T_c$  oxide superconductors[1,2,3] are quite important not only for application to electrical devices but also for studying superconducting properties of the oxides and thus contributing to the basic understanding of superconducting mechanism[4,5]. The Bi oxide superconductors have quite attractive layered structure where BiO bi-planes sandwiches SrCaCuO perovskite type layers and the origin of the high temperature superconductivity is considered to relate to the layered structure. The purpose of this research is to investigate the possibility of artificial structure control of the oxide superconductors. In this study, we used oxygen-gas-reactive[6,7] dual ion beam sputtering[8,9]. Ion beam sputtering seems to provide the best controllability for flux rate of oxide source material because of the sputtering beam stability in oxygen environment and to have an advantage for the substrate being free from the influence of sputtering plasma. The shuttering technique for epitaxial film growth is expected to enable a new artificial structure which could not be synthesized by thermal equilibrium process.

## EXPERIMENTAL

The sputtering system is provided with two sputtering sources and two shutters controlled by microcomputer connected with film thickness monitors. An electron gun is also equipped for in situ observation of reflected high energy electron diffraction(RHEED). Two Kaufman type ion sources having hollow cathode(Ion Tech) were used for sputtering and the space inside the vacuum chamber was neutralized by a hollow cathode neutralizer. Oxygen gas was directed to the substrate from the special gas nozzle which encircles the substrate to keep the uniformity of gas pressure at the substrate. The substrate temperature and the oxygen gas pressure at the substrate were fixed to typical values of 605°C and  $6 \times 10^{-5}$  torr respectively. The targets of  $\text{Bi}_2\text{O}_3$  and  $\text{Sr}_2\text{Ca}_2\text{Cu}_3\text{O}_x$  were used and film growth rate was about 0.18Å for Bi oxide and 0.10Å for SrCaCuO. Film growth by shuttering technique is performed by controlling the shutter-opening-time for each source material. In this experiments, all film structure was fixed to



first 12Å of SrCaCuO buffer layer and additional 16 periods of (BiO)(SrCaCuO) layers which is identical to 8 unit cells of bulk superconductor. The buffer layer thickness of about 12Å seems to be crucially important to achieve perfect epitaxial orientation on MgO substrate, which the buffer relaxed the lattice mismatching between the MgO substrate and film. We additionally put a 4 minute interval between each deposition. The X-ray diffraction patterns suggested the 4 minute interval dramatically improved the crystal quality of the layered structure. After film growth, films were quickly cooled down to below 150°C within 60 minutes at the same oxygen pressure for deposition. Film characterizations were carried out by mainly in-situ RHEED, X-ray diffraction and 4-probe resistivity measurement.

## RESULTS AND DISCUSSION

Film growth of artificial (BiO)(SrCaCuO) layered structures were successfully performed on (100)MgO surface with 12Å SrCaCuO buffer layer. Fig.1 shows the sequential change of RHEED patterns along  $\langle 100 \rangle$  and  $\langle 110 \rangle$  MgO azimuths during film growth. The film structure was designed to have periodicities of (BiO:5.5Å)(SrCaCuO:10Å). Fig.1(a) and (e) are the patterns of the MgO substrate with  $\langle 100 \rangle$  azimuth and  $\langle 110 \rangle$  azimuth, respectively. Fig.1(b) and (f) are the patterns after growing the 12Å of SrCaCuO buffer layer. The diffused pattern indicated the lattice relaxation of buffer at the surface. Fig.1(c) and (g) show the patterns after the growth of 8 periods ( corresponding to 4 units cell of the bulk phase ) on buffer. Fig.1(d) and (h) show the pattern after 16 unit layers. The distinct steaks suggests that the extremely smooth and highly ordered film surface. The epitaxial relationship is  $[100]\text{BiSrCaCuO}/[100]\text{MgO}$ . The center lines and the strong streaks on the both sides are indexed as (000), (200), and (200). The clear but weak superspots due to the incommensurate modulation which exist along b-axis in a bulk single crystal also appears along both the MgO  $\langle 100 \rangle$  and  $\langle 010 \rangle$  azimuth, which indicates that is composed of two sets of epitaxial grains, originating from two equivalent directions of incommensurate structure.

Table.1 Results of artificial Film Growth

Sample No	designed <BiO/SrCaCuO> (Å)	periodicity $\Lambda \times 2$ (Å)	structure second phase	Tc (k) onset-end
(a)	<5.5/13>	36.8	+	110 - 45
(b)	<5.5/8.5>	30.1	not detected	70 - 25
(c)	<5.5/6.5>	24	not detected	non super

symbol "+" indicated the film contains a small amount of second phase

The periodicities of epitaxial films were artificially controlled by adjusting the thickness of SrCaCuO layer. Fig.2 shows the X-ray diffraction patterns of the films with (a)36.8Å, (b)30.1Å, and (c)24Å phases and these result are summarized in Table.1. Diffraction patterns of Fig.(b) and (c) show the intensity oscillation at low angle diffraction caused from extremely thin and smooth film. The peak to peak angle of low angle oscillation indicated the film thickness about 300Å which is identical to the designed value of the film thickness. The superconductivity of as grown film with 18Å periodicity (which is identical to 36Å phase of bulk crystal)

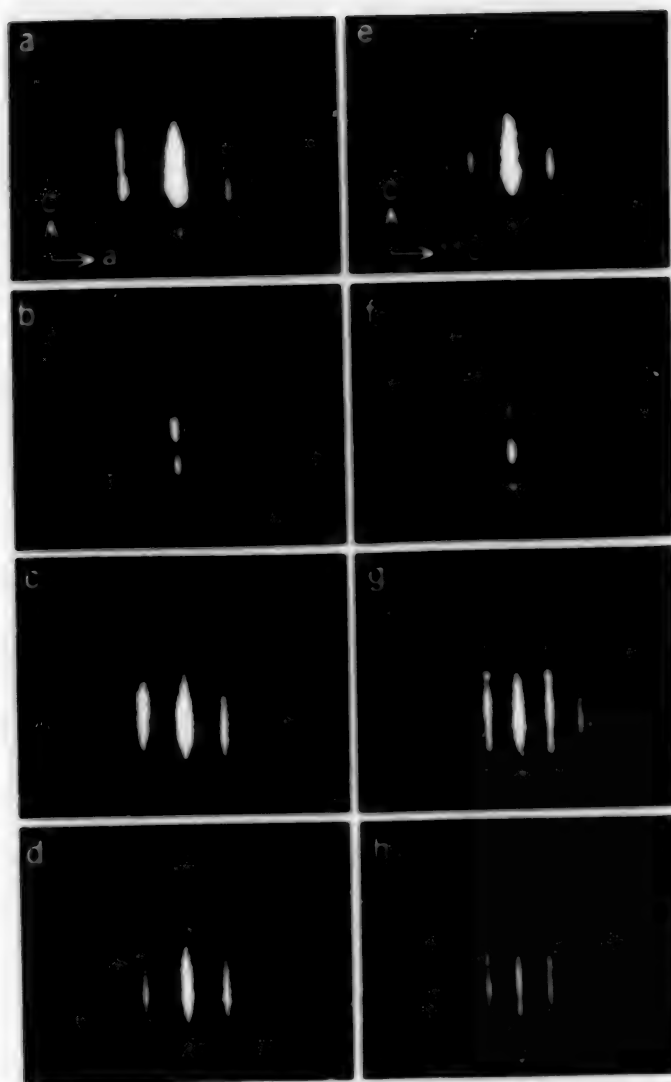


Fig.1 Sequence of RHEED pattern of perfect epitaxial film.

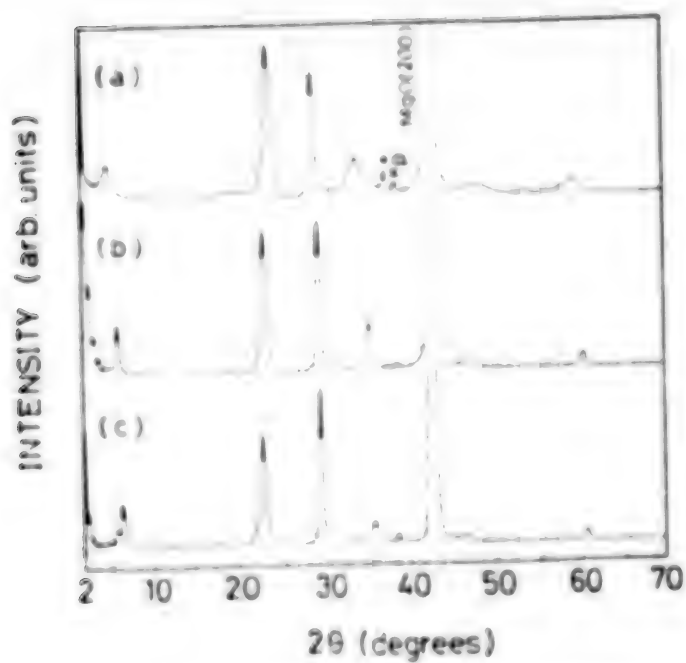


Fig.2 Typical X ray diffraction patterns.

shows a  $T_c$  onset of 110K and the end point of 45K without post-deposition annealing. The depressed  $T_c$  compared with the bulk high  $T_c$  phase may indicate the insufficient oxidation during film growth.

## SUMMARY

In conclusion, we demonstrated the artificial (BiO)/(SrCaCuO) layered structures epitaxially grown on (100) MgO substrate by using oxygen-gas-reactive dual ion beam sputtering. Films with artificial periods of 12, 15, and 18Å were selectively prepared by controlling the SrCaCuO layer thickness. The shuttering is very effective to form the smooth and epitaxial films. The layer by layer film growth seems to be achieved.

## ACKNOWLEDGMENT

The authors would like thank T.Satoh for composition analysis, M.Sugimoto for electrical measurements, and Y.Kubo for helpful discussion. We are also grateful for the support from M.Yonezawa and K.Utsumi during the course of this research.

## REFERENCE

1. J.G.Bednorz and Muller, Z.Phys.B64,189(1986).
2. M.K.Wu, J.R.Ashburn, C.J.Torng, P.H.Hor, R.L.Meng, L.Gao, Z.J.Haung, Y.Q.Wang, and C.W.Chu, Phys.Rev.Lett.58,908(1987).
3. H.Maeda, Y.Tanaka, M.Fukutomi, and T.Asano, Jpn.Appl.Phys.Lett. 27,L209(1988)
4. J.S.Tsai, I.Takeuchi, J.Fujita, T.Yohitake, S.Miura, S.Tanaka, Y.Bando, K.Iijima, and K.Yamamoto. Proceedings of the international Conference on "High Temperature Superconductors and Materials and Mechanisms of Superconductivity" Part 2,1385. February 28-march 3, 1988, Interlaken, Swizerland.
5. T.Yoshitake, T.Satoh, Y.Kubo, T.Manako, H.Igarashi, Jpn.J.Appl.Phys.Lett.27,L1094(1988)
6. T.Terashima, K.Iijima, K.Yamamoto, Y.Bando, and M.Mazaki, Jpn.J.Appl.Phys.Lett.27,L91(1988).
7. N.Missert, R.Hammond, J.E.Mooij, V.Matijasevic, P.Rosenthal, T.H.Geballe, A.Kapitulnik, M.R.Beasley, S.S.Laderman, C.Lu, E.Garwin, R.Barton. preprint
8. J.Fujita, Y.Yoshitake, A.Kamijyo, T.Satoh, and H.Igarashi, J.Appl.Phys.64,1292(1988)6.
9. J.Fujita, Y.Yoshitake, A.Kamijyo, T.Satoh, and H.Igarashi Conference Proceedings on Ion Beam Modification of Material, June 4,1988, Tokyo,Japan. submitted for publication.

## GROWTH OF C-AXIS ORIENTED Tl-Ca-Ba-Cu-O THIN FILMS

Yo ICHIKAWA, Hideaki ADACHI, Kentaro SETSUNE & Kiyotaka WASA  
CENTRAL RESEARCH LABORATORIES, MATSUSHITA ELECTRIC INDUSTRIAL CO., LTD.  
HORIGUCHI, OSAKA 570, JAPAN

### ABSTRACT

Superconducting thin films of the Tl-Ca-Ba-Cu-O system with a c-axis orientation were prepared on (100) MgO substrates by rf magnetron sputtering and subsequent annealing. The growth of superconducting phases is strongly dependent on the annealing condition. Highly c-axis oriented films comprised of 2122, 2223, 1223 and 1324 phase were synthesized by controlling the annealing conditions and varying film thickness. These annealed films exhibited superconductivity with the zero-resistance temperature above 100 K and the critical current density larger than  $10^5$  A/cm<sup>2</sup> at 77 K.

### INTRODUCTION

Rare-earth-free superconductors of the Bi-oxide system [1] and the Tl-oxide system [2] have drawn considerable attention and have been studied by many researchers. It is well known that superconducting systems have some superconducting phases with different  $T_c$  for the number of Cu-O<sub>2</sub> layers between the Bi-O or Tl-O bilayers. The number of Cu-O<sub>2</sub> layers is two for the lower  $T_c$  phase with a composition ratio of 2:1:2:2 in Bi:Ca:Sr:Cu or Tl:Ca:Ba:Cu (2122 phase) and three for the higher  $T_c$  phase with that of 2:2:2:3 (2223 phase). Recently, new phases of the form TlCa<sub>n-1</sub>Ba<sub>2</sub>Cu<sub>n</sub>O<sub>2n+3</sub> were discovered for n=1-5 [3,4]. This new Tl oxide system contains n Cu-O<sub>2</sub> layers between the Tl-O monolayer. In order to investigate an essential mechanism of these superconductors and apply to electronic devices, much effort has been paid for the development of the high-quality superconducting thin films [5-7]. We have succeeded in the preparation of highly oriented c-axis Tl<sub>2</sub>Ca<sub>2</sub>Ba<sub>2</sub>Cu<sub>3</sub>O<sub>x</sub> [8], Tl<sub>2</sub>Ca<sub>1</sub>Ba<sub>2</sub>Cu<sub>2</sub>O<sub>x</sub> [9] and Tl<sub>1</sub>Ca<sub>3</sub>Ba<sub>2</sub>Cu<sub>4</sub>O<sub>x</sub> [10] thin films by rf magnetron sputtering. In this paper, growth conditions of some superconducting phases in thin films are reported.

### EXPERIMENTAL RESULTS AND DISCUSSION

Tl-Ca-Ba-Cu-O thin films were deposited onto polished (100) MgO substrates using an rf-planar magnetron sputtering system. The target was obtained by reacting a mixture of BaCO<sub>3</sub> (99.9%) and CuO (99.9%) at 880 °C for about 8 h in air followed by sintering a mixture of Tl<sub>2</sub>O<sub>3</sub> (99.5%), CaCO<sub>3</sub> (99%) and previously reacted BaCO<sub>3</sub>+CuO powders in a covered alumina crucible at 910 °C for about 8 h in air. The typical sputtering conditions are shown in Table I. The sputtering time was changed between 1 h and 10 h yielding thicknesses of the as-sputtered films ranging from 0.4 μm to 4 μm. The structure of the films was characterized by an X-ray diffraction technique with Cu K<sub>α</sub> radiation. The composition of the films was determined by inductively coupled plasma-emission spectrometry and electron-probe X-ray microanalyses. The temperature dependence of the resistivity was measured by the standard dc four-probe method with



Table I. Sputtering conditions.

Target	Tl:Ca:Ba:Cu=2:2:1-2:3 (10 cm in diameter)
Substrate	(100)MgO
Substrate temperature	200 °C (not controlled)
Sputtering gas	Ar:O <sub>2</sub> =1:1
Gas pressure	0.5 Pa
rf input power	100 W
Deposition rate	0.4 μm/h

gold electrodes deposited on the films surface. The as-sputtered films were generally an insulator in the amorphous state.

In order to obtain superconductivity, heat treatments were carried out in an electric furnace under oxygen gas stream. Following two methods were tried for these treatments; (1) the specimens were annealed in the alumina crucible supplying Tl vapor, (2) the specimens were wrapped in gold foil and annealed.

First, the results for the former annealing method with the supply of Tl vapor are reported. The Tl-Ca-Ba-Cu-O thin films of 0.4 μm and 2 μm in thickness were annealed at 900 °C for 1 min in order to investigate the growth of superconducting phase in the different film thickness. The deposited films were obtained from the sputtering target of Tl<sub>2</sub>Ca<sub>2</sub>Ba<sub>1</sub>Cu<sub>3</sub>O<sub>x</sub>. By XRD analyses, the 2122 phase was confirmed for the 0.4-μm thick film and the 2122 and 2223 phases were confirmed for the 2-μm thick film.

The XRD patterns of 2-μm thick Tl-Ca-Ba-Cu-O thin films obtained for various annealing time at 900 °C are shown in Fig.1. The 2122 phase was dominant in the films annealed for the annealing time shorter than 3 min. On the other hand, in the films annealed for the annealing time longer than 3 min, the 2223 phase was dominant. In case of the annealing time longer than 10 min, only the 2223 phase was observed. This film showed highly c-axis orientation with lattice constant c of 35.6 Å. The highest onset temperature of 125 K and the zero-resistance temperature of 118 K were obtained when the film was annealed for 13 min at 900 °C. The critical current density was larger than 10<sup>5</sup> A/cm<sup>2</sup>. When the 2-μm thick film was annealed at 890 °C for 13 min, the crystal structure consisted of the 2122 and the 2223 phases. When films were annealed at 910 °C for 13 min, crystal structure constructed by single phase of 2223 was obtained, but these onset temperatures were lower than those for the films annealed at 900 °C for 13 min. Further, the thin film of the 2122 phase with the zero-resistance temperature of 102 K and the critical current density larger than 10<sup>5</sup> A/cm<sup>2</sup> at 77 K could be obtained when the 0.4-μm film was prepared from the Tl<sub>2</sub>Ca<sub>2</sub>Ba<sub>2</sub>Cu<sub>3</sub>O<sub>x</sub> sputtering target and annealed at 900 °C for 1 min. This film exhibited a highly c-axis orientation with lattice constant of c=29.25 Å.

Secondly, the results obtained for the annealing by using gold foil are referred. In order to investigate the effect of the annealing conditions on the crystal structure and the superconducting properties of the films, the annealing temperature was varied between 890 and 910 °C, and the annealing time was set to 1 or 2 min. Figure 2 shows the X-ray diffraction patterns for four annealed films with different thickness. The films were prepared from a Tl<sub>2</sub>Ca<sub>2</sub>Ba<sub>1</sub>Cu<sub>3</sub>O<sub>x</sub> target and annealed at 900 °C for 1 min. As is seen in Fig.2, all of the X-ray patterns show sharp

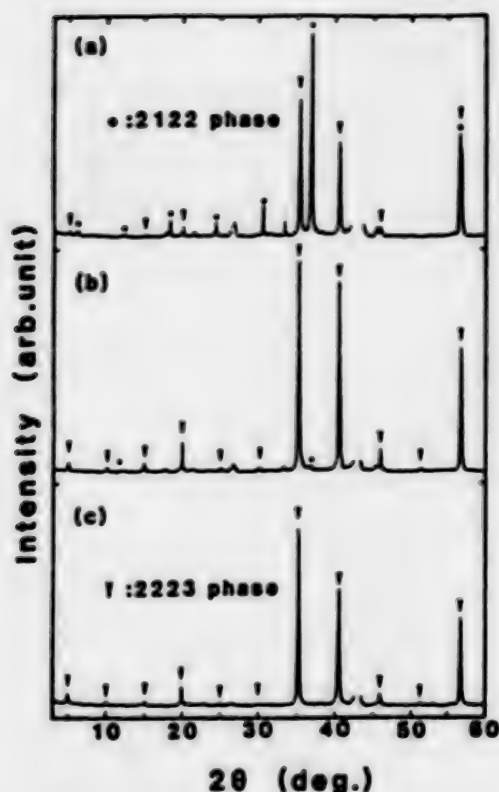


FIG.1. X-ray diffraction patterns for 2- $\mu$ m thick Tl-Ca-Ba-Cu-O films annealed by supplying Tl vapor at 900 °C for different time: (a) 3, (b) 5 and (c) 11 min. Dark spots and arrows indicate c-planes of 2122 phase and 2223 phase, respectively.

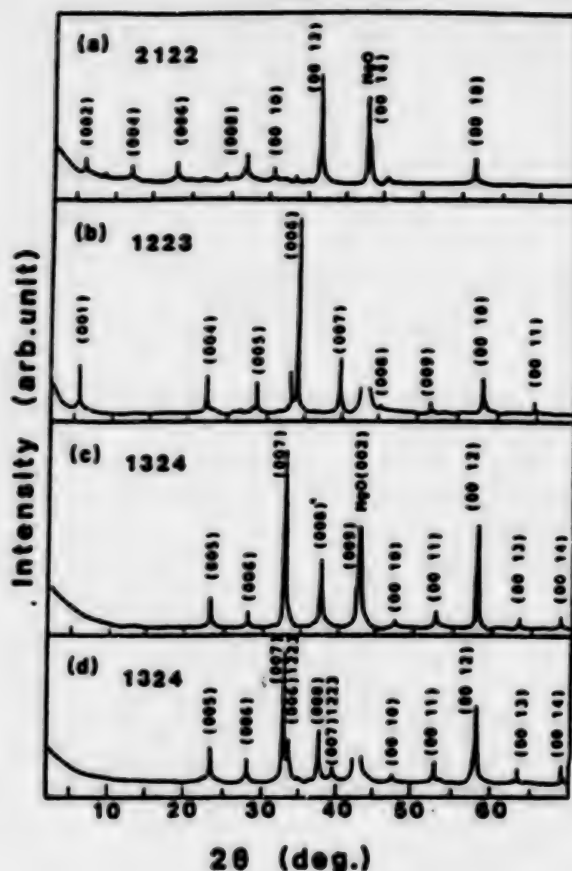


FIG.2. X-ray diffraction patterns for Tl-Ca-Ba-Cu-O films annealed by Au foil at 900 °C for 1 min with different thickness: (a) 0.4, (b) 1.2, (c) 2 and (d) 2.8  $\mu$ m.

periodical peaks. These patterns suggest that the c-axis orientation normal to substrate surface was obtained on the crystal structure of these films. For the films with 2 and 2.8  $\mu$ m thicknesses, their (00m) peaks shown in Figs.2(c) and (d) can be assigned by the diffraction of the  $\text{Tl}_1\text{Ca}_3\text{Ba}_2\text{Cu}_4\text{O}_x$  (1324 phase) with the lattice constant  $c=19.05$  Å. This value agrees well with the result reported for bulk materials [4]. The appearance of the peaks corresponding to the  $\text{Tl}_1\text{Ca}_2\text{Ba}_2\text{Cu}_3\text{O}_x$  (1223 phase) in the diffraction pattern of the 2.8- $\mu$ m thick film indicates that this sample also contains a small amount of the 1223 phase. In both annealed films, the (001) reflection was not observed. For the film with 0.4  $\mu$ m thickness, its diffraction pattern shown in Fig.2(a) is dominated by the regularly spaced (00m) peaks of the 2122 phase. The diffraction pattern for the 1.2  $\mu$ m thick film shown in Fig.2(b) is found to correspond to the 1223 phase with lattice constant of  $c=15.9$  Å [7]. The above experimental results indicate that the growth of these phases under the same annealing conditions depends on the thickness of the films. This phenomenon may be attributed to the decrease of the Tl content in films with the increase

of the film thickness. The 2- $\mu\text{m}$  thick film showed the highest onset temperature of 120 K and zero-resistance temperature of 113 K in these annealed films. The critical current density of about  $10^5 \text{ A/cm}^2$  was obtained at 77 K.

To obtain the optimum annealing conditions for the formation of the 1324 phase with a high c-axis orientation, the 2- and 2.8- $\mu\text{m}$  thick films were annealed at various temperature for 1 and/or 2 min. The crystal phases, onset temperature and zero-resistance temperature were investigated on these annealed films. The 1223 phase appeared when the films were annealed at 900 °C for 2 min and at 910 °C for 1 or 2 min. The onset temperature and contents of Ca and Cu decreased with the increase of the annealing temperature and annealing time. It can be concluded that the annealing at 900 °C for 1 min is most suitable to obtain the 1324 phase. The increase of the annealing temperature and time resulted in the relative decrease of Cu content. This decrease is considered to be the cause for growth of 1223 phase. We believe that relatively high Cu and Ca contents are necessary for the formation of the 1324 phase in thin films. The annealing at 890 °C usually gives the 2122 phase which contains a higher Tl content than the 1324 and/or the 1223 phase.

In conclusion, we have succeeded in the preparation of highly oriented c-axis Tl-Ca-Ba-Cu-O thin films with 2122, 2223 and 1324 phases by rf magnetron sputtering and post annealing. It can be concluded that the annealing with supplying Tl vapor is suitable to obtain the phase with the Cu-O<sub>2</sub> layers between the Tl-O bilayers and the annealing with Au foil to avoid a decrease of Tl is suitable to obtain the phase with the Cu-O<sub>2</sub> layers between Tl-O monolayers. The critical current density at 77 K was larger than  $10^5 \text{ A/cm}^2$  for all the superconducting phases. The larger critical current density can be expected by the finer controlled supply of Tl vapor at the annealing.

The authors would like to thank Drs. S.Hatta, J.Zhou, S.Kawashima and T.Mitsuyu for their useful discussions.

## REFERENCES

1. H.Maeda, Y.Tanaka, M.Fukutomi and T.Asano: Jpn.J.Appl.Phys. 27(1988)L209.
2. Z.Z Sheng and A.M.Hermann: Nature 332(1988)138.
3. S.S.P.Parkin, V.Y.Lee, A.I.Nazzari, R.Savoy and R.Beyers: Phys.Rev.Lett. 61(1988)750.
4. H.Ihara, R.Sugise, M.Hirabayashi, N.Terada, M.Jo, K.Hayashi, A.Negishi, M.Tokumoto, Y.Kimura and T.Shimomura: Nature 334 (1988)510.
5. M.Nakao, R.Yuasa, M.Nemoto, H.Kuwahara, H.Mukada and A.Mizukami: Jpn.J.Appl.Phys. 27(1988)L849.
6. W.Y.Lee, V.Y.Lee, J.Salem, T.C.Huang, R.Savoy, D.C.Bullock and S.S.P.Parkin: Appl.Phys.Lett. 53(1988)329.
7. T.C.Huang, W.Y.Lee, V.Y.Lee and R.Karimi: Jpn.J.Appl.Phys. 27(1988)L1498.
8. H.Adachi, K.Wasa, Y.Ichikawa, K.Hirochi and K.Setsune: J. Cryst. Growth 91(1988)352.
9. Y.Ichikawa, H.Adachi, K.Setsune, S.Hatta, K.Hirochi and K.Wasa: Appl.Phys.Lett. 53(1988)919.
10. J.Zhou, Y.Ichikawa, H.Adachi, T.Mitsuyu and K.Wasa: Jpn. J. Appl. Phys. 27(1988)L2321.

MICROSTRUCTURE DEPENDENCE OF CRITICAL CURRENT DENSITY  
IN Ag SHEATHED  $\text{Ba}_2\text{YCu}_3\text{O}_{6+x}$  TAPES

K. OSAMURA  
DEPARTMENT OF METALLURGY, KYOTO UNIVERSITY  
SAKYO-KU, KYOTO 606, JAPAN

## ABSTRACT

In order to improve the critical current density of Ag sheathed tapes, various attempts have been tried to make tapes as thin as possible. The pressing was most effective at present for obtaining a large critical current density. Also the use of hydrogen gas reduced powder was effective to eliminate the thermal induced microcracks and resulted in the improvement of the critical current. The best value of the critical current density in the present study was  $3280 \text{ A/cm}^2$  at 77K.

## INTRODUCTION

The present oxide,  $\text{Ba}_2\text{YCu}_3\text{O}_{6+x}$ , was found to have potentially the promising superconducting properties. The superconducting critical current of the thin film prepared by CVD technique has been recently reported to be very high at 77.3 K, exceeding  $6 \times 10^4 \text{ A/cm}^2$  even at 27 T [1]. In the technological view point for manufacturing the long scale magnetic wires, it is necessary to develop a more sophisticated mass productive process. The so called powder-in-tube technique is very vital for this purpose. In order to achieve high transport critical current for the composites of sintered powder sheathed by silver tube, several techniques for improving this process have been developed till now. The situation has been recently reviewed [2]. In this report, the effect of cold-working on the critical current density as well as the use of hydrogen gas reduced powder will be discussed from the microstructural viewpoint.

## EXPERIMENTAL PROCEDURE

The process employed here was essentially a conventional powder-in-tube method, of which the detail was reported elsewhere [3,4]. The mixture of  $\text{BaCO}_3$ ,  $\text{Y}_2\text{O}_3$  and  $\text{CuO}$  powders with stoichiometric proportion according to the formula  $\text{Ba}_2\text{YCu}_3\text{O}_{6+x}$  was calcined at 1173 K for 173 ks. Instead of  $\text{Y}_2\text{O}_3$ , the rare earth oxide,  $\text{Ho}_2\text{O}_3$ , was used in a part of the experiments. The product was reground and filled in a silver tube with inner diameter (I.D.) of 4 mm. The composite was deformed to the tape by the following alternative cold - working techniques. (1) After it was thinned intermediately by a grooved - rolling, the wire with I.D. of about 1 mm was cold-rolled to make tape specimen. The thickness of oxide layer in the tape was controlled in the range between 500 and  $30 \mu\text{m}$ . (2) After it was thinned by wire - drawing up to 0.2 mm I.D., the wire was finally cold - pressed. The above two techniques are called "cold - rolling" and "cold - pressing", respectively. Both silver sheathed tape specimens were heat - treated at 1203 K for 72 ks and then cooled gradually with cooling rate of 5 K/min. In case of the cold-rolling technique, the hydrogen gas reduced powder was partially used, of which details have been reported elsewhere [3]. The reduced powder consisted of  $\text{BaO}$ ,  $\text{Y}_2\text{O}_3$  (or  $\text{Ho}_2\text{O}_3$ ) and metallic copper.



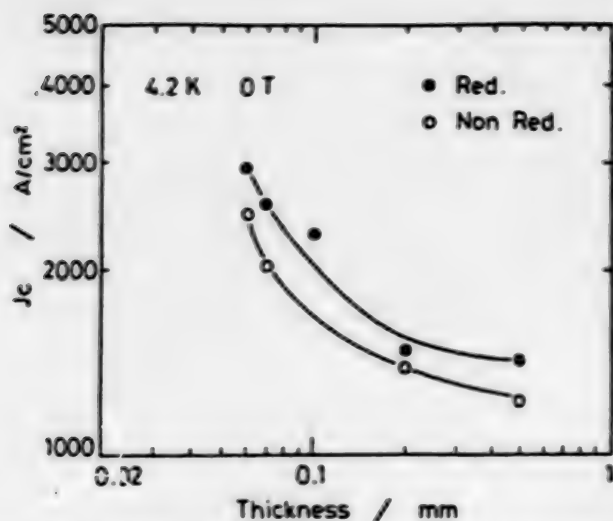


Fig. 1 Critical current density as a function of tape-thickness of  $\text{Ba}_2\text{YCu}_3\text{O}_{6+x}$  measured at 4.2K.

The transport critical current measurements have been performed at both temperatures of 77 K and 4.2 K with criterion of  $1 \mu\text{V}/\text{cm}$ . The critical current density is defined as the current divided by the cross sectional area of oxide phase. After the partial removal of silver sheath and polishment of the tape specimen, the microstructure was examined by a polarization microscope. The crystallographical orientation of grains was investigated by X-ray pole figure technique.

## RESULTS AND DISCUSSION

**Effect of Hydrogen Gas Reduction:** The present process seemed to be advantageous in several points. The metallic composite has a high workability. The generation of cracks due to thermal tensile stress during heating is essentially avoided. At the stage of oxidation, the oxide layer is grown under compressive stress and a preferred orientation is obtainable in arrangement of grains. Fig. 1 shows the change of critical current density as a function of tape thickness of specimens. At 4.2K,

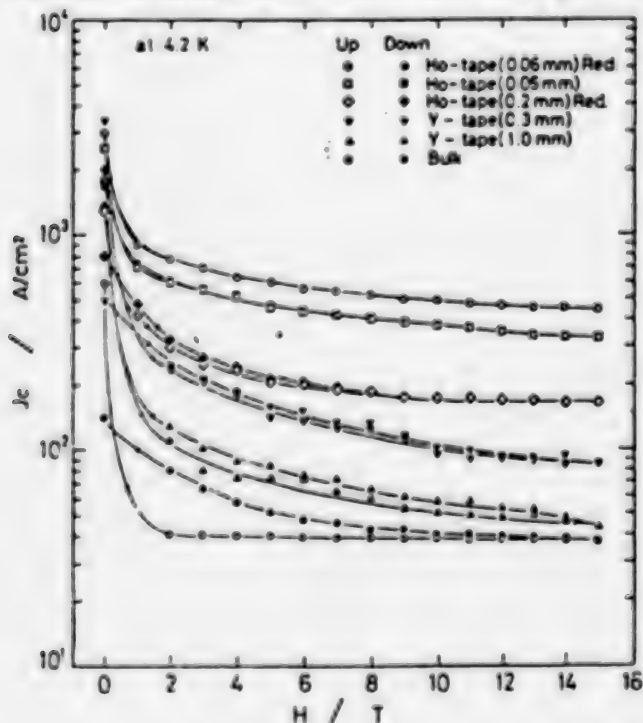


Fig. 2 Magnetic field dependence of critical current density at 4.2 K.

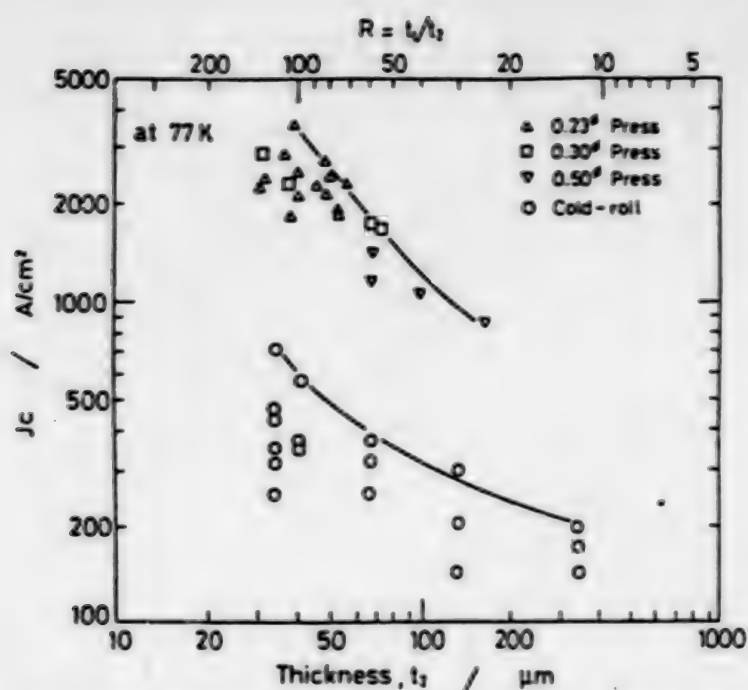


Fig. 3 Critical current density at 77 K as a function of thickness of  $\text{Ba}_2\text{YCu}_3\text{O}_{6+x}$  oxide layers made by both cold-rolling and pressing.



Fig. 4 Microstructure at the cross-section of tape specimens.

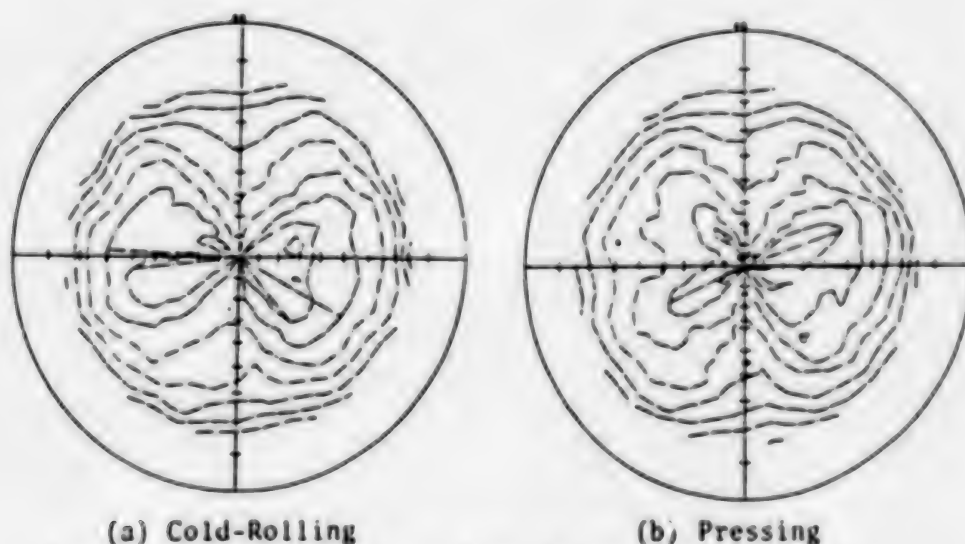


Fig. 5 (003) pole figure from the tape surface.

the current density stayed maximumly up to  $3000 \text{ A/cm}^2$ . The current density for the specimens made from the hydrogen gas reduced powder became larger than that for the conventional specimens. As shown in Fig. 2, it is clearly seen that the hydrogen reduced specimen is superior in the magnetic field dependence of critical current density.

Effect of Cold-Working on Critical Current: As shown in Figs. 1 and 2, the current density increased with decreasing the tape thickness for the specimens made by cold-rolling technique. In Fig. 3, the current density for the specimens made by both cold-rolling and cold-pressing techniques. The same results have been already reported from Sumitomo Electronics [2]. Clearly the current density increases with decreasing thickness for both groups of experimental data obtained by different techniques of cold-working. The cold-working induced resultantly a textured structure in the sintered oxide layer as shown in Fig. 4. For the tapes with the higher degree of cold-working, the number of voids among grains was observed to decrease, suggesting the higher densification of the sintered body. Fig. 5 shows a typical result of (003) pole figure for the specimen made by cold-rolling. Two intensity maxima appear at symmetrical positions indicating that the c-axis inclines in average by about 30 degree from the surface normal. Fig. 5(b) shows the pole figure for the specimen made by pressing. The intensity profile is similar with the former one, but is concentrated much more in the centered region, indicating that the c-axis tends to become more parallel to the surface normal.

Comparing with the results for the epitaxially grown thin films [1], the transport critical current densities are very limited for the polycrystalline tape specimens. This might be attributed to weak links associated with the grain boundaries [5]. The direct mechanism explaining the increase of critical current by the texturing has not been yet made clear. Dimos et al [5] reported that even only minor misorientations of neighbouring grains sharing a parallel c-axis produces a drastically reduced intergrain critical current density. Furthermore it is suggested that Josephson barrier at the grain boundary contacting with each a-b plane is very weak and resultantly the critical current density becomes very small. From such an argument, it is possible to explain the big change of critical current density depending on the different cold-working technique. Conclusively, the increase of critical current density with increasing degree of cold working might be attributed to the formation of {001} alignment of grains parallel to the tape surface.

#### Acknowledgements

The critical current measurements have been partially performed at HFLSM of Tohoku University. This study was made possible by a Scientific Research Grant in-Aid (Proj. No. 62124055) from the Ministry of Education.

#### References

- 1) K.Watanabe, H.Yamane, H.Kurosawa, T.Hirai, N.Kobayashi, H.Iwasaki, K.Noto and Y. Muto; Appl. Phys. Lett., (1988) submitted.
- 2) M.Nagata, K.Ohmatsu, H.Mukai, T.Hikata, Y.Yosoda, N.Shibuta and M.Kawashima; Report of Sumitomo Electronics, 133 (1988) 7-14.
- 3) K.Osamura, T.Takayama and S.Ochiai; Proc.of ICEC12 (July, 1988, Southampton)
- 4) T.Takayama, K.Osamura, S.Ochiai and H.Tabata; Proc.of Osaka University Inter. Symp. (Oct., 1988, Suita).
- 5) D.Dimos, P.Chaudhari, J.Mannhart and F.K.LeGoues; Phys.Rev.Lett., 61 (1988) 219-222.

## Ag-SHEATHED HIGH $T_c$ SUPERCONDUCTING TAPE WITH $J_c=10^4$ A/cm<sup>2</sup>

T. MATSUMOTO, M. OKADA, R. HISIWAKI, T. KAMO,  
K. AIHARA and S. MATSUDA

HITACHI, LTD., HITACHI RESEARCH LABORATORY  
4026 Kuji, Hitachi, Ibaraki, 319-12, Japan

M. SEIDO

HITACHI CABLE, LTD. METAL RESEARCH LABORATORY  
3550 Kidamari, Tsuchiura, Ibaraki 300, Japan

K. OZAWA

HITACHI, LTD., ENERGY RESEARCH LABORATORY  
1168 Moriyama, Hitachi, Ibaraki, 316, Japan

Y. MORII and S. FURAHASHI

JAPAN ATOMIC ENERGY RESEARCH INSTITUTE  
Tokai, Naka, Ibaraki, 319-11, Japan

### ABSTRACT

Ag-sheathed high  $T_c$  superconducting tapes were fabricated by a drawing-rolling method, using  $YBaCuO$  (YBCO),  $TlBaCaCuO$  (TBCCO) and  $Tl(Ba,Sr)CaCuO$  (TBSCCO). The critical current density  $J_c$  reached 3300 A/cm<sup>2</sup> and  $10^4$  A/cm<sup>2</sup> at 77 K in the YBCO and TBSCCO tape, respectively. A series of SEM observation and neutron diffraction analysis revealed that crystallite alignment was enhanced through the cold rolling process and the subsequent heat treatment.

### INTRODUCTION

Since the discovery of high  $T_c$  oxide superconductors, a number of studies have been made on the preparation of wires by powder methods. The  $J_c$ 's of the superconducting wires reported so far are, however, in the order of  $10^4$  A/cm<sup>2</sup> at 77K in the absence of external magnetic field. For the power applications, it is prerequisite to develop a superconducting wire with  $J_c$  above  $10^4$  A/cm<sup>2</sup> in the presence of magnetic field. The authors have developed Ag-sheathed superconducting tape by a drawing-rolling method<sup>1,2</sup>. In this paper, the  $J_c$ 's of the superconducting tape are discussed in relation to the microstructure of superconducting crystallites.

### EXPERIMENTAL

Ag-sheathed superconducting tapes were fabricated by the drawing-rolling method shown in Fig.1, using YBCO ( $T_{c,0} = 90$  K), TBCCO ( $T_{c,0} = 118$  K) and TBSCCO ( $T_{c,0} = 115$  K) powders. The  $T_{c,0}$  values in the parentheses were resistively measured, using a respective pellet. The YBCO powder was prepared from  $Y_2O_3$ ,  $BaCO_3$  and  $CuO$  with the purity of 99.9 %. The TBCCO and TBSCCO powders



were prepared from  $Tl_2O_3$ ,  $BaCO_3$ ,  $SrCO_3$  (used only for TBSCCO),  $CaCO_3$ , and  $CuO$ . It has been found that  $Tl-Sr-Ca-Cu-O$  system gives superconductor with  $T_c$  100 K<sup>11</sup>, and the TBSCCO has a higher superconducting volume fraction than the TBCCO. The  $J_c$  of the superconducting tape was resistively measured in the absence and presence of external magnetic field up to 9T. The criterion for the  $J_c$  was 1  $\mu V/cm$ . The microstructure of the superconducting core was examined by SEM observation and neutron diffraction analysis.

## RESULTS AND DISCUSSION

### $J_c$ 's of Ag-sheathed superconducting tapes

Figure 2 shows the  $J_c$ 's of Ag-sheathed superconducting tapes in relation to their thickness, measured at 77 K in the absence of external magnetic field. The heat treatment condition was 910 °C-2h for the YBCO tape and 845 °C-2h for the TBSCCO tape in a flowing oxygen atmosphere. It is clearly observed that the  $J_c$  increases with decreasing the tape thickness and the  $J_c$  of the TBSCCO tape is much higher than that of the YBCO tape. The difference in  $J_c$  was probably caused by the difference in  $T_c$  between the YBCO and TBSCCO powder. The  $J_c$  has reached 3300 A/cm<sup>2</sup> and 10<sup>4</sup> A/cm<sup>2</sup> in the YBCO<sup>11</sup> and TBSCCO tape, respectively.

### Heat treatment on Tl-based superconducting tape

Thallium oxide has a relatively high vapor pressure in the temperature range of calcination so that the high  $T_c$  phase of Thallium-based superconductor may be transformed into another phases during the heat treatment. Figure 3 shows the effect of the heat treatment condition on the  $J_c$  of the TBCCO tapes<sup>11</sup>. The optimum heat treatment should be conducted in a temperature range between 845 °C and 860 °C for about 2h. An EDX analysis revealed that the atomic ratio of Tl:Ba:Ca:Cu was approximately 2:2:2:3 in the superconducting core of the tape heat treated under these conditions.

### SEM images of superconducting core

Figure 4 shows the SEM images of the YBCO core surface contact with the Ag-sheath of the tape with the thickness of 0.06 mm<sup>11</sup>. Figure 4(a) shows plate-shaped grains. Figure 4(b) shows alternating bright and dark bands due to the twin lamellas. The bands penetrate through grain boundaries. These observation suggests that the YBCO grains have been partially aligned in the Ag-sheathed tape.

## Crystallite alignment in Ag-sheathed tape

It was confirmed" through the neutron diffraction analysis that the YBCO crystallites were partially aligned in the YBCO tape with the thickness of 0.1mm". Figure 5 shows the crystallite alignment of the YBCO crystals in the Ag-sheathed tapes with various thickness. The Std. Dev. means the standard deviation of the intensity distribution of the diffracted neutron from the (001) plane of the YBCO crystallite in the crystal rotation method. The a-b planes of YBCO crystallite are aligned along the rolling surface within the angle designated as the Std. Dev. with the probability of 68 %. According to Fig.5, the YBCO crystallites exhibit a considerable alignment even under the as rolled condition and the crystallite alignment is enhanced by the subsequent heat treatment. The effect is more pronounced as the tape thickness becomes thin. It is suggested that the  $J_c$  of the Ag-sheathed tape increases through the enhanced crystallite alignment.

## $J_c$ in magnetic field

Figure 6 shows the  $J_c$  in external magnetic field on the TBCCO (0.07mm thick) and YBCO (0.10mm thick) tapes". Both  $J_c$ 's decrease sharply even in the low magnetic field below 0.1 T. The  $J_c$  of the TBCCO tape is, however, improved markedly in comparison with the YBCO tape. As shown in Fig.6(b), the  $J_c$  is about  $10^4$  A/cm<sup>2</sup> at 20 K in the external magnetic field of 9 T.

## CONCLUSIONS

- (1) The  $J_c$  of the Ag-sheathed TBCCO tape reached  $10^4$  A/cm<sup>2</sup> at 77K.
- (2) The YBCO crystallites in the Ag-sheathed tape exhibit a considerable alignment under the as rolled condition and the crystallite alignment is enhanced by the subsequent heat treatment.
- (3) The  $J_c$  of the Ag-sheathed tape decreases sharply in the presence of external magnetic field.

## REFERENCES

- 1) M. Okada et al.: Jpn. J. Appl. Phys. 27(1988)L185.
- 2) M. Okada et al.: Jpn. J. Appl. Phys. 27(1988)L2345
- 3) T. Matsumoto et al.: Progress in High Temperature Superconductivity-8(1988)321
- 4) M. Okada et al.: Jpn. J. Appl. Phys. 27(1988)L1715
- 5) M. Matsuda et al.: Jpn. J. Appl. Phys. 27(1988)pp2062

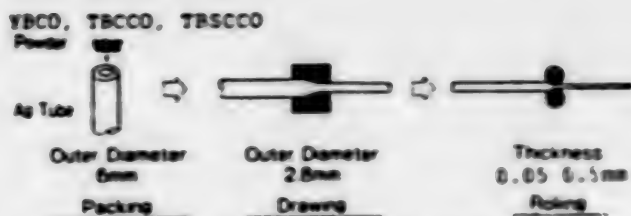


Fig.1 Drawing-rolling method

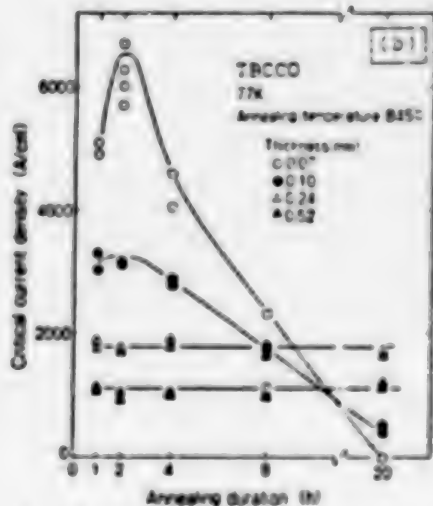
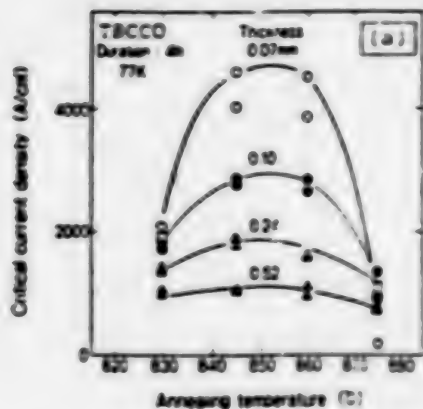


Fig.3 Effect of heat treatment condition on  $J_c$

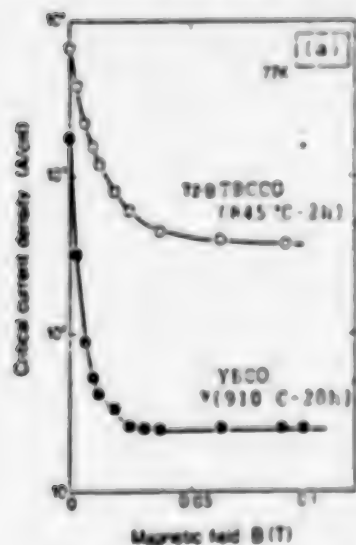


Fig.6  $J_c$  in external magnetic field

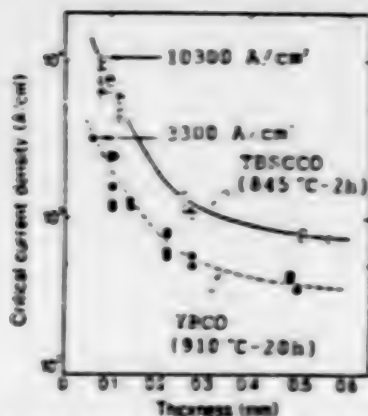


Fig.2  $J_c$ 's of Ag-sheathed tape

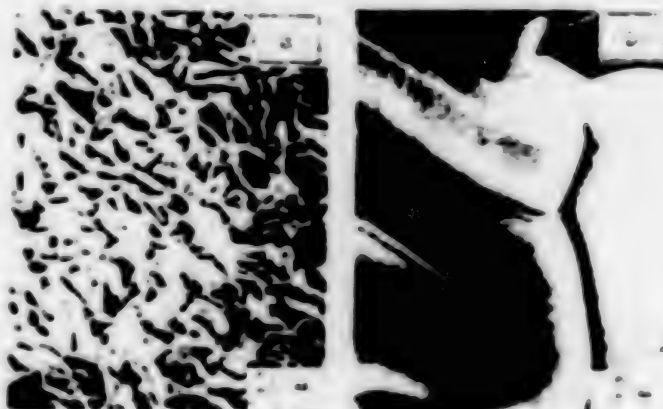


Fig.4 SEM images of superconducting core surface

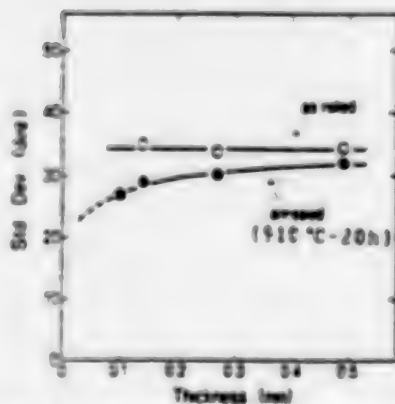
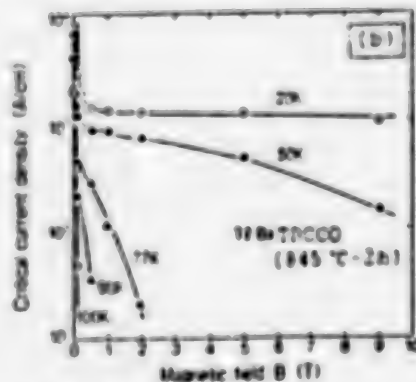


Fig.5 Alignment of YBCO crystallite



# CRITICAL CURRENT DENSITY OF Bi(Pb)-Sr-Ca-Cu-O TAPE

K. TOGANO

NATIONAL RESEARCH INSTITUTE FOR METALS

1-2-1, Sengen, Tsukuba-city, Ibaraki 305, JAPAN

## ABSTRACT

Flexible tape conductors of high- $T_c$  Bi(Pb)-Sr-Ca-Cu-O were prepared by doctor blading and Ag-sheathing techniques. The tapes have a highly oriented grain structure, which can result in a improvement in electrical coupling between grains, and hence improved transport  $J_c$  characteristics.

## INTRODUCTION

Discovery of superconductivity in Bi-Sr-Ca-Cu-O superconductor with transition temperatures,  $T_c$ , above 100K, has brought about a new phase in the research of high- $T_c$  oxide superconductors(1). However, the transport critical current density  $J_c$  for this Bi-based compound prepared by the conventional sintering method still remains very low compared to the level of practical application. In particular, the  $J_c$  drastically decreases with increasing the applied magnetic field as in the case of Y-Ba-Cu-O compound, probably due to the weakness of the coupling between adjacent grains.

In this paper, we present a result in which a significant improvement in transport  $J_c$  has been achieved in the Pb-doped Bi-Sr-Ca-Cu-O tapes prepared by the powder techniques of doctor blading (2) and Ag-sheathing (3).

## EXPERIMENTAL

The appropriate amounts of  $Bi_2O_3$ ,  $Pb_2O_3$ ,  $SrCO_3$ ,  $CaCO_3$  and  $CuO$  powders were mixed, calcined and heat treated at  $845^\circ C$  for 120h to form high- $T_c$  phase of the Bi-Sr-Ca-Cu-O system. This was milled into a fine powder for subsequent processing. Organic formulation consisting of solvent, binder and dispersant was then added and again milled together. The resulting slurry was cast under a doctor blade into a green tape of 50-150  $\mu m$  thickness on the carrier sheet. Ribbon samples, typically 3mm in width and 100mm in length, were cut from the tape and heat treated at  $500^\circ C$  for 1h. The ribbon was then sandwiched between stainless steel sheets and cold rolled together. A small reduction of total cross sectional area results in an effective densification of the oxide ribbon. The ribbon was then subjected to a final heat treatment of sintering.

Tape conductors have also been prepared by conventional fabrication methods of powder using Ag-sheath. The oxide powder of Bi(Pb)-Sr-Ca-Cu-O was prepared by mixing the appropriate amounts of reagents and calcination at  $800^\circ C$  for 12h. The powder was then packed into a Ag-tube and cold worked to a tape of 0.5mm in thickness by swaging and rolling. The tape was then cut into 3cm length and the short samples were then subjected to the combination process of sintering and intermediate cold rolling.





Fig. 1  
BSE image of the longitudinal cross-section at the center of the Ag-sheathed tape prepared by adding intermediate cold rolling during sintering process. H, F and R denote the High- $T_c$  phase, Bi-free phase and Bi-rich phase, respectively

## RESULTS AND DISCUSSION

Both of the doctor blade processed (DBP) and Ag-sheathed tapes have a highly oriented grain structure, which is caused by the addition of intermediate cold rolling process. Figure 1 shows the back-scattered electron image of the longitudinal cross section at the center of the Ag-sheathed tape, showing that the high- $T_c$  plate-like grains are aligned in parallel direction to the tape surface, i.e., c-axis alignment perpendicular to the surface. The addition of rolling also greatly improves the packing density and flexibility especially for the DBP-tape. The DBP-tape after the final sintering can be bent elastically into a small diameter of about 30mm without any breakage. Figure 2 shows the DBP-tape bent on a 38mm-diameter bobbin.



Fig. 2  
DBP tape bent on a 38mm-diameter bobbin.

The inclusion of the intermediate rolling process was also found to greatly improve the superconducting properties of the tape. Figure 3 shows the  $J_c$  of the Ag-sheathed tape. The tape was initially sintered at 835°C for 80h and then subjected to the combination process of sintering at 835°C and cold rolling, and the  $J_c$  is plotted as a function of total sintering time. The highest  $J_c$  is 3050A/cm<sup>2</sup>. Similar improvement of  $J_c$  was also obtained for the DBP-tape. The DBP-tape processed without rolling has a  $T_c$  of 97K and a poor  $J_c$  of less than 10A/cm<sup>2</sup> at 77K and 0T. However, by the addition of the rolling process,  $T_c$  above 100K and  $J_c$  in excess of 1000A/cm<sup>2</sup> were easily obtained. The highest  $J_c$  obtained so far is 1850A/cm<sup>2</sup>.

Figure 4 shows the  $J_c$  of the DBP-tape as a function of magnetic field.  $J_c$ -H curves of a bulk sample prepared by the conventional sintering are also shown in the figure.  $J_c$  of the tape is much larger than that of the sintered bulk sample at entire magnetic fields. Especially,  $J_c$  degradation with increasing magnetic field is significantly decreased for the tape. This improved  $J_c$  property in magnetic fields suggests that the coupling of grains along the current direction is improved in the tape. Both of the tape and bulk samples show hysteresis in the  $J_c$ -H curve as shown in Fig. 4. Similar hysteresis was also reported for sintered Y-Ba-Cu-O(4). It is considered that the hysteresis is attributed to the grain boundaries having weak coupling nature which was affected by the local magnetic field induced by the large shielding current.

This improvement in coupling nature was also confirmed by the A.C. susceptibility measurement(5). Both the tape and bulk samples showed a two step transition in  $\chi'$  vs. temperature curve in large A.C. field amplitude, higher and lower temperature transitions corresponding to the intragrain and intergrain superconductivities, respectively. However, the curve for the tape shows a strong dependence on the field direction, i.e., the lower temperature transition is much smaller in the field perpendicular to the tape surface, while it becomes much larger in the parallel field compared to those of the bulk sample. This result indicates that the intergrain coupling along the tape direction is improved in the tape.

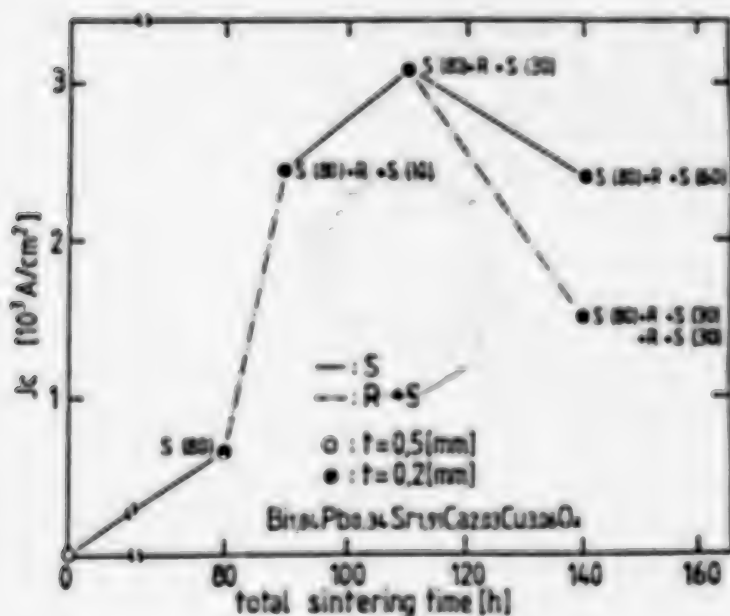


Fig. 3  
 $J_c$  of the Ag-sheathed tape as a function of the total sintering time. S(t) denotes the sintering and its time, and R denotes the rolling process.

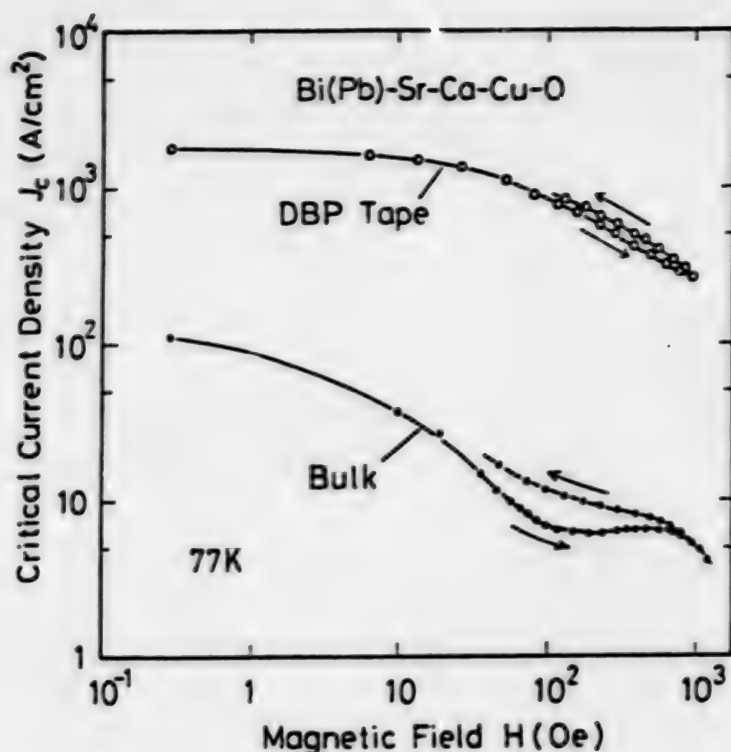


Fig. 4  
 $J_c$  versus  $H$  curves for DBP-tape. The results for bulk sample prepared by conventional sintering process are shown for comparison.

## CONCLUSIONS

Highly oriented grain structure in which the grains are aligned in such a way to maximize the intergrain electronic coupling has been obtained for the Bi(Pb)-Sr-Ca-Cu-O tapes prepared by the modified doctor blading and Ag-sheathing techniques. This structure results in a significantly improved transport  $J_c$ - $H$  characteristics for the tape. The tape processed by the modified doctor blading shows a sufficient flexibility to be bent into a small diameter of about 30mm.

## ACKNOWLEDGEMENTS

The author is very grateful for the cooperation of Drs. H.Kumakura and D.R.Dietderich of National Research Institute for Metals, Mr. A.Yanagisawa (Asahi Glass Co.) and Mr. M.Mimura (Furukawa Elec. Co) to do this work.

## REFERENCES

1. H.Maeda, Y.Tanaka, M.Fukutomi and T.Asano, Jpn. J. Appl. Phys., 27, L209(1988).
2. K.Togano, H.Kumakura, H.Maeda, E.Yanagisawa, N.Irisawa, J.Shimoyama and T.Morimoto, Jpn. J. Appl. Phys, 28, L278(1989).
3. M.Mimura, H.Kumakura, K.Togano and H.Maeda, submitted to Appl. Phys. Lett.
4. K.Noto, H.Morita, K.Watanabe, T.Murakami, Y.Koyanagi, I.Yoshii, I.Sato, H.Sugawara, N.Kobayashi, H.Fujimori and Y.Muto, Physica 148B, 239(1987).
5. H.Kumakura, K.Togano, H.Maeda, E.Yanagisawa and T.Morimoto, to appear in Jpn. J. Appl. Phys.

# BiPbSrCaCuO SUPERCONDUCTING WIRES WITH HIGH CRITICAL CURRENT DENSITY

KEN-ICHI SATO, TAKESHI HIKATA, HIDEHITO MUKAI  
and HAJIME HITOTSUYANAGI

OSAKA RESEARCH LABORATORIES, SUMITOMO ELECTRIC INDUSTRIES LTD.,  
1-1-3 SHIMAYA, KONOYAMA-KU, OSAKA, 554 JAPAN

## ABSTRACT

Through the solid reaction methods, silver sheathed BiPbSrCaCuO superconducting wires were fabricated. The maximum transport current density was 10,600 A/cm<sup>2</sup> at 77.3K in a zero magnetic field. These wires had critical temperature:  $T_c$  ( $R=0$ ) = 104K. The magnetic field dependence of  $J_c$  (0.1  $\mu$ V/cm criterion) was summarized as follows for the sample of  $J_c=10,600$  A/cm<sup>2</sup> in a zero magnetic field: 2,850 A/cm<sup>2</sup> ( $H \perp I$ ,  $H \parallel c$ -plane, 0.1T), 1,220 A/cm<sup>2</sup> ( $H \perp I$ ,  $H \perp c$ -plane, 0.1T). The low- $J_c$  sample has a two-step decrease in  $J_c$  versus  $H$ , while the high- $J_c$  sample has only a one-step decrease in the higher magnetic field. The rapid decrease of  $J_c$  in a relatively low magnetic field, i.e. 100 gauss, of the low- $J_c$  sample was caused by the weak link, confirmed by investigating the history effects of  $J_c$  during the increase and decrease of the magnetic field. XRD analysis shows the series of (00 $l$ ) peaks of the high- $T_c$  phase (110K) with the characteristic (002) peak at  $2\theta=4.7^\circ$ . The grains in the 110K phase were found to be oriented with the  $c$ -axis perpendicular to the wide plane of the taped superconducting wire. It was observed that the non-superconducting phase,  $Ca_2PbO_4$ , remained. SEM photographs of the fracture surface show that the high- $J_c$  sample had grain boundaries composed of the grains aligned in the same orientation in the  $c$ -planes, bonded strongly in the direction of alignment.

## INTRODUCTION

One of the most convenient methods for producing high- $T_c$  oxide superconducting wires is a metal sheathing method employing powder in tube, which was fabricated by various metal working processes, such as drawing, swaging, rolling and pressing. These wires are required to transport high superconducting currents in a high magnetic field for application to transformers, power cables, NRI magnets and other various superconducting magnets.

Since a new oxide superconductor, Bi-Sr-Ca-Cu-O system with a high- $T_c$  phase (110K) and low- $T_c$  phase (80K) was reported by Maeda et al.,<sup>(1)</sup> there have been many related investigations. It was reported that substituting a part of Bi for Pb produced a stable high- $T_c$  phase.<sup>(2)</sup> Bi-Pb-Sr-Ca-Cu-O with a high- $T_c$  phase is expected to have a higher  $J_c$  because of a larger margin between its  $T_c$  and the liquid nitrogen temperature (77.3K). To obtain a higher  $J_c$  wire, it is important to align the superconducting grains and strengthen the contact at the grain boundaries, adding homogenization of the high- $T_c$  phase.<sup>(3)</sup>

## EXPERIMENTAL



Appropriate amounts of  $\text{Bi}_2\text{O}_3$ ,  $\text{PbO}$ ,  $\text{SrCO}_3$ ,  $\text{CaCO}_3$  and  $\text{CuO}$  powders with 3 to 4 N purity were mixed into the composition ( $\text{Bi}:\text{Pb}:\text{Sr}:\text{Ca}:\text{Cu}=1.6:0.4:2:2:3$ ) basically, calcined and sintered from  $750^\circ\text{C}$  to  $870^\circ\text{C}$  for 8 to 200h in air, and then ground into powder. The powder was put into silver tubes. The composites were swaged and drawn, and then fabricated into wires by rolling or pressing. The wires were sintered from  $800^\circ\text{C}$  to  $870^\circ\text{C}$  for 8-800h in air. The thickness of the wires ranged from 0.1mm to 0.4mm.

The measurements of critical transport current and critical temperature were carried out by the 4-probe dc method. The magnetic field was applied perpendicularly to a transport current up to 2.5T. The criterion for  $J_c$  determination was defined as  $1\mu\text{V}/\text{cm}$  in a zero magnetic field and  $0.1\mu\text{V}/\text{cm}$  in a magnetic field. X-ray diffraction analysis using  $\text{Cu-K}\alpha$  radiation was performed on the wide surface of each oxide superconducting specimen after the Ag-sheath was stripped. The fracture surface of each specimen was observed by SEM.

## RESULTS AND DISCUSSION

The wires had a critical temperature  $T_c$  with zero resistivity of about 104 K when sintered for over 50 hours at  $845^\circ\text{C}$ . Figure 1 shows the X-ray diffraction pattern for the specimen with  $J_c$  of  $10,600\text{ A}/\text{cm}^2$ . The series of peaks of the high- $T_c$  phase (110K) with the characteristic (002) peak at  $2\theta=4.7^\circ$  was observed, while the low  $T_c$  phases (80K, 7K) with the characteristic (002) peaks,  $2\theta=5.7^\circ, 7.2^\circ$ , could not be observed. Therefore the only superconducting phase of this specimen was the 110K phase. However, it was observed that the non-superconducting phase,  $\text{Ca}_2\text{PbO}_4$ , remained. The grains in the 110K phase were found to be oriented with the c-axis perpendicular to the wide plane of the wire specimen.

Figure 2 shows the  $J_c$  versus cross sectional area of the wire including silver sheath. From this figure, it can be seen that  $\text{BiPbSrCaCuO}$  wires have high  $J_c$  properties at large dimensions.

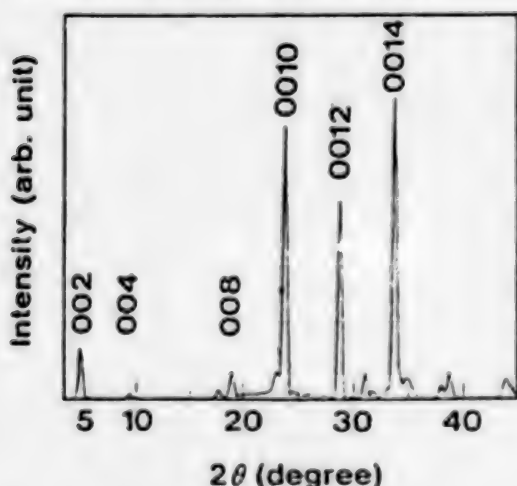


Fig. 1. X-ray diffraction pattern for the wide surface of  $\text{BiPbSrCaCuO}$  specimen with  $10,600\text{ A}/\text{cm}^2$  after stripping of the Ag-sheath.

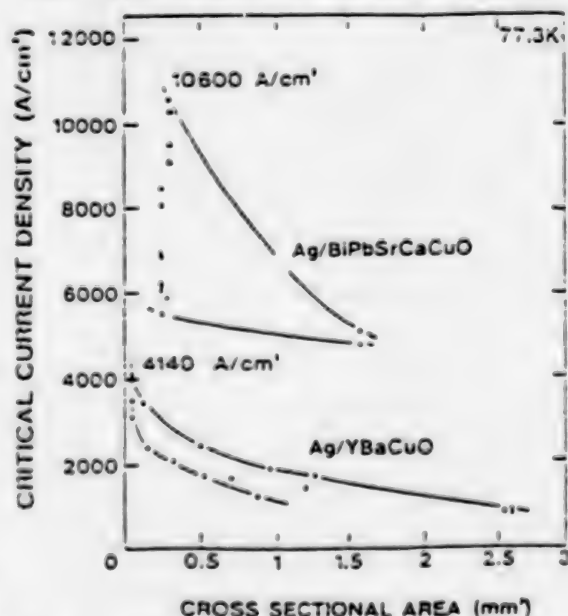


Fig. 2.  $J_c$  of  $\text{BiPbSrCaCuO}$  superconducting wires.

Figure 3 shows the magnetic field dependencies of  $J_c$  for specimen A ( $10,600 \text{ A/cm}^2$ ), B ( $1,650 \text{ A/cm}^2$ ). The thickness of specimen A was  $0.12 \text{ mm}$ , and that of specimen B was  $0.2 \text{ mm}$ . The magnetic field was applied in two dimensions: perpendicular and parallel to the wide plane of the wire specimens.

The magnetic field dependence of these specimens had anisotropy for the applied direction of magnetic field. The  $J_c$  in the magnetic field was improved greatly when  $J_c$  was increased in a zero field, but the decrease at the higher magnetic field remained. Figure 3 shows that specimen B has a two-step decrease in  $J_c$  versus  $H$ , while specimen A has only a one-step decrease in the higher magnetic field. The reason was revealed in an observation of SEM photographs of the fracture surface of specimen A and B in Fig. 4. It was found that specimen B had grain boundaries composed of grains with a difference in crystal orientation, as shown in Fig. 4(b), while specimen A had grain boundaries composed of the grains' aligned in the same orientation in the c-planes, as shown in Fig. 4(a). Therefore, it was considered that the superconducting current in specimen A must flow through the grain

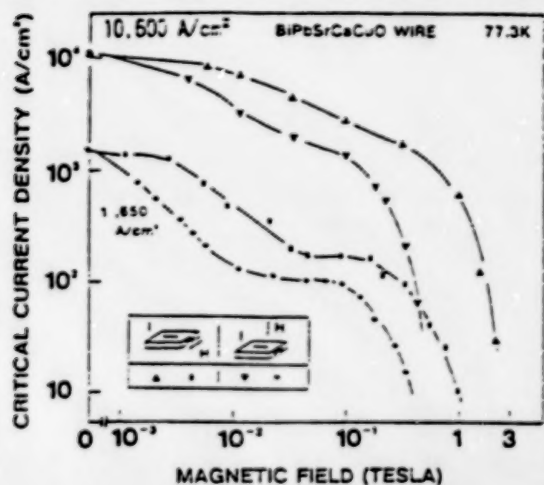


Fig. 3. Magnetic field dependence of critical current density of specimen A ( $10,600 \text{ A/cm}^2$ ) and B ( $1,650 \text{ A/cm}^2$ ) during increase in the magnetic field. Lines are drawn as a guide for the eye.



Fig. 4. Fracture surface of BiPbSrCaCuO oxide superconductor inside a Ag-sheathed taped wire. a) specimen A. b) specimen B.

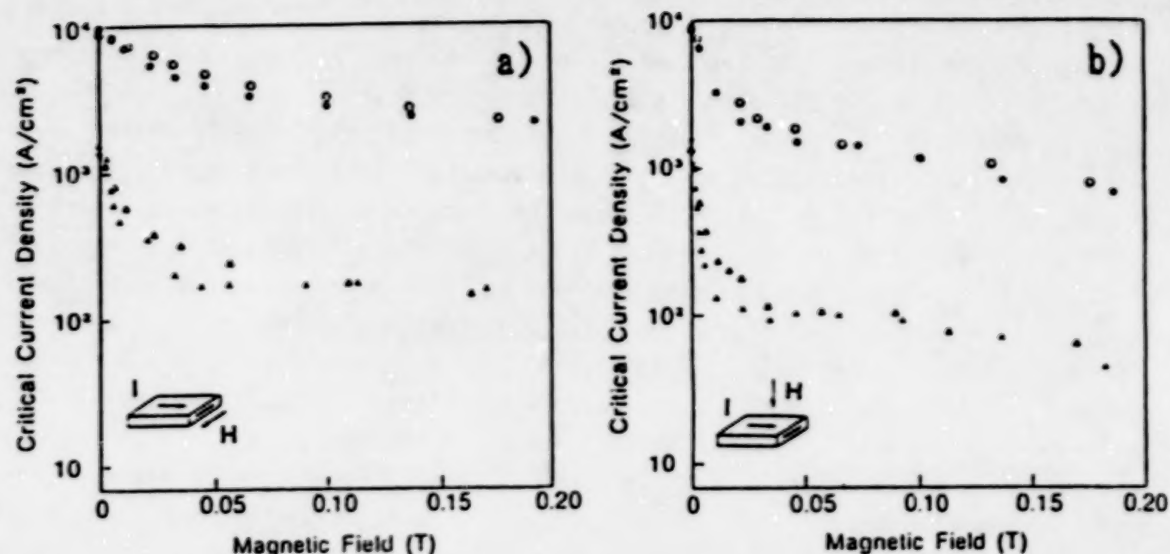


Fig. 5. The history of  $J_c$  during the increase and decrease of H for specimen A and B. a) H parallel to wide plane of the specimens. b) H perpendicular to wide plane of the specimens. Solid circles and triangles represent  $J_c$  during an increase in the magnetic field; open circles and triangles represent  $J_c$  during a decrease in the field.

boundaries securely along the aligned c-planes. The bonds never weaken in a low magnetic field. Figure 5 shows the history effect of  $J_c$  during the increase and decrease of the magnetic field. The hysteresis appeared at a low magnetic field below 0.1 T and showed anisotropy for the magnetic field direction. The hysteresis of specimen A was small, while specimen B had large hysteresis. Therefore, the hysteresis must be caused mainly by the weak link shown in Fig. 4(b).

In summary, we developed Ag-sheathed Bi-Pb-Sr-Ca-Cu-O superconducting wires with high current capacities by solid reaction method. The maximum  $J_c$  was 10,600 A/cm². The  $J_c$  in 0.1 T was 2,850 A/cm² when the magnetic field was parallel to the wide plane of the taped wire, and 1,220 A/cm² when it was perpendicular to it. The reason for these improvements were homogenization of the high- $T_c$  phase (110K), preferred alignment of the superconducting grains, and good contact at the grain boundaries.

#### REFERENCES

- [1] H.Naeda, Y.Tanaka, M.Fukutomi and T.Asano: Jpn. J. Appl. Phys. 27 (1988) L209.
- [2] M.Takano, J.Takada, K.Oda, H.Kitaguchi, Y.Miura, Y.Ikeda, Y.Tomii and H.Hazaki: Jpn. J. Appl. Phys. 27 (1988) L1041.
- [3] T.Hikata, K.Sato and H.Hitotsuyanagi: Jpn. J. Appl. Phys. 28 (1989) No.1.

- END -

This is a U.S. Government publication. Its contents in no way represent the policies, views, or attitudes of the U.S. Government. Users of this publication may cite FBIS or JPRS provided they do so in a manner clearly identifying them as the secondary source.

Foreign Broadcast Information Service (FBIS) and Joint Publications Research Service (JPRS) publications contain political, economic, military, and sociological news, commentary, and other information, as well as scientific and technical data and reports. All information has been obtained from foreign radio and television broadcasts, news agency transmissions, newspapers, books, and periodicals. Items generally are processed from the first or best available source; it should not be inferred that they have been disseminated only in the medium, in the language, or to the area indicated. Items from foreign language sources are translated; those from English-language sources are transcribed, with personal and place names rendered in accordance with FBIS transliteration style.

Headlines, editorial reports, and material enclosed in brackets [ ] are supplied by FBIS/JPRS. Processing indicators such as [Text] or [Excerpts] in the first line of each item indicate how the information was processed from the original. Unfamiliar names rendered phonetically are enclosed in parentheses. Words or names preceded by a question mark and enclosed in parentheses were not clear from the original source but have been supplied as appropriate to the context. Other unattributed parenthetical notes within the body of an item originate with the source. Times within items are as given by the source. Passages in boldface or italics are as published.

#### SUBSCRIPTION/PROCUREMENT INFORMATION

The FBIS DAILY REPORT contains current news and information and is published Monday through Friday in eight volumes: China, East Europe, Soviet Union, East Asia, Near East & South Asia, Sub-Saharan Africa, Latin America, and West Europe. Supplements to the DAILY REPORTs may also be available periodically and will be distributed to regular DAILY REPORT subscribers. JPRS publications, which include approximately 50 regional, worldwide, and topical reports, generally contain less time-sensitive information and are published periodically.

Current DAILY REPORTs and JPRS publications are listed in *Government Reports Announcements* issued semimonthly by the National Technical Information Service (NTIS), 5285 Port Royal Road, Springfield, Virginia 22161 and the *Monthly Catalog of U.S. Government Publications* issued by the Superintendent of Documents, U.S. Government Printing Office, Washington, D.C. 20402.

The public may subscribe to either hardcover or microfiche versions of the DAILY REPORTs and JPRS publications through NTIS at the above address or by calling (703) 487-4630. Subscription rates will be

provided by NTIS upon request. Subscriptions are available outside the United States from NTIS or appointed foreign dealers. New subscribers should expect a 30-day delay in receipt of the first issue.

U.S. Government offices may obtain subscriptions to the DAILY REPORTs or JPRS publications (hardcover or microfiche) at no charge through their sponsoring organizations. For additional information or assistance, call FBIS, (202) 338-6735, or write to P.O. Box 2604, Washington, D.C. 20013. Department of Defense consumers are required to submit requests through appropriate command validation channels to DIA, RTS-2C, Washington, D.C. 20301 (Telephone: (202) 373-3771, Autovon: 243-3771).

Back issues or single copies of the DAILY REPORTs and JPRS publications are not available. Both the DAILY REPORTs and the JPRS publications are on file for public reference at the Library of Congress and at many Federal Depository Libraries. Reference copies may also be seen at many public and university libraries throughout the United States.



**END OF**

**FICHE**

**DATE FILMED**

**22 MAY 89**